Vaisala 3TIER Services
Wind Energy Due Diligence

PROJECT

Busch Ranch II : Las Animas and Huerfano Counties, Colorado

using 27 Vestas V120-2.2MW wind turbines at 80 m

FOR

Black Hills Corp.

DATE

6 December, 2017

CONTACT

ph: +1 206.325.1573
2001 6th Avenue, Suite 2100
Seattle, WA 98121
www.vaisala.com/energy

VAISALA

Process Versioning

Employed Version	6.12
Most Recent Validated Version	6.5
Process Updates Since Validation	• Extreme Cold Temperature Derating Algorithm • Topographic Data Improvement in United States • Turbulence Intensity Loss Algorithm • Turbine Specific Wind Energy Sensitivity • Climate Variability Uncertainty Algorithm

Report Creation

Author	First Reviewer	Second Reviewer
		
Mike Burghart	Matthew Wiley	Annie Guiler

Report Specifications

Date	6 December, 2017
Client	Black Hills Corp.
Project	Busch Ranch II
Issue	A
Version ID	Y7wlxllX+zv9Ysev59chyDVxLPIPRJoL5TWfV63JUA==

Disclaimer

Contents

1 EXECUTIVE SUMMARY

Vaisala has conducted a wind resource assessment of the Busch Ranch II project, located in Las Animas and Huerfano Counties, Colorado. This project consists of 27 Vestas V120-2.2MW wind turbines at $80\,m$, for a total capacity of $59.4\,MW$. The project is located in rangeland approximately $30\,km$ northeast of Walsenburg.

A summary of the major results is provided here. Table 1 provides configuration details of the project as well as primary wind speed, generation and uncertainty results. Table 2 shows the probability of exceedance levels associated with the P50 project estimate. The long-term reference period used in this analysis extends over 37 years (January, 1980 – September, 2017). The wind resource assessment yields a gross project-average long-term wind speed estimate, at hub height, of $\mathbf{7.62\,m/s}$. The long-term mean gross generation estimate is $\mathbf{248.2\,GWh}$, with a corresponding gross capacity factor of $47.7\,\%$. Loss factors are considered, leading to a net energy estimate of $\mathbf{201.5\,GWh}$, with a corresponding net capacity factor of $38.7\,\%$.

A map of the hub height long-term mean wind speed values across the Busch Ranch II project area is displayed in Wind Speed Maps.

Project Size	$59.4\,MW$
Number of Turbines	27
Turbine Type	Vestas V120-2.2MW
Hub Height	$80\,m$
Project-Average Wind Speed	$7.62\,m/s$
Project-Average Density	$0.990\,kg/m^3$
Gross Generation	$248.2\,GWh$
Net Generation	$201.5\,GWh$
Gross Capacity Factor	$47.7\,\%$
Net Capacity Factor	$38.7\,\%$
Aggregate Loss Factor	$81.2\,\%$
Standard Error of 20-year Estimate	$7.0\,\%$

Table 1: Project Overview

	1-year	10-year	20-year
Gross-P50	248.2	248.2	248.2
Net-P50	201.5	201.5	201.5
Net-P75	190.8	191.9	192.0
Net-P90	181.2	183.3	183.4
Net-P95	175.5	178.1	178.3
Net-P99	164.7	168.4	168.7

Table 2: Probability of Exceedance Values (GWh)

1.1 Wind Speed Maps

This section contains a map of MOS-corrected long-term mean wind speed values at hub height ($80\,m$) across the Busch Ranch II project area.

1.1.1 80 m Hub Height

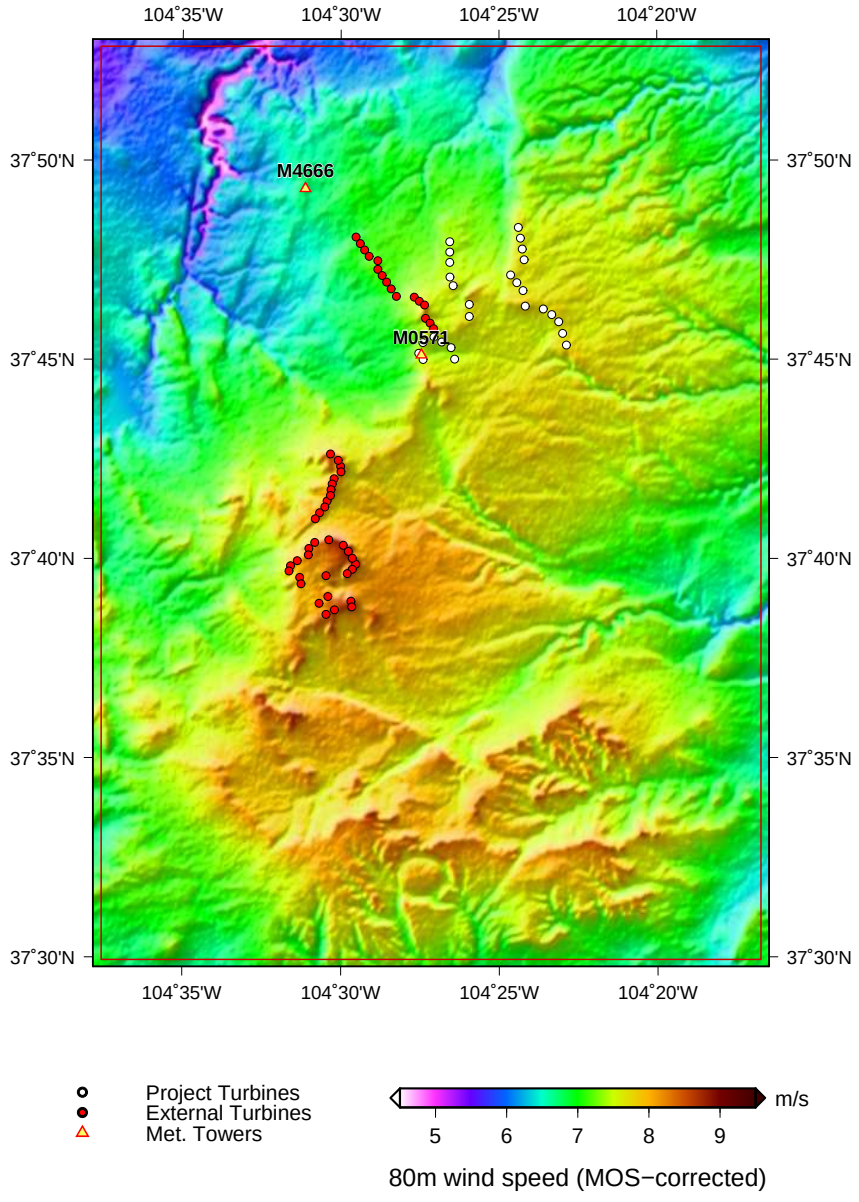

Figure 1: 37-year (January, 1980 – September, 2017) mean wind speed at $80\,m$.

2 METHODOLOGY

Vaisala's wind resource assessments are conducted using the 3TIER Services' NWP modeling platform that combines on-site observations with mesoscale and microscale weather simulation models. The output from the modeling system is a four-dimensional data set of modeled historical weather for each meteorological (met) tower and wind turbine location. Model output is statistically calibrated using observed data from met towers. The resulting data sets are the basis for analysis of the wind resource.

The core of this modeling system is the Weather Research and Forecasting (WRF) Numerical Weather Prediction (NWP) model, developed in a partnership between U.S. federal agencies and universities. WRF is suitable for a broad spectrum of applications including air quality plume modeling, wind resource assessment, and climate modeling. WRF provides a flexible and computationally efficient framework that allows the worldwide academic, government, and private research communities to contribute advancements in physics, numerical methods, and data assimilation.

The WRF model uses reanalysis data for initial and boundary conditions, and for continuous assimilation of gridded analysis into the simulations. A reanalysis data set is a coarse resolution, observational-based data set that exists for the past several decades. WRF relies on the reanalysis data set to provide an accurate representation of the large-scale (hundreds of kilometers) historic flow patterns throughout the atmosphere (e.g. the location of high and low pressure centers, the position of the jet stream, etc). In addition, WRF requires as input high-resolution topographic and land-use data in order to accurately represent surface conditions. Land surface characteristics are derived from the 10 arc second (approximately $300\,m$) resolution European Space Agency (ESA) GlobCover data set [1]. Topographic data are sourced from the Shuttle Radar Topography Mission (SRTM) data set at 3 arc-second (approximately $90\,m$) resolution [2]. With these primary inputs, WRF then solves the dynamical and physical equations that describe the processes of the atmosphere. A nested grid configuration is used to simulate the fine-resolution, local-scale flow conditions given the large-scale state of the atmosphere (as described by the reanalysis data).

The 3TIER Services Time-Varying Microscale (TVM) Model enables high-resolution mapping of meteorological fields without the computational cost of running an NWP model, such as the WRF model, at such fine spatial resolution. TVM uses several techniques to analyze microscale winds. Terrain effects that are unresolved by the mesoscale NWP model are estimated by considering both the variability of the elevation and the depth of the atmospheric mixed layer [3]. This is followed by a divergence minimization that enforces conservation of mass and further redistributed the wind velocity field. These effects are computed at each time step in the study period and are based not only on wind speed and elevation, but also on other quantities, including wind direction and the thermodynamic properties of the lower atmosphere. This enables a sophisticated time-varying spatial analysis at high-resolution.

On-site observational data are incorporated into the analysis to validate and correct the raw model data from WRF and TVM using a process of Model Output Statistics (MOS) correction. MOS uses multi-linear regression equations to remove bias and adjust the variance of the raw model output to improve the match with observational data at met tower locations. The MOS equation for each met tower is fit to the observational period of record. The MOS equation is then applied over the entire data set, correcting the historical period during which direct observational data are unavailable. MOS corrections are distributed across the model domain using a weighting scheme that depends on horizontal and vertical distance from the met tower.

A detailed analysis of the data set from each met tower ensures the integrity of the observational data before MOS-correction. Data are reviewed to ensure that:

- The functions to convert anemometer output to wind speed are appropriate, assuming raw data logger files and conversion functions are provided.
- Periods of icing affecting the accuracy of wind speed and direction measurement are excluded.
- Sensor data affected by the tower structures may be properly accounted for.
- Periods of anemometer dragging and/or malfunction are excluded.

During wind project development, met tower sensors are usually placed lower than the hub height of the proposed wind turbines. The analysis process must extrapolate the sensor data to hub height using a wind shear coefficient. Wind shear is a meteorological phenomenon in which wind speed values generally increase with height above ground level (AGL); the surrounding ground cover, trees, and topographic features such as hills and valleys can significantly affect the measured wind shear. The analysis calculates the shear coefficient from the observed data and then applies the coefficient to highest observed wind speed data to estimate wind speed values at hub height.

Long-term time series at each proposed turbine location are extracted from the MOS-corrected data set. These hourly time series are then combined with the manufacturer's specified power curve to compute gross capacity factor values. Applying site-specific loss factor estimates to the mean P50 gross capacity factor yields the P50 net capacity factor. Uncertainty of the measured data and modeling data is then estimated to calculate the final net capacity factors at various probabilities of exceedance.

2.1 Wind Resource Assessment Steps

To determine the energy production potential of the proposed Busch Ranch II wind project, the following procedure was implemented:

1. For the ERA-I [4], NCAR/NCEP [5], and MERRA-2 [6] reanalysis data sets, simulate 37 years at $4.5\,km$ resolution using WRF to understand the long-term temporal variability of weather over the project site.
2. When on-site observational data are available, validate time series data collected from each measurement location, and then perform correlation analysis between observations and $4.5\,km$ model results to determine primary reanalysis data set for NWP modeling.
3. Simulate 1 year at $500\,m$ resolution using WRF to understand the spatial variability of the wind resource at the site.
4. Run TVM to downscale $500\,m$ WRF simulation to $90\,m$ spatial resolution.
5. Perform ensemble analysis to integrate effects of each long-term data set including consistency checks to determine usefulness of entire 37 year period for each data set.
6. Combine the high-resolution spatial model data with the ensemble-adjusted coarser resolution long-term data, creating the final $90\,m$ resolution long-term data set.
7. When on-site observational data are available, compute and apply MOS to eliminate temporal bias and mitigate spatial bias of WRF/TVM model output.
8. Calculate the expected (P50) gross capacity factor using modeled long-term time series at each turbine location in combination with the appropriate power curve.
9. Perform numerical wake and turbulence modeling.
10. Apply wake deficit as well as other site-specific loss factor estimates to the gross capacity factor data, yielding the expected (P50) net capacity factor.
11. Perform uncertainty analysis using the 3TIER Services' Energy Risk Framework.
12. Calculate probability of exceedance levels for the net capacity factor data using the results of the uncertainty analysis.

The following sections provide detail regarding the process outlined above as applied to the Busch Ranch II wind project.

3 OBSERVATIONAL DATA

Black Hills Corp. provided observational data from the following towers at the proposed Busch Ranch II site:

- Tower M0571
- Tower M4666

The location of each tower and the proposed turbine locations are shown in Wind Speed Maps, and a summary of each tower is presented in Table 3. Vaisala did not perform a site visit of the Busch Ranch II wind project. Quality control of the observed data for each tower are described in detail within the following sections.

	M0571	**M4666**
Latitude	37.75192°	37.82153°
Longitude	-104.45762°	-104.51877°
Time Series Start	2008-Nov-07	2013-Apr-19
Time Series End	2014-Jan-14	2014-Apr-28
Observed 10 m Wind Speed	5.82	5.46
Observed 32 m Wind Speed	6.82	6.35
Observed 50 m Wind Speed	7.38	6.72
Observed 59 m Wind Speed	–	6.73
Observed 60 m Wind Speed	7.52	–
Average Shear	0.15	0.10
Hub Height 80 m Wind Speed	7.85	6.95
Long-term 80 m Wind Speed	7.52	6.76
Long-term 80 m Adjustment Factor	95.9 %	97.3 %
Mean Turbulence Intensity (TI) 80 m	8.1 %	9.4 %
Characteristic TI 80 m	11.1 %	12.3 %

Table 3: On-site met tower summary. Hub height wind speeds are extrapolated unless there is a sensor at the hub height. Wind speed values shown above are in units of m/s. Mean and characteristic turbulence intensity are at 15 m/s.

3.1 Tower M0571

The M0571 Tower is located at $37.75192^\circ\,N$, $104.45762^\circ\,W$. The location of the tower and the turbine locations are shown in Wind Speed Maps. The tower is located near the southwestern edge of the project area. The tower has instrumentation up to $59.9\,m$, with anemometers at four heights and wind vanes at two heights. A summary of instruments installed on the tower is shown in Table 4.

Instrument	Height (m)	Boom Orientation	Recovery Rate
Anemometer	59.9	314°	81.6 %
Anemometer	59.9	177°	82.5 %
Anemometer	50.0	315°	71.1 %
Anemometer	31.5	320°	81.9 %
Anemometer	31.5	181°	82.4 %
Anemometer	10.2	317°	75.4 %
Wind Vane	56.5	355°	90.3 %
Wind Vane	49.0	356°	90.3 %

Table 4: M0571 Tower instrumentation.

3.1.1 Quality Control

The observed data at the M0571 Tower were quality controlled to check for instrument malfunction and tower shadow. The data record provided extended from 7 November 2008 to 15 January 2014. Raw data were processed using calibrated transfer functions based on client provided commissioning documentation. Redundant tower anemometers exhibited intermittent periods of distortion due to dry friction whip from the start of the data record until replacement on 20 April 2013. Data from this period were included in the analysis because the omission of the data would lead to an inadequate data record length for a quality due diligence analysis. Higher measurement uncertainty was assigned during 3TIER Services' Energy Risk Framework to account for issues related to dry friction whip. There were no significant periods of sensor failure, with the majority of data removal due to tower shadowing. The selectively averaged $59.9\,m$ wind speed data recovery rate was 90.3%.

3.1.2 Shear Extrapolation

Observed anemometer data from M0571 were used for extrapolating top sensor level wind speed data to $80\,m$ hub height level. A 12-by-24 table, see Figure 2 below, was developed based on observed data from the anemometers at all of the available sensor levels. These shear exponent values were then applied to the observed data using the power law extrapolation method to calculate wind speed values at $80\,m$.

Hour of Day (Local)	Jan	Feb	Mar	Apr	May	Jun	Jly	Aug	Sep	Oct	Nov	Dec	Avg
0	0.22	0.20	0.19	0.18	0.22	0.21	0.22	0.23	0.22	0.22	0.21	0.21	0.21
1	0.22	0.19	0.19	0.17	0.21	0.20	0.22	0.22	0.23	0.21	0.21	0.21	0.21
2	0.22	0.18	0.19	0.17	0.21	0.20	0.22	0.22	0.23	0.21	0.21	0.20	0.21
3	0.22	0.18	0.19	0.18	0.21	0.20	0.22	0.22	0.23	0.21	0.21	0.20	0.21
4	0.22	0.18	0.19	0.18	0.21	0.20	0.21	0.22	0.24	0.22	0.21	0.19	0.21
5	0.22	0.18	0.19	0.17	0.18	0.18	0.19	0.21	0.23	0.22	0.22	0.20	0.20
6	0.22	0.18	0.18	0.14	0.12	0.14	0.14	0.17	0.20	0.20	0.21	0.20	0.18
7	0.21	0.15	0.13	0.09	0.07	0.08	0.08	0.11	0.14	0.16	0.19	0.19	0.13
8	0.18	0.12	0.09	0.06	0.05	0.05	0.04	0.06	0.09	0.11	0.14	0.17	0.09
9	0.13	0.08	0.05	0.04	0.04	0.04	0.03	0.04	0.06	0.07	0.09	0.13	0.07
10	0.09	0.07	0.04	0.04	0.04	0.04	0.03	0.04	0.06	0.06	0.07	0.10	0.06
11	0.07	0.06	0.04	0.04	0.05	0.04	0.03	0.04	0.06	0.06	0.06	0.08	0.05
12	0.07	0.06	0.04	0.04	0.05	0.05	0.04	0.04	0.06	0.06	0.06	0.07	0.05
13	0.07	0.06	0.04	0.04	0.05	0.05	0.04	0.05	0.06	0.06	0.06	0.07	0.05
14	0.07	0.06	0.04	0.05	0.05	0.06	0.05	0.05	0.06	0.06	0.08	0.09	0.06
15	0.10	0.07	0.05	0.05	0.06	0.06	0.06	0.06	0.07	0.08	0.10	0.11	0.07
16	0.15	0.10	0.08	0.07	0.07	0.07	0.07	0.08	0.09	0.12	0.15	0.15	0.10
17	0.19	0.14	0.12	0.10	0.10	0.09	0.10	0.12	0.14	0.16	0.19	0.18	0.14
18	0.21	0.18	0.17	0.13	0.15	0.14	0.14	0.18	0.20	0.20	0.21	0.20	0.18
19	0.21	0.19	0.20	0.16	0.19	0.19	0.18	0.22	0.24	0.21	0.22	0.21	0.20
20	0.21	0.19	0.20	0.18	0.22	0.22	0.20	0.24	0.24	0.21	0.21	0.21	0.21
21	0.21	0.19	0.20	0.18	0.22	0.23	0.21	0.24	0.24	0.21	0.21	0.20	0.21
22	0.22	0.19	0.21	0.18	0.22	0.22	0.21	0.24	0.23	0.22	0.21	0.21	0.21
23	0.22	0.19	0.20	0.18	0.22	0.21	0.21	0.24	0.23	0.22	0.21	0.21	0.21
Avg	0.17	0.14	0.13	0.12	0.13	0.13	0.13	0.15	0.16	0.16	0.16	0.17	0.15

Figure 2: Shear exponent values for the M0571 Tower.

3.2 Tower M4666

The M4666 Tower is located at $37.82153^\circ\,N$, $104.51877^\circ\,W$. The location of the tower and the turbine locations are shown in Wind Speed Maps. The tower is located approximately $7\,km$ northwest of the project area. The tower has instrumentation up to $59\,m$, with anemometers at four heights and wind vanes at two heights. A summary of instruments installed on the tower is shown in Table 5.

Instrument	Height (m)	Boom Orientation	Recovery Rate
Anemometer	58.5	315°	88.5 %
Anemometer	58.5	180°	87.1 %
Anemometer	50.0	315°	88.7 %
Anemometer	31.7	315°	88.6 %
Anemometer	31.7	180°	87.2 %
Anemometer	9.8	315°	88.7 %
Wind Vane	56.5	1°	94.6 %
Wind Vane	48.0	1°	94.6 %

Table 5: M4666 Tower instrumentation.

3.2.1 Quality Control

The observed data at the M4666 Tower were quality controlled to check for instrument malfunction and tower shadow. The data provided extended from 19 April 2013 to 28 April 2014. Raw data were processed using calibrated transfer functions based on client provided commissioning documentation. There were no significant periods of sensor failure, with the majority of data removal due to tower shadowing and icing. The selectively averaged $58.5\,m$ wind speed data recovery rate was 94.6%.

3.2.2 Shear Extrapolation

Observed anemometer data from M4666 were used for extrapolating top sensor level wind speed data to $80\,m$ hub height level. A 12-by-24 table, see Figure 3 below, was developed based on observed data from the anemometers at all of the available sensor levels. These shear exponent values were then applied to the observed data using the power law extrapolation method to calculate wind speed values at $80\,m$.

Hour of Day (Local)	Jan	Feb	Mar	Apr	May	Jun	Jly	Aug	Sep	Oct	Nov	Dec	Avg
0	0.13	0.15	0.16	0.14	0.15	0.15	0.14	0.15	0.17	0.14	0.09	0.11	0.14
1	0.13	0.17	0.15	0.13	0.13	0.14	0.14	0.14	0.17	0.13	0.09	0.13	0.14
2	0.13	0.18	0.14	0.10	0.12	0.14	0.11	0.13	0.16	0.13	0.12	0.14	0.13
3	0.12	0.19	0.15	0.08	0.13	0.13	0.07	0.12	0.16	0.14	0.14	0.15	0.13
4	0.12	0.18	0.16	0.09	0.13	0.13	0.02	0.10	0.15	0.13	0.15	0.14	0.12
5	0.12	0.17	0.16	0.10	0.12	0.12	0.01	0.06	0.14	0.12	0.15	0.12	0.11
6	0.12	0.16	0.14	0.09	0.08	0.08	0.01	0.02	0.13	0.11	0.14	0.11	0.10
7	0.11	0.14	0.12	0.08	0.05	0.04	0.01	0.01	0.10	0.10	0.13	0.11	0.08
8	0.10	0.11	0.09	0.06	0.03	0.02	0.01	0.01	0.07	0.08	0.11	0.12	0.07
9	0.07	0.07	0.06	0.05	0.02	0.02	0.01	0.01	0.05	0.06	0.09	0.10	0.05
10	0.06	0.05	0.06	0.05	0.02	0.03	0.01	0.01	0.05	0.05	0.07	0.07	0.04
11	0.05	0.04	0.06	0.05	0.02	0.03	0.01	0.01	0.05	0.05	0.07	0.06	0.04
12	0.04	0.04	0.06	0.05	0.02	0.03	0.01	0.01	0.05	0.05	0.07	0.05	0.04
13	0.05	0.04	0.06	0.05	0.02	0.04	0.02	0.01	0.05	0.05	0.07	0.05	0.04
14	0.06	0.05	0.06	0.05	0.03	0.04	0.02	0.02	0.05	0.05	0.07	0.07	0.05
15	0.08	0.06	0.07	0.06	0.03	0.05	0.03	0.03	0.06	0.06	0.09	0.09	0.06
16	0.10	0.08	0.08	0.07	0.05	0.05	0.03	0.05	0.08	0.08	0.11	0.13	0.08
17	0.13	0.11	0.11	0.09	0.07	0.07	0.05	0.08	0.12	0.11	0.13	0.16	0.10
18	0.14	0.14	0.14	0.11	0.10	0.11	0.08	0.12	0.15	0.13	0.14	0.18	0.13
19	0.14	0.16	0.16	0.14	0.14	0.14	0.12	0.15	0.18	0.13	0.14	0.17	0.15
20	0.15	0.17	0.17	0.16	0.16	0.16	0.14	0.16	0.18	0.14	0.14	0.15	0.16
21	0.15	0.17	0.17	0.17	0.17	0.17	0.15	0.16	0.18	0.14	0.13	0.14	0.16
22	0.15	0.17	0.17	0.16	0.17	0.17	0.15	0.15	0.18	0.14	0.12	0.12	0.15
23	0.14	0.16	0.17	0.16	0.17	0.16	0.15	0.15	0.18	0.14	0.10	0.11	0.15
Avg	0.11	0.12	0.12	0.09	0.09	0.09	0.06	0.08	0.12	0.10	0.11	0.12	0.10

Figure 3: Shear exponent values for the M4666 Tower.

4 LONG-TERM REFERENCE

In order to put the short-term observational data into the climatological context, Vaisala performed a review of several long term climate data sources. Vaisala primarily relies on global reanalysis data sets for understanding long-term climate variability. The reanalysis data sets are derived from thousands of global observations, including ground based weather stations, ocean surface buoys, satellites, and weather balloons.

Vaisala analyzed three major reanalysis data sets that are each produced independently by various institutions. Each data set offers an independent view of the climate, and Vaisala will consider each in determining the most appropriate data set. The statistics relating each met tower to the reanalysis data sets reviewed are shown below in Table 6, including the daily-mean explained variance, long-term climate adjustment, and considered start year statistics. Figure 4 shows the annual-mean wind speed values extracted from each reanalysis data set across the period of record. Each time series shown in Figure 4 has been MOS-corrected using the observed data at Tower M0571.

Tower	Data Set	Explained Variance (R^2)	Climate Adjustment	Start Year
M0571	ECMWF ERA-I	82.6%	96.1%	1980
M0571	MERRA2	81.0%	96.5%	1980
M0571	NCEP/NCAR	73.3%	96.8%	1980
M4666	ECMWF ERA-I	75.3%	96.3%	1980
M4666	MERRA2	74.0%	96.3%	1980
M4666	NCEP/NCAR	65.4%	98.7%	1985

Table 6: Daily explained variance and long-term climate adjustment values for the considered reanalysis data sets.

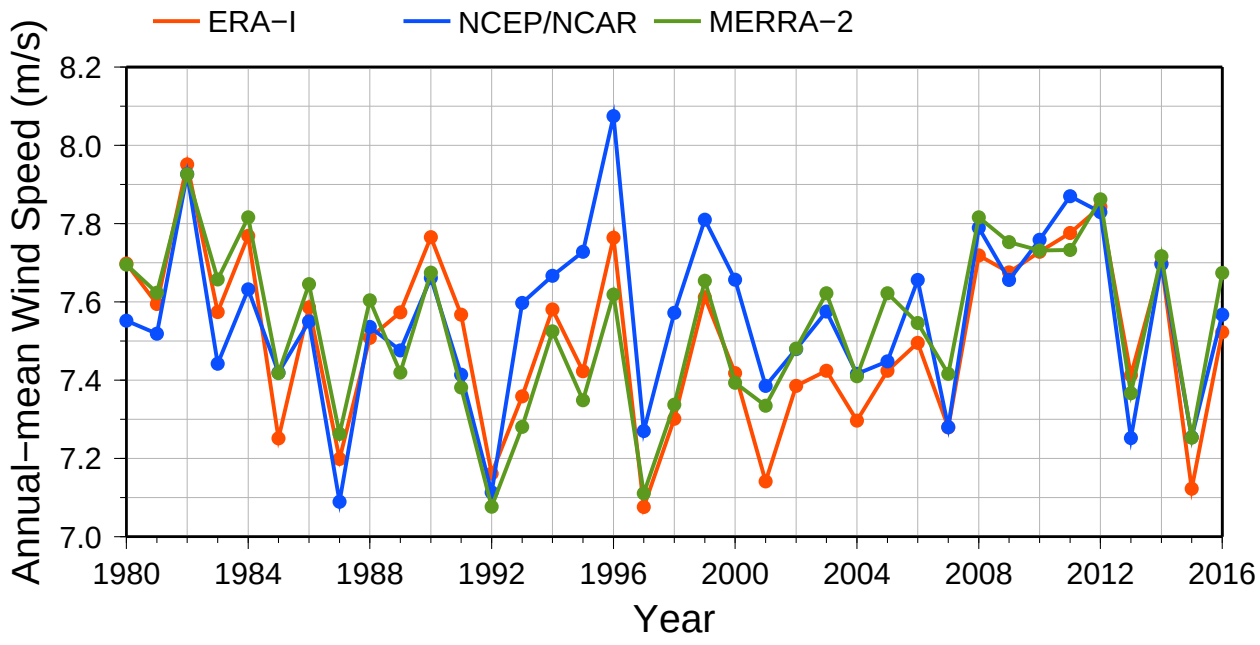

Figure 4: Time series of annual-mean wind speed data for each considered reanalysis data set.

5 GROSS GENERATION

5.1 Wind Resource Variability

This section provides an analysis of the MOS-corrected model-simulated project-average wind resource at hub height. To generate the project-average wind resource time series, MOS-corrected wind resource time series data are extracted at each turbine location at the appropriate height ($80\,m$) and then averaged across all 27 turbine locations.

Based on the results of the 3TIER Services' Energy Risk Framework, the last 37 years (January, 1980 – September, 2017) of data have been utilized for estimating the expected future generation at Busch Ranch II. The long-term mean project-average wind speed at hub height is $\mathbf{7.62\,m/s}$. A map of the 37-year average wind speed values at $80\,m$ is displayed in Figure 1. Gross wind speed values and average density values at each of the 27 turbine locations are provided in Appendix Turbine Means. The project-average density value at hub height is $0.990\,kg/m^3$.

The distribution of hourly MOS-corrected project-average wind speed values is shown below in Figure 5. The distribution is based on the 37 years of modeled data. The annual wind rose is shown in Figure 6. Figure 7 displays the time series of gross project-average annual-mean wind speed values. Tables 8 and 9 shown on the following pages contain tabular-formatted month-hour and monthly-mean wind speed values, respectively. Table 8, often referred to as a '12x24' table, shows the average diurnal profile of wind speed values for each month of the calendar year. Table 9 shows the monthly-mean wind speed value for each month of the 37-year analysis period. Annual-mean wind speed values are also displayed in the right-most column of data in Table 9. Additional analysis of the long-term variability is available in Project-average Long-term Wind Resource Assessment.

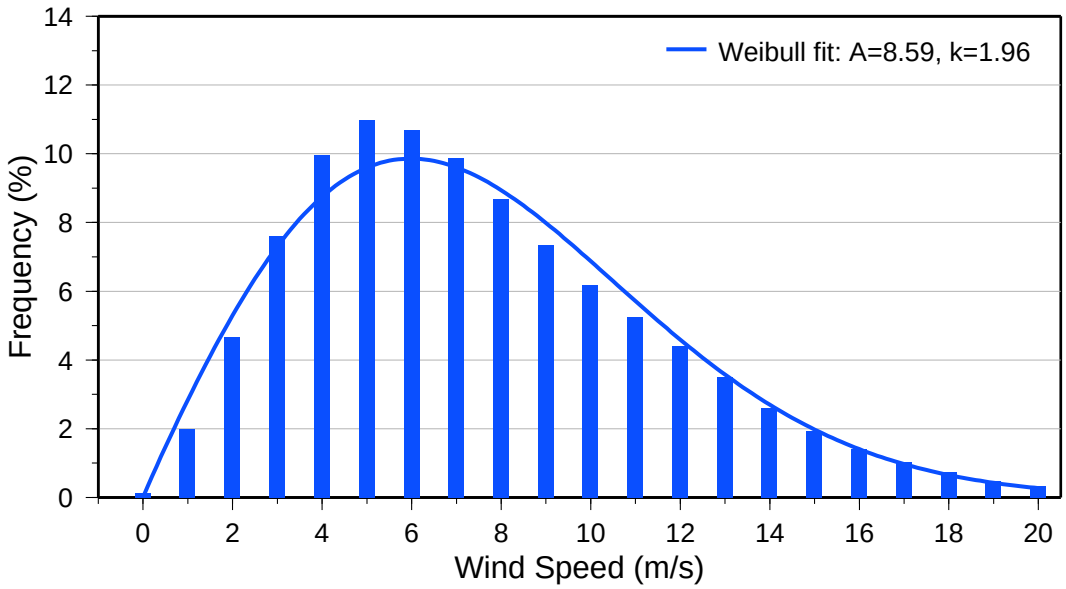

Figure 5: Hourly distribution of simulated project-average wind speed using $1\,m/s$ bins. ($0\,m/s$ bin contains only values ≤ 0.5.) Weibull distribution is also shown with the scale (A) and shape (k) parameters listed in the legend.

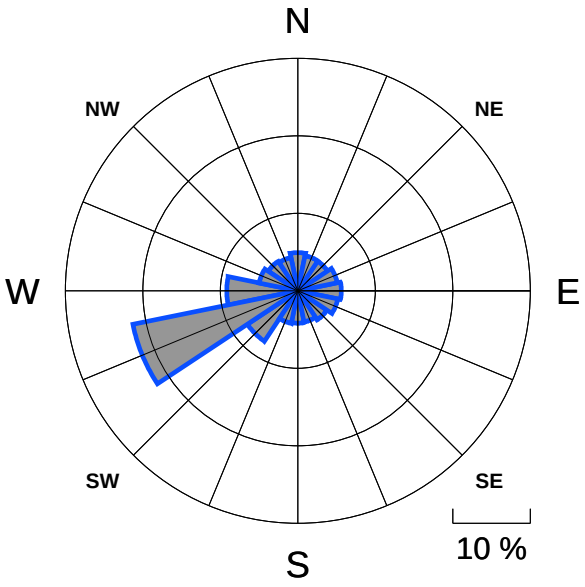

Figure 6: Annual wind rose of the hourly-mean project-average wind direction time series. Directional bins are 22.5° wide, and the radial contour interval is 10%.

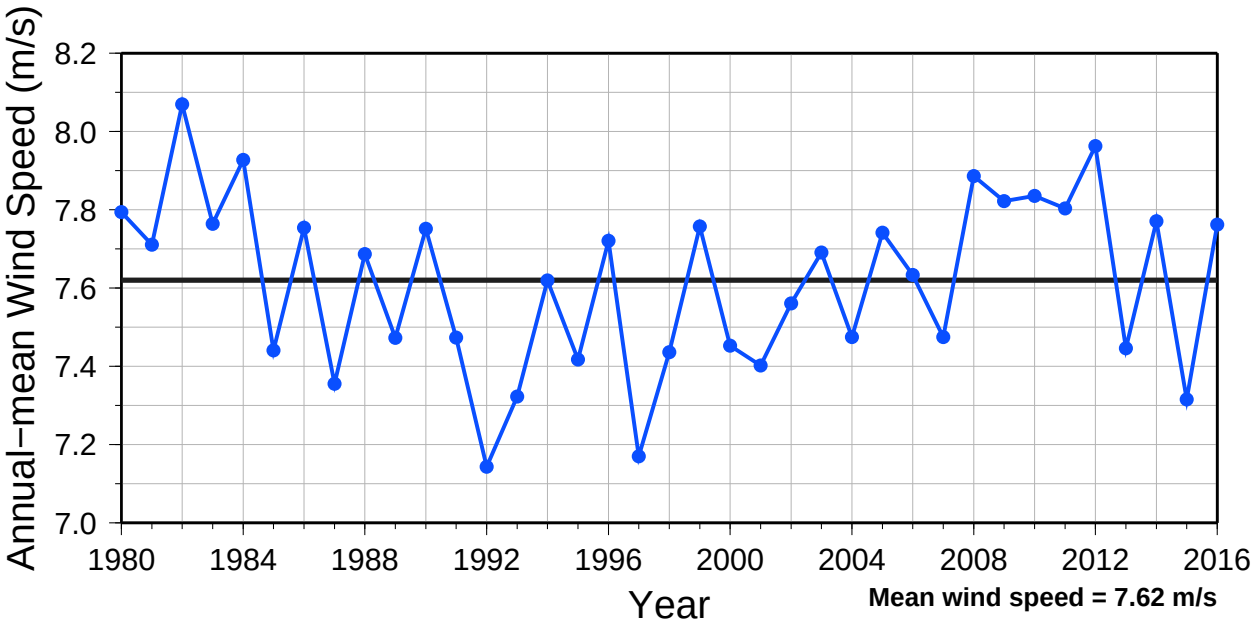

Figure 7: Time series of annual-mean project-average wind speed. Black line denotes the long-term mean.

Hour of Day (Local)	Jan	Feb	Mar	Apr	May	Jun	Jly	Aug	Sep	Oct	Nov	Dec	Avg
0	8.48	7.90	8.31	8.66	8.21	8.81	8.12	7.94	8.13	7.66	8.41	8.29	8.24
1	8.48	8.05	8.07	8.27	7.70	8.27	7.83	7.67	7.49	7.62	8.58	8.57	8.05
2	8.57	8.17	8.05	8.26	7.62	7.89	7.57	7.40	7.30	7.52	8.54	8.84	7.98
3	8.50	7.96	7.85	7.99	7.58	7.64	7.18	7.32	7.22	7.54	8.55	8.78	7.84
4	8.50	7.82	7.88	7.83	7.43	7.40	6.69	7.18	7.20	7.60	8.81	8.58	7.74
5	8.86	8.07	8.11	7.71	7.08	7.05	6.38	6.85	7.12	7.75	8.80	8.61	7.69
6	8.57	7.92	7.94	7.85	6.86	6.44	6.04	6.61	6.95	7.62	8.44	8.30	7.45
7	8.25	7.69	7.61	7.66	6.36	5.94	5.33	5.95	6.56	7.49	8.32	8.11	7.10
8	8.22	7.78	7.37	7.07	5.81	5.58	4.78	5.06	5.83	7.09	8.09	8.02	6.71
9	7.91	7.60	7.13	7.08	5.77	5.52	4.72	4.79	5.52	6.69	7.62	7.86	6.50
10	7.50	7.63	7.37	7.20	5.97	5.60	4.74	4.67	5.52	6.58	7.47	7.69	6.48
11	7.41	7.53	7.53	7.32	6.37	5.96	4.69	4.59	5.62	6.54	7.42	7.57	6.53
12	7.49	7.41	7.67	7.58	6.86	6.46	4.83	4.68	5.67	6.33	7.31	7.75	6.66
13	7.40	7.45	7.75	7.81	7.10	6.46	5.06	4.93	5.93	6.48	7.61	7.83	6.81
14	7.50	7.51	8.07	8.11	7.64	7.12	5.52	5.51	6.21	6.68	7.60	7.84	7.10
15	7.37	7.37	8.25	8.42	8.28	8.04	6.02	5.85	6.36	6.92	7.69	7.61	7.35
16	7.28	7.49	8.70	8.24	8.36	8.56	6.70	6.30	6.68	7.49	7.93	7.65	7.62
17	7.67	7.96	8.69	8.46	8.68	9.21	7.70	7.16	7.15	7.91	8.27	7.93	8.06
18	8.27	8.11	8.69	8.77	9.07	9.37	7.97	7.66	7.91	8.23	8.68	8.51	8.44
19	8.31	8.08	8.59	9.07	9.05	9.68	7.91	7.73	8.42	8.32	8.90	8.68	8.56
20	8.36	8.38	8.67	9.05	9.12	9.54	8.55	8.09	8.29	8.30	8.99	8.63	8.66
21	8.46	8.14	8.63	9.06	8.74	9.20	8.63	7.95	8.53	8.10	8.80	8.64	8.57
22	8.36	7.92	8.43	8.94	8.66	9.04	8.10	7.90	8.36	7.80	8.33	8.49	8.36
23	8.41	8.04	8.34	8.72	8.62	9.13	8.12	8.02	8.33	7.68	8.24	8.28	8.33
Avg	8.09	7.83	8.07	8.13	7.62	7.66	6.63	6.58	7.01	7.41	8.23	8.21	7.62

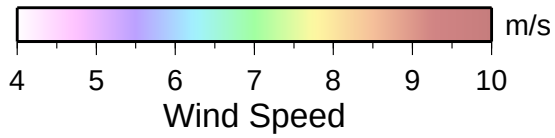

Figure 8: Hourly-mean values of simulated project-average wind speed. Vertical axis is local time.

Year	Jan	Feb	Mar	Apr	May	Jun	Jly	Aug	Sep	Oct	Nov	Dec	Avg
1980	8.43	7.92	9.09	7.31	7.96	8.25	6.78	8.10	7.43	7.09	7.59	7.55	7.79
1981	6.70	7.86	8.24	8.30	8.17	8.09	6.73	6.33	6.70	8.38	8.25	8.81	7.71
1982	10.63	7.64	8.99	8.83	7.06	7.23	7.19	6.36	7.32	7.87	8.45	9.19	8.07
1983	7.50	7.91	8.25	7.90	7.73	7.63	7.60	6.60	7.76	7.39	9.11	7.84	7.76
1984	6.94	8.39	7.68	8.83	7.63	8.04	6.99	6.32	7.36	8.08	9.86	9.11	7.93
1985	6.49	7.46	9.62	7.76	7.28	7.19	6.32	7.11	7.71	7.55	8.16	6.67	7.44
1986	8.45	9.40	7.56	8.84	7.70	7.07	7.51	6.59	8.23	7.17	8.86	5.91	7.75
1987	8.42	7.21	8.05	7.35	7.37	7.00	8.24	6.69	6.13	6.17	7.56	8.01	7.36
1988	8.42	7.23	7.94	7.68	8.72	7.42	6.58	7.29	7.51	6.30	8.90	8.24	7.69
1989	9.11	6.36	8.99	7.33	7.70	6.84	6.80	6.96	7.11	7.25	8.46	6.65	7.47
1990	9.63	8.03	6.97	7.33	8.45	8.66	6.33	6.84	6.57	7.77	8.90	7.56	7.75
1991	6.85	6.98	9.65	7.80	8.65	8.05	6.42	6.18	6.96	7.18	7.71	7.22	7.47
1992	7.36	7.41	7.14	7.18	6.71	6.78	6.65	6.22	7.48	6.91	6.80	9.09	7.14
1993	7.43	7.41	6.53	7.66	6.89	8.32	7.41	6.75	6.50	6.36	8.20	8.47	7.32
1994	7.64	9.05	7.67	8.12	7.25	7.67	6.32	6.43	6.87	7.26	9.63	7.71	7.62
1995	7.69	7.26	8.27	8.09	7.67	7.62	6.60	6.58	6.36	7.55	8.31	7.02	7.42
1996	8.95	7.82	7.36	8.59	7.82	6.69	5.97	6.13	6.91	8.07	7.61	10.72	7.72
1997	8.60	6.89	7.55	7.27	6.37	7.07	7.07	5.86	6.24	8.09	7.21	7.76	7.17
1998	8.28	6.96	7.25	7.40	8.20	8.63	6.26	5.95	7.00	7.49	8.51	7.31	7.44
1999	8.69	9.31	8.18	8.80	8.06	7.80	7.15	6.78	6.33	6.88	7.28	7.95	7.76
2000	7.92	8.31	7.30	7.96	8.44	7.84	6.50	6.53	7.27	7.14	6.94	7.34	7.45
2001	6.99	7.60	6.57	9.12	6.84	7.83	7.13	6.70	6.44	7.95	7.36	8.34	7.40
2002	7.96	7.86	8.32	8.69	7.70	8.01	5.87	6.89	7.35	6.62	7.34	8.19	7.56
2003	6.93	6.83	8.56	9.74	7.49	6.97	6.94	6.59	6.75	7.34	8.82	9.29	7.69
2004	7.86	7.14	7.07	7.60	8.22	7.12	6.02	6.65	7.60	8.47	7.20	8.70	7.47
2005	8.11	7.18	7.97	8.18	7.45	8.21	6.79	6.14	7.74	7.20	9.36	8.60	7.74
2006	10.37	7.36	9.11	9.28	6.53	7.35	5.88	5.95	6.35	7.34	8.07	8.02	7.63
2007	7.58	8.46	7.22	7.62	6.92	7.43	5.81	6.68	7.66	8.08	7.32	9.01	7.47
2008	9.93	8.37	8.38	8.11	8.39	7.35	6.49	6.65	6.63	7.22	7.45	9.62	7.89
2009	8.61	9.26	9.38	8.80	7.14	7.84	6.17	6.75	6.64	7.91	7.36	8.12	7.82
2010	7.31	5.86	7.79	9.47	8.63	8.10	6.96	7.22	7.59	7.53	8.95	8.52	7.84
2011	7.31	8.89	8.34	9.20	8.30	8.51	6.76	6.55	6.18	7.10	9.73	6.94	7.80
2012	8.68	8.57	9.43	7.82	7.92	8.93	6.25	6.63	5.79	7.34	8.69	9.53	7.96
2013	7.54	7.34	7.47	7.10	7.27	7.98	6.34	6.32	8.05	7.78	8.00	8.19	7.45
2014	8.58	8.63	8.81	8.32	7.51	8.61	6.20	6.70	6.88	6.83	9.24	7.11	7.77
2015	6.95	7.08	6.53	8.11	7.03	6.89	6.39	6.49	6.67	7.13	8.85	9.68	7.32
2016	7.61	7.85	8.73	7.36	7.47	6.80	6.94	6.29	7.46	8.49	8.30	9.82	7.76
2017	8.94	10.48	8.74	8.06	7.03	7.35	5.73	6.07	6.88				––
Avg	8.09	7.83	8.07	8.13	7.62	7.66	6.63	6.58	7.01	7.41	8.23	8.21	**7.62**

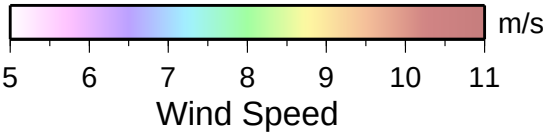

Figure 9: Monthly-mean values of simulated project-average wind speed.

5.2 Gross Generation Variability

Following WRF/TVM modeling and MOS correction, 37 years of hourly wind speed, wind direction, temperature, and pressure time series data were extracted for each proposed turbine location at hub height. The simulated temperature and pressure data are used to normalize simulated wind speed data to the power curve's reference density with the equation

$$V_{norm} = V\left((\frac{\rho}{\rho_0})^{1/3}\right)$$

where V_{norm} is normalized hourly wind speed at hub height, V is simulated hourly wind speed at hub height, ρ is density calculated from simulated hourly temperature and pressure at hub height using the Ideal Gas Law, and ρ_0 is the reference density of the power curve.

The turbine power curve is then applied to the normalized wind speed data using piecewise linear interpolation between the power curve points supplied by the manufacturer. Turbine specific cut-in and cut-out limits on wind speed are also applied. This allows the manufacturer's power curve to be applied to the wind speed time series to calculate gross expected energy for all proposed turbine locations for each hour over the past 37 years.

Computing the nameplate capacity factor at each turbine and then averaging across all 27 turbines yields the project-wide gross capacity factor value. A turbine-by-turbine gross energy estimate is calculated by multiplying the nameplate capacity factor at each turbine by the turbine-specific nameplate capacity, and by 8766 hours. Summing these across all 27 turbines yields the project-average gross energy estimate.

Based on the results of the 3TIER Services' Energy Risk Framework, the last 37 years (January, 1980 – September, 2017) of data have been utilized for estimating the expected future generation at Busch Ranch II. The 37-year long-term mean gross energy estimate at the proposed Busch Ranch II project is **248.2 GWh**. Figure 10 below shows the time series of gross project-average annual-mean energy values. Gross energy values at each of the 27 turbine locations are provided in Appendix Turbine Means. Additional analysis of the long-term variability is available in Project-average Long-term Gross Power Capacity Assessment.

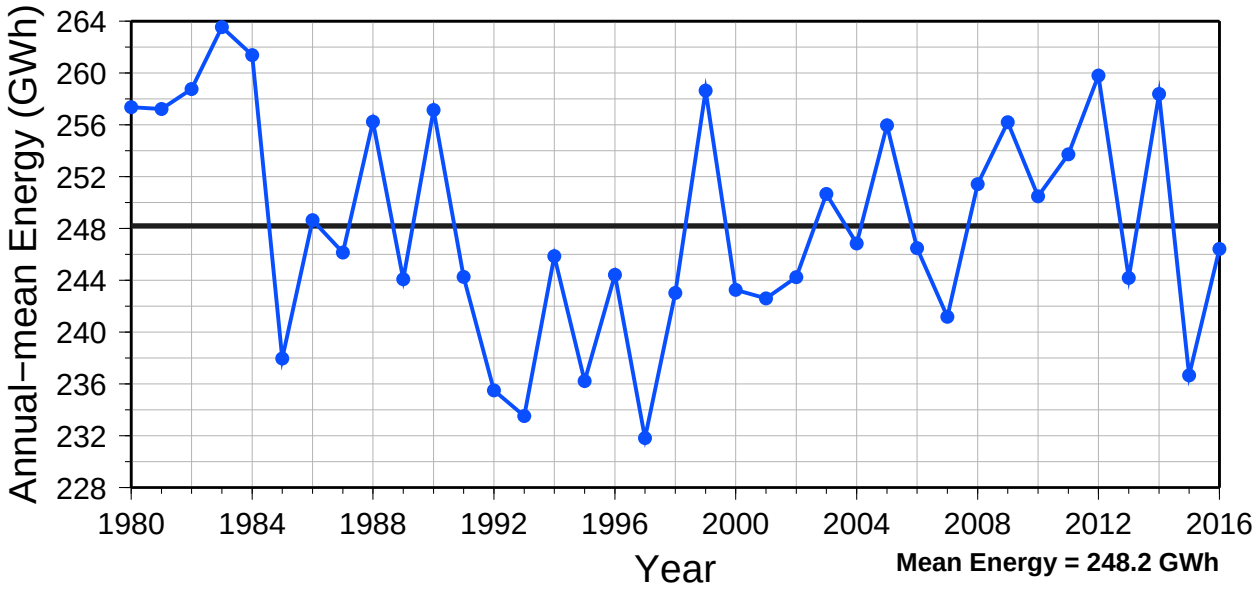

Figure 10: Time series of annual-mean project-average gross energy. Black line denotes the long-term mean.

5.3 Power Curves

It is expected that Vestas V120-2.2MW wind turbines at a hub height of $80\,m$ will be erected at the site. The Vestas V120-2.2MW power curve is shown in Figure 11 and Table 7. The reference density for each power curve is shown in the caption of each respective Figure and Table below.

5.3.1 Vestas V120-2.2MW

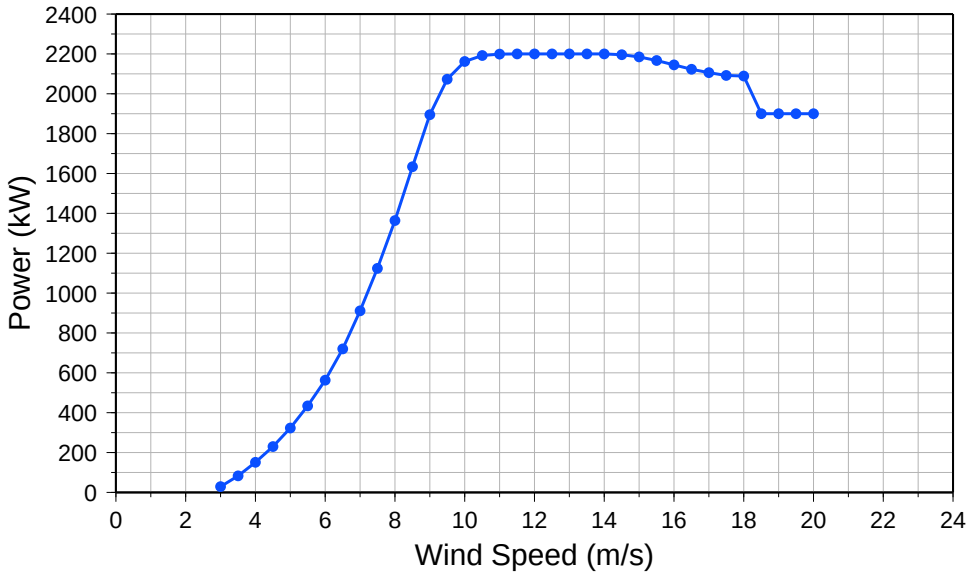

Figure 11: Power curve values for a Vestas V120-2.2MW turbine with a reference density of $1.0\,kg/m^3$.

Wind Speed ($\frac{m}{s}$)	Power (kW)	Wind Speed ($\frac{m}{s}$)	Power (kW)	Wind Speed ($\frac{m}{s}$)	Power (kW)
3.0	29.0	9.0	1895.0	15.0	2185.0
3.5	83.0	9.5	2073.0	15.5	2167.0
4.0	151.0	10.0	2162.0	16.0	2145.0
4.5	230.0	10.5	2192.0	16.5	2123.0
5.0	323.0	11.0	2199.0	17.0	2106.0
5.5	434.0	11.5	2200.0	17.5	2092.0
6.0	563.0	12.0	2200.0	18.0	2089.0
6.5	720.0	12.5	2200.0	18.5	1900.0
7.0	911.0	13.0	2200.0	19.0	1900.0
7.5	1124.0	13.5	2200.0	19.5	1900.0
8.0	1364.0	14.0	2200.0	20.0	1900.0
8.5	1634.0	14.5	2196.0		

Table 7: Power curve values for a Vestas V120-2.2MW turbine with a reference density of $1.0\,kg/m^3$.

6 LOSS FACTORS

To convert from expected gross generation to expected net generation, the following loss factor categories are considered: availability, curtailment, wake deficit, electrical efficiency, turbine efficiency, and environmental. Details for each loss factor are discussed below.

6.1 Availability

Availability losses include losses driven by turbine and transmission shutdowns caused by planned and unexpected faults.

6.1.1 Turbine Availability

Vaisala has observed that turbine availability at newly constructed wind farms achieve 96.0% or higher availability when averaged over an entire calendar year. Therefore, the turbine availability loss factor is estimated to be **96.0%**.

6.1.2 Grid Availability

The ability of the electric grid to receive and transmit wind power to load centers varies by year, season and location. Issues with grid availability are very dynamic and may actually be worsened as wind penetration levels increase. Grid availability is expected to be high across the United States. Vaisala has assumed a regional grid availability loss factor of **99.5%** for the Busch Ranch II wind energy project.

6.1.3 Balance of Plant Availability

The balance of the plant availability is based on a total of 24 hours of outage time per year per turbine for transformer inspections and maintenance. Therefore, the balance of plant availability loss factor is estimated to be **99.7%**.

6.2 Curtailment

Curtailment losses are based on forced wind plant shutdowns resulting from environmental conditions that can adversely effect the turbines. These curtailments include wind driven sector management, high wind hysteresis, extreme icing events, and extreme temperatures.

6.2.1 Sector Management

Standard minimum turbine spacing of three rotor diameters perpendicular to the dominant wind direction and five rotor diameters parallel to the dominant wind direction was tested against the layout. Turbine spacing perpendicular to the prevailing wind direction is less than three rotor diameters for four turbines. These spacing violations are considered trivial. Therefore the curtailment loss factor associated with sector management is estimated to be **100.0%**.

6.2.2 High Wind Hysteresis

High wind speed hysteresis loss potentially occurs after a turbine has shut down because of a high wind speed cut-out event. Before the turbine can re-start, the wind speed must slow down to the hysteresis cut-in wind speed. If wind speed values reduce to below the cut-out wind speed, but remain above the hysteresis cut-in wind speed, then hysteresis loss will occur. Based on 37 years of modeled hourly wind speed data, cut-out wind speed events are rare, and the hysteresis loss factor is expected to be negligible. A high wind speed hysteresis loss factor of **98.8%** is applied.

6.2.3 Extreme Temperature

The Vestas V120-2.2MW turbines planned for the site allow for normal operation between $-20°C$ and $30°C$. A de-rating scheme is applied on the Vestas V120-2.2MW turbine for temperatures between $30°C$ and $45°C$. The Vestas V120-2.2MW de-rating scheme limits the rated power, which means the de-rating scheme only reduces power output when wind speed values are high. Based on 37 years of MOS-corrected temperature data, the extreme temperature loss factor for the project is estimated to be **100.0%**.

6.2.4 Icing Shutdown

Observational data were inspected for significant icing events that may lead an operator to shutdown the wind farm. The observational data suggest a curtailment associated with icing events of **99.0%**.

6.3 Wake Deficit

The 3TIER Services' time-varying wake model is used to determine the expected wake deficit for the turbine layout. The magnitude of the losses at any given time is a combination of the gross wind field and ambient turbulence intensity across the park, the turbine layout, and physical characteristics of the installed turbines. Vaisala analyzes wakes using a proprietary time-varying wake model that analyzes the wake at every individual time within the simulated record, rather than relying on bulk statistical descriptions of the wind field. Wakes for each turbine are computed individually and interact in a physically consistent way, eliminating the need for posterior models to combine wakes from multiple turbines or add in deep-array effects. The single turbine wake model is based on concepts originally presented by Larsen et al. (1996). [7] Vaisala's internal research has shown that the low bias associated with other Larsen-derived wake models [8] is a result of poorly handled wake addition rather than the underlying model. The full system has been calibrated using production numbers from permanently installed turbines under a wide range of environmental conditions, including a broad span of turbulence intensities and stability regimes. The outputs from the model are wake-induced velocity deficit and turbulence intensity at all turbine locations, and can include additional reference locations.

6.3.1 Internal Wakes

Internal wakes represent wakes caused by turbines within the project. The effect of wake deficit on energy output for the layout leads to an internal wake loss factor of **96.4%**.

6.3.2 External Wakes

External wakes represent additional wakes caused by turbines from surrounding wind farms. An additional 16 Vestas V100-1.8MW turbines and 34 GE 1.79-100 turbines have been included as external turbines in the wake model. The location of all the external turbines are shown in Wind Speed Maps. The effect of wake deficit on energy output due to external turbines is **98.8%**.

6.3.3 Future Wakes

Future wakes represent wakes caused by turbines that will be built in the future, not related to this project. Vaisala performed a review of the potential impact of future wakes due to nearby developments using the FAA's Obstruction Evaluation / Airport Airspace Analysis (OEAAA) website [9]. At this time Vaisala is unaware of any planned wind farms in the region, therefore this loss factor is **100%**.

6.3.4 Total Wakes

The total wake loss factor, including the project (i.e. internal) turbines, and external turbines, is **95.3%**. Waked generation values for each individual turbine are shown in Appendix Turbine Means.

6.4 Electrical Efficiency

Electrical efficiency considers losses associated with the electrical systems connecting the turbines to the metering point. These systems include the on-site collection system, the substation power transformer, and the transmission line depending on the meter location. Vaisala assumes the wind farm will be metered on the high side of the substation power transformer. Given this assumption, the electrical system efficiency is expected to be **97.5%**.

6.4.1 Collection System Efficiency

The collection system efficiency covers the efficiency of all components from the turbines to the pooling substation, including the medium voltage transformer efficiency that steps up the turbine voltage to the collection system voltage. These losses are inherent in the electrical system efficiency loss factor.

6.4.2 Substation Power Transformer Efficiency

The substation power transformer converts the voltage of the collection system to the voltage of the high voltage transmission line. Vaisala assumes the plant will be metered at the high side of the substation transformer; therefore, substation power transformer losses are applicable.

6.4.3 High Voltage Transmission Line Efficiency

Transmission line efficiency is dependent on the cable type, voltage, load, and the distance from the pooling substation to the plant metering point. Vaisala assumes the plant will be metered at the high side of the substation transformer; therefore, high voltage transmission line losses are applicable.

6.4.4 Consumptive Power

Consumptive power considers the fact that a wind farm consumes electrical power when generation levels are very low. This is primarily due to power required to keep generators and transformers active and ready for operations. When the plant is operating, consumptive power is inherent to the turbine power curve and electrical efficiency assumptions. Vaisala assumes that consumptive power of the wind farm will be metered separately from the export power generated by the wind turbines, i.e. net metering is not applicable. Based on this assumption, consumptive power will not lead to a reduction in the export power; thus, a loss factor of **100.0%** is applied for consumptive power.

6.5 Turbine Efficiency

Turbine efficiency is based on the ability of the turbines to perform at a level relative to the manufacturer's suggested performance rating. This can be affected by many factors, including the manufacturer's warranted performance level, the turbulence, and inflow angle.

6.5.1 Turbine Performance

Based on Vaisala's experience with operating wind farms, a loss factor should be applied for turbine performance. This loss factor is related to turbines not performing at the manufacturer's rated power curve. It is suggested that a turbine performance loss factor of **98.0%** be applied to account for the risk that the turbines do not perform exactly at the manufacturer's rated power curve.

6.5.2 Turbulence Intensity

Research has linked turbine under performance to stable atmospheric conditions, which are often accompanied by low turbulence intensity and high vertical wind shear. In addition, periods of low or high turbulence intensity can affect the specified power curve by creating a statistical averaging effect. The statistical averaging effect is assessed by comparing the average of the instantaneous wind speeds using a theoretical zero turbulence power curve against the manufacturer's power curve at given turbulence level. Vaisala analyzes the potential for both of these effects using the measured turbulence intensity and has calculated a loss factor of **98.2%**.

6.5.3 Inflow Angle

Reduced efficiency associated with extreme inflow angles is expected to be negligible; therefore, an inflow angle loss factor of **100.0%** is applied.

6.6 Environmental

Potential environmental losses include turbine under-performance caused by turbine blade soiling and degradation, extreme weather conditions such as icing and thunderstorms, and changes to the surrounding environment such as tree growth.

6.6.1 Blade Soiling

In locations where the ground is dry and the soil is loose, turbine blades can build up substantial amounts of soil, leading to a power curve derating. Vaisala has analyzed projects in similar terrain and has calculated a standard loss factor for shrub-steppe conditions. A loss factor of **98.5%** is applied for blade soiling.

6.6.2 Blade Degradation

Blade degradation, unlike blade soiling, is permanent damage caused to the turbine blades by material in hitting the blades. This can include corrosive material, such as sodium chloride (sea salt), and larger diameter soil and dirt particles. Vaisala has analyzed projects in similar terrain and has calculated a standard loss factor for shrub-steppe conditions. A loss factor of **99.5%** is applied for blade degradation.

6.6.3 Soft Icing

Soft icing occurs when ice builds up on the turbine blades and affects the ability of the turbine to operate optimally. Soft icing is often found as shoulder events to hard ice in which loads are exceeded and turbine shutdown occurs. A loss factor of **99.5%** is applied for soft icing.

6.6.4 Other Environmental Losses

Additional environmental losses such as thunderstorms and tree growth have not been evaluated, but are expected to be negligible.

6.7 Aggregate Loss Factor

Table 8 below shows the individual loss factors for all considered categories and the aggregate loss factor. The product of all considered losses is **81.2%**. The expected gross P50 generation is $248.2\,GWh$; therefore, the net P50 generation is the product of 81.2% and $248.2\,GWh$, which equals $\mathbf{201.5\,GWh}$. Table 9 displays the monthly-mean net values as a percent of the expected annual-mean generation value (GWh).

Loss Factor	Percent Loss
Project Availability	
Turbine Availability	96.0 %
Balance Of Plant Availability	99.7 %
Grid Availability	99.5 %
Environmental Curtailment	
Sector Management	100.0 %
High Wind Hysteresis	98.8 %
Icing	99.0 %
Extreme Temperature	100.0 %
Wake Deficit	
Total Wakes	95.3 %
Electrical Efficiency	
Total Electrical Efficiency	97.5 %
Consumptive Power	100.0 %
Turbine Efficiency	
Turbine Performance	98.0 %
Turbulence Intensity	98.2 %
Inflow Angle	100.0 %
Environmental	
Blade Soiling	98.5 %
Blade Degradation	99.5 %
Soft Icing	99.5 %
Aggregate Loss Factor	**81.2 %**

Table 8: Summary of loss factors.

Month	GWh (%)
January	9.2 %
February	7.9 %
March	9.1 %
April	9.1 %
May	8.8 %
June	8.4 %
July	7.0 %
August	6.9 %
September	7.5 %
October	8.2 %
November	8.8 %
December	9.1 %

Table 9: Monthly-mean net values as a percent of the total annual-mean generation.

7 UNCERTAINTY ANALYSIS

To calculate uncertainty and estimates of probabilities of exceedance, Vaisala has utilized the 3TIER Services' Energy Risk Framework. This framework is based on theoretical propagation of error theory and models hundreds of sources of uncertainty and their relationships throughout the modeling process. Each source of uncertainty is treated in a separate model that interacts with the framework through overlying covariance models. The analysis considers the following sources of uncertainty: measurement, vertical extrapolation, MOS correction, climate variability, spatial modeling, and power modeling.

7.1 Uncertainty Methodology

7.1.1 Measurement Uncertainty

Measurement uncertainty captures the uncertainties related to the on-site measured data utilized in the energy assessment. It is a measure of the confidence that the recorded data, which are presumed to represent the truth, actually do represent the truth. Individual components of measurement uncertainty include the following: anemometer uncertainty, benefits of utilizing redundant sensors, measurement height uncertainty, and the statistical propagation of these uncertainties through the wind shear and extrapolation calculations to estimate hub height wind speed values. Uncertainty is separately estimated for each measurement sensor, and the sensor uncertainties are aggregated together to represent the total measurement uncertainty at hub height level for each met tower. Measurement uncertainty estimates at each met tower are considered to be independent when predicting measurement uncertainty at each turbine location.

7.1.2 Vertical Extrapolation Uncertainty

If on-site measurements are not directly recorded at hub height, an uncertainty exists that the true vertical wind speed profile may differ from the assumed power law profile. A vertical extrapolation uncertainty is required to account for this uncertainty. Remote sensing and/or hub height measurements can reduce and potentially eliminate this uncertainty.

Vertical extrapolation uncertainty is estimated at each met tower individually and, met tower estimates are combined assuming partial dependency on the mast and turbine heights when estimating vertical extrapolation uncertainty at the turbine locations. For example, if met towers are located in meteorologically similar environments, risk is increased that common errors are present in the vertical extrapolation process.

7.1.3 MOS Correction Uncertainty

A MOS Correction uncertainty is applied at each met tower that accounts for the probability that the statistical correction applied to the long term climate signal will accurately capture the true historic climate variability. The uncertainty associated with the 3TIER Services' MOS correction algorithm decreases as the training period increases. The uncertainty depends on the length of data available at the met tower and the quality of the relationship between the met tower and the long term data set.

MOS correction uncertainty is estimated at each met tower, and then individual uncertainties are combined to predict the uncertainty at each turbine location assuming partial dependence between each met tower. This dependence is a function of the concurrency of measurements between the met towers, since the uncertainty of this relationship will depend on common errors in the climate signal used as the reference.

7.1.4 Climate Variability Uncertainty

Climate variability uncertainty is comprised of the following individual component uncertainties: historic climate, future climate, climate change, and climate signal consistency. Historic and future climate uncertainties represent the uncertainty associated with the natural variability of the climate and whether the climate reference period or future prediction period will capture the true climate. These uncertainties are a function of the inter-annual variability and auto-correlation of the climate signal. Climate change and climate signal consistency uncertainties represent the probability of error of the future prediction because the climate of the future may not be accurately represented by the climate of the past. These uncertainties are higher if the past few years show potential trends that may point towards a changing pattern.

Climate variability uncertainty is considered common across all met towers and is modeled with complete dependence in the uncertainty framework.

7.1.5 Spatial Modeling Uncertainty

Spatial modeling uncertainty is estimated by calibrating a spatial model for each met tower that applies the MOS correction derived at that met tower to all the turbine locations. The individual spatial models are combined at each turbine location using weights that are a function of the total uncertainty at each met tower considering dependence and independence of each component uncertainty. Spatial uncertainties are a function of the geographic covariance between each met tower and turbine location. Vaisala applies two spatial modeling uncertainties: micro spatial uncertainty and macro spatial uncertainty. Micro spatial uncertainty represents the uncertainty associated with the grid resolution of the spatial model and whether the model is capturing micro scale effects. Macro spatial uncertainty represents the risk that a spatial model calibration at the location of a met tower is applicable at distances away from that met tower.

This complex uncertainty is a function of all the prior uncertainties and relative proximity and complexity of each geospatial relationship. The dependence on prior uncertainties is driven by the weighting scheme of each met tower, which has uncertainty dependence. Spatial covariance is also considered when aggregating each individual turbine uncertainty into a project average uncertainty.

7.1.6 Power Modeling Uncertainty

Power modeling uncertainty considers each step in converting wind speed estimates into energy estimates. In this step, wind speed uncertainties are expanded by the wind speed to energy relationship and then the following is considered: representativeness of the modeled frequency distribution when applying the specified power curve, wakes, availabilities, electrical losses, and all other losses considered in the loss evaluation process. Power modeling uncertainties are considered to be dependent between each turbine location.

7.2 Uncertainty Framework Results

The primary source of uncertainty for the Busch Ranch II project originates in spatial modeling. There is only one met tower sited within the project array, and the weighted average turbine to tower distance of $5.8\,km$ is high for a quality due diligence analysis. Measurement uncertainty is also elevated because Vaisala included data from M0571 affected by dry friction whip in order maintain an adequate data record for the tower. Overall project uncertainty is relatively low, but could be further reduced with the installation of additional towers within the project array.

7.2.1 Met Tower Uncertainty

Uncertainty values for each met tower are presented as a function of wind speed below in Table 10.

	M0571	M4666
Measurement	2.8	1.9
Vertical Extrapolation	1.4	1.5
MOS Correction	0.3	2.4
Climate Variability	1.2	1.3
Combined Uncertainty	**3.4**	**3.6**

Table 10: Standard error of wind speed estimation at each met tower (%)

7.2.2 Combined Project Uncertainties

The total project uncertainties, represented as a percent of the P50 estimate are presented in Table 11 as a function of energy.

	1-year	10-year	20-year
Measurement	2.6	2.6	2.6
Vertical Extrapolation	1.6	1.6	1.6
MOS Correction	0.8	0.8	0.8
Climate Variability	3.8	1.6	1.4
Spatial Modeling	4.2	4.2	4.2
Power Modeling	4.4	4.4	4.4
Total Uncertainty	**7.9**	**7.1**	**7.0**

Table 11: Standard error of wind energy estimation (%)

8 PROBABILITY OF EXCEEDANCES

Based on the estimated total project uncertainties, Tables 12 and 13 present the probability of exceedance levels associated with the P50 project estimate. Table 12 provides results in terms of GWh, while Table 13 shows results in terms of project-average capacity factor (%). Table 14 shows the net P50, P75, and P90 values for each calendar month.

	1-year	10-year	20-year
Gross-P50	248.2	248.2	248.2
Net-P50	201.5	201.5	201.5
Net-P75	190.8	191.9	192.0
Net-P90	181.2	183.3	183.4
Net-P95	175.5	178.1	178.3
Net-P99	164.7	168.4	168.7

Table 12: Probability of Exceedance Values (GWh)

	1-year	10-year	20-year
Gross-P50	47.7	47.7	47.7
Net-P50	38.7	38.7	38.7
Net-P75	36.6	36.9	36.9
Net-P90	34.8	35.2	35.2
Net-P95	33.7	34.2	34.2
Net-P99	31.6	32.3	32.4

Table 13: Probability of Exceedance Values (%)

	Net P50	20-year Net P75	20-year Net P90
January	18.2	17.3	16.5
February	16.0	15.2	14.4
March	18.4	17.5	16.7
April	18.4	17.5	16.7
May	17.7	16.7	15.9
June	17.0	16.1	15.3
July	14.0	13.1	12.4
August	13.9	13.1	12.3
September	15.2	14.3	13.4
October	16.6	15.7	14.9
November	17.7	16.9	16.2
December	18.4	17.5	16.8

Table 14: Monthly Probability of Exceedance Values (GWh). The monthly P75 and P90 values are not expected to sum to the annual values, since the variability of the monthly-means is greater than the variability of the annual-mean.

9 CONCLUSION

Vaisala has conducted a wind resource assessment of the Busch Ranch II project. The assessment is based on a wind turbine layout consisting of 27 Vestas V120-2.2MW wind turbines at $80\,m$. The wind resource assessment yields a gross energy value of $248.2\,GWh$. Loss factors were considered, leading to a net energy estimate of $201.5\,GWh$. Turbine-wise values of gross energy, wake loss, and net energy are available in Appendix Turbine Means. Following the uncertainty assessment of wind speed measurement and energy modeling analysis, net probabilities of exceedance were calculated. 20-year P75 and P90 cases are $192.0\,GWh$ and $183.4\,GWh$, respectively.

10 APPENDIX TURBINE MEANS

This section contains turbine-specific elevation, wind speed, and air density, along with gross energy values, wake loss, and net energy values for each of the 27 turbines at the Busch Ranch II project.

10.1 Vestas V120-2.2MW wind turbines at 80 m

ID	Latitude ($degrees$)	Longitude ($degrees$)	Elevation (m)	Wind Speed ($\frac{m}{s}$)	Air Density ($\frac{kg}{m^3}$)	Gross Generation (MWh :: %)	Wake Loss (%)	Net Generation (MWh :: %)
T01	37.75707	-104.45678	1896	7.44	0.987	8851 :: 45.9	95.6	7190 :: 37.3
T02	37.75262	-104.45902	1895	7.47	0.987	8896 :: 46.1	95.6	7229 :: 37.5
T03	37.75001	-104.45671	1895	7.52	0.987	8979 :: 46.6	96.3	7346 :: 38.1
T04	37.75947	-104.45094	1896	7.52	0.986	8988 :: 46.6	91.3	6975 :: 36.2
T05	37.75735	-104.44690	1884	7.50	0.987	8976 :: 46.5	92.9	7092 :: 36.8
T06	37.75501	-104.44193	1866	7.44	0.989	8912 :: 46.2	94.3	7158 :: 37.1
T07	37.75020	-104.44006	1860	7.47	0.990	8968 :: 46.5	96.4	7367 :: 38.2
T08	37.79499	-104.44260	1836	7.44	0.992	8970 :: 46.5	95.3	7296 :: 37.8
T09	37.79932	-104.44260	1830	7.41	0.992	8933 :: 46.3	96.3	7346 :: 38.1
T10	37.77233	-104.40287	1859	7.88	0.989	9577 :: 49.7	95.6	7785 :: 40.4
T11	37.77117	-104.39332	1838	7.71	0.991	9370 :: 48.6	95.4	7626 :: 39.5
T12	37.76876	-104.38889	1832	7.73	0.992	9399 :: 48.7	95.1	7624 :: 39.5
T13	37.76578	-104.38520	1828	7.75	0.992	9429 :: 48.9	96.0	7718 :: 40.0
T14	37.76091	-104.38317	1819	7.71	0.993	9378 :: 48.6	96.3	7711 :: 40.0
T15	37.75602	-104.38121	1823	7.79	0.993	9487 :: 49.2	97.4	7876 :: 40.8
T16	37.79065	-104.44259	1840	7.44	0.991	8954 :: 46.4	95.2	7273 :: 37.7
T17	37.78454	-104.44258	1853	7.50	0.990	9012 :: 46.7	94.6	7263 :: 37.7
T18	37.78091	-104.44086	1871	7.69	0.988	9260 :: 48.0	94.7	7451 :: 38.6
T19	37.77306	-104.43238	1873	7.73	0.988	9310 :: 48.3	95.1	7518 :: 39.0
T20	37.76801	-104.43238	1874	7.69	0.988	9255 :: 48.0	94.6	7444 :: 38.6
T21	37.80529	-104.40644	1830	7.67	0.992	9280 :: 48.1	96.7	7652 :: 39.7
T22	37.80078	-104.40544	1834	7.69	0.992	9311 :: 48.3	95.7	7603 :: 39.4
T23	37.79625	-104.40444	1834	7.66	0.992	9283 :: 48.1	95.4	7560 :: 39.2
T24	37.79172	-104.40343	1840	7.71	0.991	9349 :: 48.5	95.8	7641 :: 39.6
T25	37.78542	-104.41060	1848	7.76	0.990	9415 :: 48.8	95.7	7672 :: 39.8
T26	37.78215	-104.40729	1844	7.68	0.990	9307 :: 48.3	94.4	7497 :: 38.9
T27	37.77888	-104.40399	1848	7.74	0.990	9390 :: 48.7	94.8	7589 :: 39.4

Table 15: Turbine-specific 37-year mean values for 27 Vestas V120-2.2MW wind turbines at $80\,m$. Generation values are provided in terms of energy and capacity factor.

ID	Net P50 (MWh :: %)	Net P75 (MWh :: %)	Net P90 (MWh :: %)	Net P95 (MWh :: %)	Net P99 (MWh :: %)
T01	7190 :: 37.3	6861 :: 35.6	6565 :: 34.0	6388 :: 33.1	6056 :: 31.4
T02	7229 :: 37.5	6901 :: 35.8	6606 :: 34.3	6429 :: 33.3	6097 :: 31.6
T03	7346 :: 38.1	7015 :: 36.4	6716 :: 34.8	6537 :: 33.9	6202 :: 32.2
T04	6975 :: 36.2	6649 :: 34.5	6356 :: 33.0	6181 :: 32.0	5852 :: 30.3
T05	7092 :: 36.8	6745 :: 35.0	6433 :: 33.4	6247 :: 32.4	5897 :: 30.6
T06	7158 :: 37.1	6788 :: 35.2	6455 :: 33.5	6255 :: 32.4	5881 :: 30.5
T07	7367 :: 38.2	6985 :: 36.2	6641 :: 34.4	6435 :: 33.4	6049 :: 31.4
T08	7296 :: 37.8	6944 :: 36.0	6628 :: 34.4	6439 :: 33.4	6083 :: 31.5
T09	7346 :: 38.1	6992 :: 36.3	6673 :: 34.6	6483 :: 33.6	6125 :: 31.8
T10	7785 :: 40.4	7432 :: 38.5	7115 :: 36.9	6925 :: 35.9	6568 :: 34.1
T11	7626 :: 39.5	7267 :: 37.7	6945 :: 36.0	6752 :: 35.0	6389 :: 33.1
T12	7624 :: 39.5	7266 :: 37.7	6945 :: 36.0	6753 :: 35.0	6392 :: 33.1
T13	7718 :: 40.0	7357 :: 38.1	7033 :: 36.5	6838 :: 35.5	6474 :: 33.6
T14	7711 :: 40.0	7346 :: 38.1	7017 :: 36.4	6821 :: 35.4	6452 :: 33.5
T15	7876 :: 40.8	7511 :: 38.9	7181 :: 37.2	6985 :: 36.2	6615 :: 34.3
T16	7273 :: 37.7	6920 :: 35.9	6602 :: 34.2	6412 :: 33.2	6054 :: 31.4
T17	7263 :: 37.7	6910 :: 35.8	6592 :: 34.2	6402 :: 33.2	6045 :: 31.3
T18	7451 :: 38.6	7098 :: 36.8	6780 :: 35.2	6590 :: 34.2	6233 :: 32.3
T19	7518 :: 39.0	7161 :: 37.1	6839 :: 35.5	6647 :: 34.5	6286 :: 32.6
T20	7444 :: 38.6	7084 :: 36.7	6760 :: 35.1	6566 :: 34.0	6203 :: 32.2
T21	7652 :: 39.7	7292 :: 37.8	6968 :: 36.1	6774 :: 35.1	6410 :: 33.2
T22	7603 :: 39.4	7247 :: 37.6	6926 :: 35.9	6734 :: 34.9	6373 :: 33.0
T23	7560 :: 39.2	7204 :: 37.4	6884 :: 35.7	6692 :: 34.7	6332 :: 32.8
T24	7641 :: 39.6	7284 :: 37.8	6962 :: 36.1	6769 :: 35.1	6408 :: 33.2
T25	7672 :: 39.8	7317 :: 37.9	6997 :: 36.3	6805 :: 35.3	6446 :: 33.4
T26	7497 :: 38.9	7143 :: 37.0	6825 :: 35.4	6634 :: 34.4	6277 :: 32.5
T27	7589 :: 39.4	7236 :: 37.5	6918 :: 35.9	6727 :: 34.9	6370 :: 33.0

Table 16: Turbine-specific 20-year generation probability of exceedance values (P-values) for 27 Vestas V120-2.2MW wind turbines at $80\,m$.

11 APPENDIX GROSS LONG-TERM VARIABILITY

11.1 Summary

This section provides a retrospective analysis of the past 37 years of wind speed and power at the Busch Ranch II location. These data were derived from a mesoscale Numerical Weather Prediction (NWP) model that has been statistically calibrated to match the observed data during the measurement period at each meteorological tower for which data were provided (Towers M0571 and M4666). Due to long-term climate variability and/or change the historic distributions of wind and power capacity described here may not be indicative of future conditions.

Based on the results of the 3TIER Services' Energy Risk Framework, the last 37 years (January, 1980 – September, 2017) of data have been utilized for estimating the expected future generation at Busch Ranch II. The average MOS-corrected simulated wind speed at hub height ($80\,m$) during the past 37 years of record (January, 1980 – September, 2017) across all 27 turbines is $\mathbf{7.62\,m/s}$. The average MOS-corrected simulated gross power capacity at hub height during the past 37 years across all 27 turbines is $\mathbf{47.7\%}$. A map of average MOS-corrected gross power capacity values across the Busch Ranch II project area using the power curve for the Vestas V120-2.2MW wind turbines is displayed in Power Capacity Maps.

All power capacities presented in this section are gross power capacities.

11.2 Power Capacity Maps

This section contains a map of MOS-corrected long-term mean gross power capacity values across the Busch Ranch II project area for each turbine model and hub height.

11.2.1 Vestas V120-2.2MW at 80 m

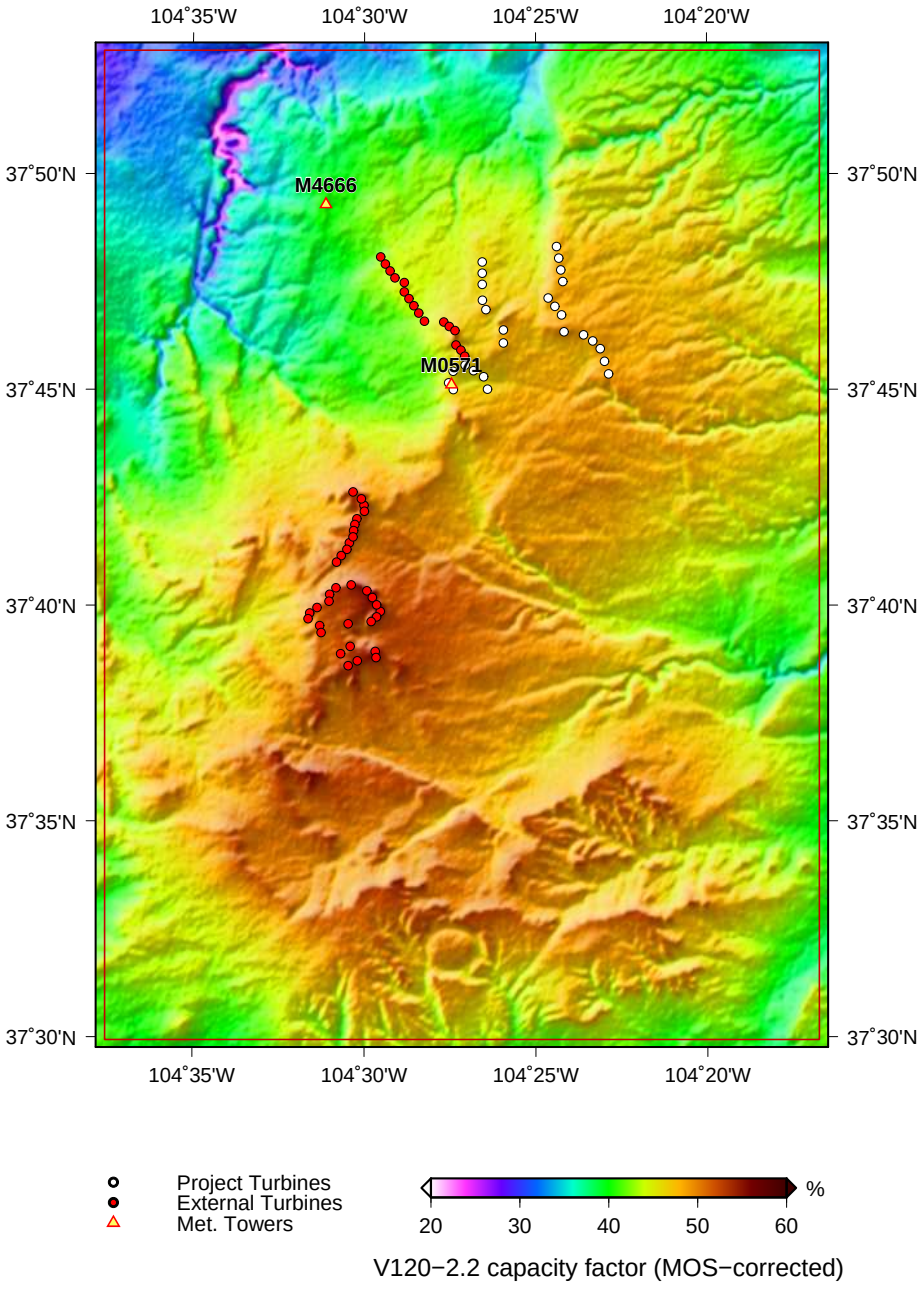

Figure 12: 37-year mean capacity factor at $80\,m$.

11.3 Model Simulations By Vaisala

The assessment of the wind resource across the Busch Ranch II project presented in this section is based on 37 years of simulated data (January, 1980 – September, 2017) using a numerical weather prediction (NWP) model of the atmosphere.

The 37-year simulated data set is constructed from two separate model runs:

1. a 1-year, $500\,m$ resolution simulation (where the year of each calendar day is chosen sequentially from the last 10 years (2007 – 2016)), and
2. a 37-year continuous $4.5\,km$ resolution simulation.

The NWP model represents atmospheric processes in the boundary layer, including the roughness of the underlying terrain or water, stability within the boundary layer, heat and moisture fluxes into the atmosphere, wind shear, and turbulence within the boundary layer. The model outputs winds at fixed vertical levels, and there are 6 such levels in the lowest $600\,m$ of the atmosphere. To determine winds at specific hub heights, model data are interpolated between fixed vertical levels using "power-law interpolation". This process essentially uses the standard power-law shear formula, where the shear exponent is determined exactly from the winds at the two bracketing levels, rather than assuming a fixed shear exponent.

Vaisala configured the NWP model using nested grids to simulate the wind resource over the Busch Ranch II region. Some details of the NWP configuration are shown below in Table 17. The extent of the coarsest grid was selected to capture the effect of synoptic weather events on the wind resource at the site, as well as to allow the model to develop regional, thermally-driven circulations. The increasingly fine $40.5\,km$, $13.5\,km$, $4.5\,km$, $1.5\,km$ and $500\,m$ grids were selected to model the effect of local terrain and local scale atmospheric circulations.

After the NWP model simulations finished, a Time-Varying Microscale (TVM) model was employed to downscale the $500\,m$ horizontal resolution NWP model output to the final $90\,m$ horizontal resolution. All deliverables and model data shown in this section are derived from the $90\,m$ resolution model grids. A map of the $90\,m$ TVM grid is shown in Figure 13.

Based on a comparison of the NWP output with observations from each meteorological tower for which data were provided (Towers M0571 and M4666), a linear statistical model was constructed to remove the bias and adjust the variance of the raw NWP simulated winds.

Parameter	Value
Mesoscale numerical weather prediction model	WRF
Horizontal resolution of valid study area	$500\,m$
Final downscaled horizontal resolution	$90\,m$
Number of vertical levels	31
Elevation database	3 second SRTM
Vegetation database	1 second NLCD01
Surface parameterization	Monin-Obukhov similarity model
Boundary layer parameterization	Mellor-Yamada-Janjic TKE
Land surface scheme	5-layer soil diffusivity model

Table 17: Numerical weather prediction model configuration

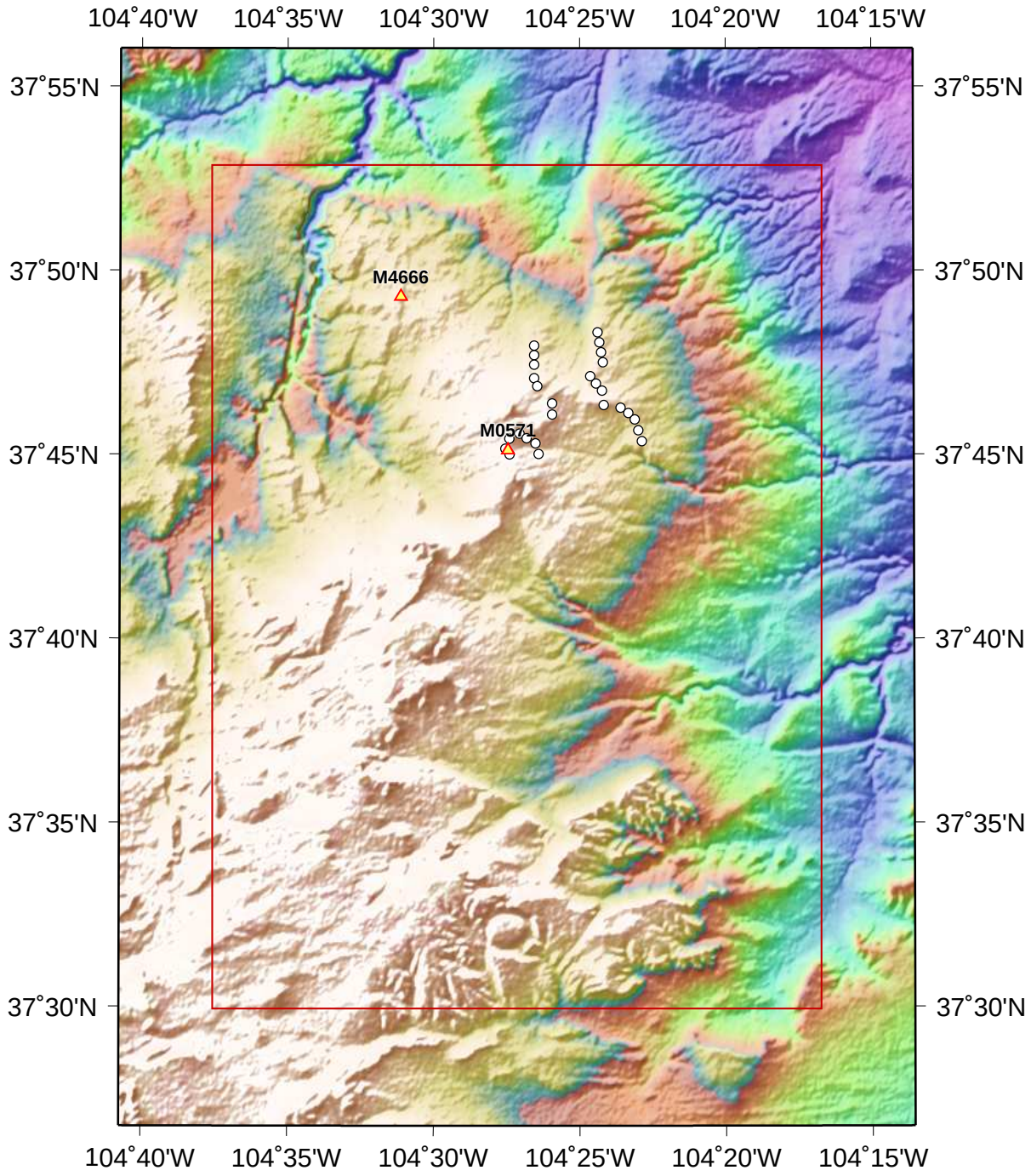

Figure 13: Map of the $90\,m$ resolution NWP model domain. The bold red box marks the boundary of the valid study area. The yellow triangles denote locations of meteorological towers and white dots indicate wind turbines.

11.4 Project-average Long-term Wind Resource Assessment

11.4.1 Monthly-mean Variability of Wind Speed

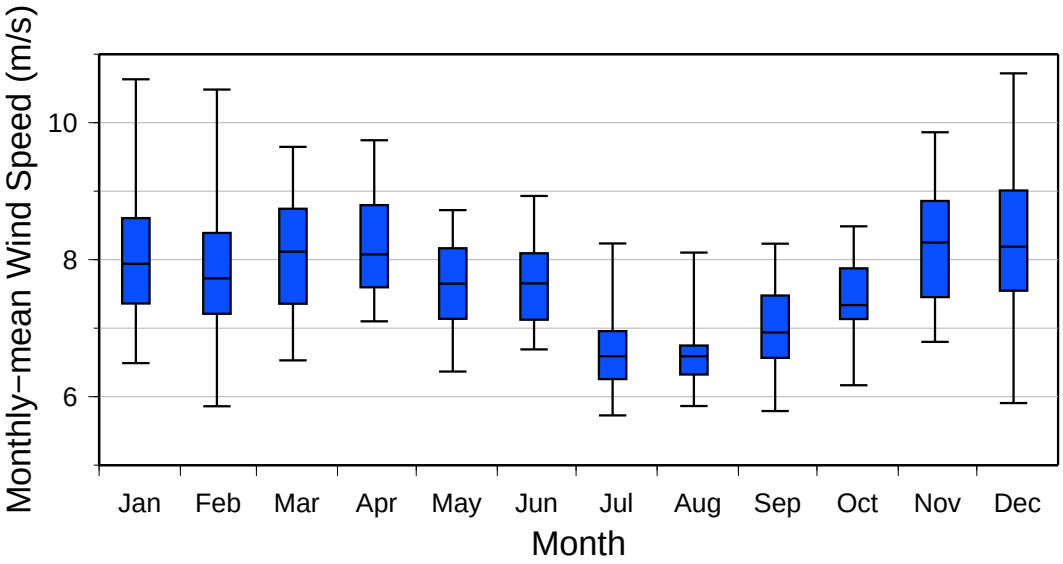

Figure 14: Box-and-whisker plot of monthly-mean project-average wind speed. This figure displays the expected variability of monthly-mean project-average wind speeds. Median wind speed denoted by solid line within the shaded box. Upper and lower boundaries of the shaded box correspond to the 75% and 25% quartiles, while the whiskers denote the maximum and minimum monthly-mean wind speeds.

11.4.2 Annual-mean Variability of Wind Speed

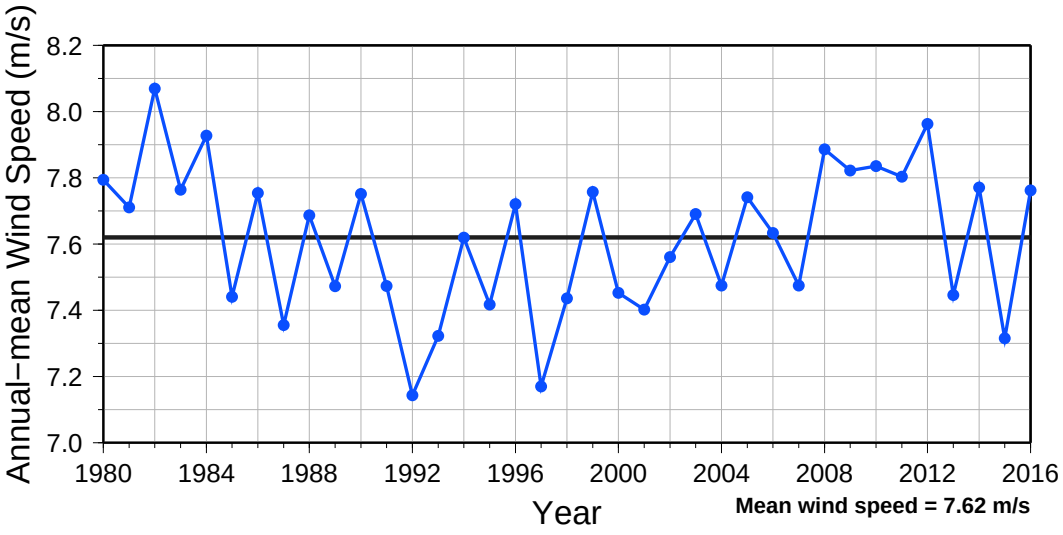

Figure 15: Time series of annual-mean project-average wind speed. Black line denotes the long-term mean.

11.4.3 Wind Speed Distribution

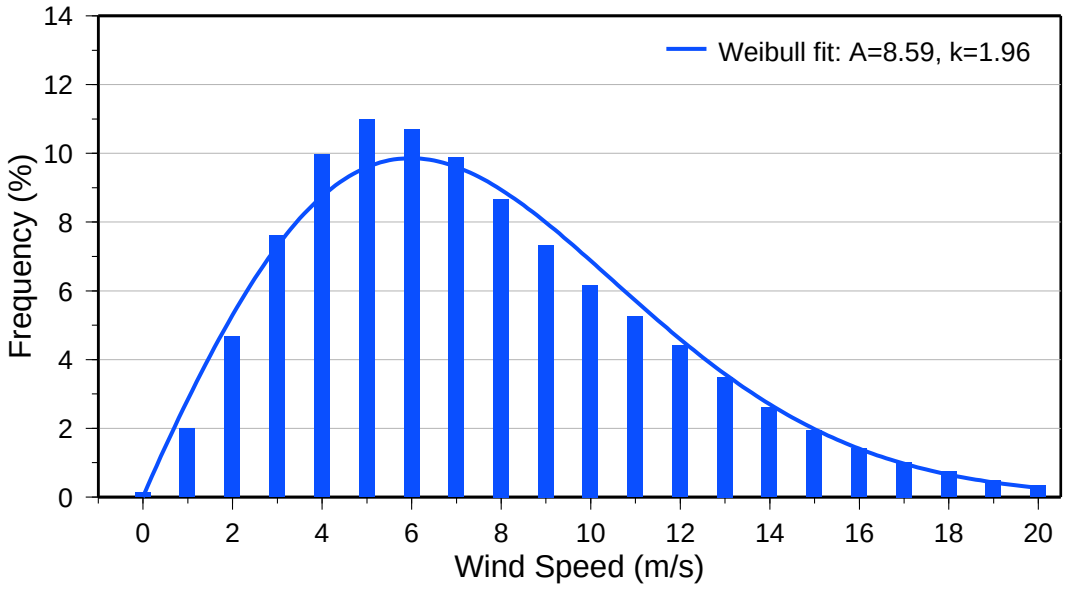

Figure 16: Hourly distribution of simulated project-average wind speed using $1\,m/s$ bins. ($0\,m/s$ bin contains only values ≤ 0.5.) Weibull distribution is also shown with the scale (A) and shape (k) parameters listed in the legend.

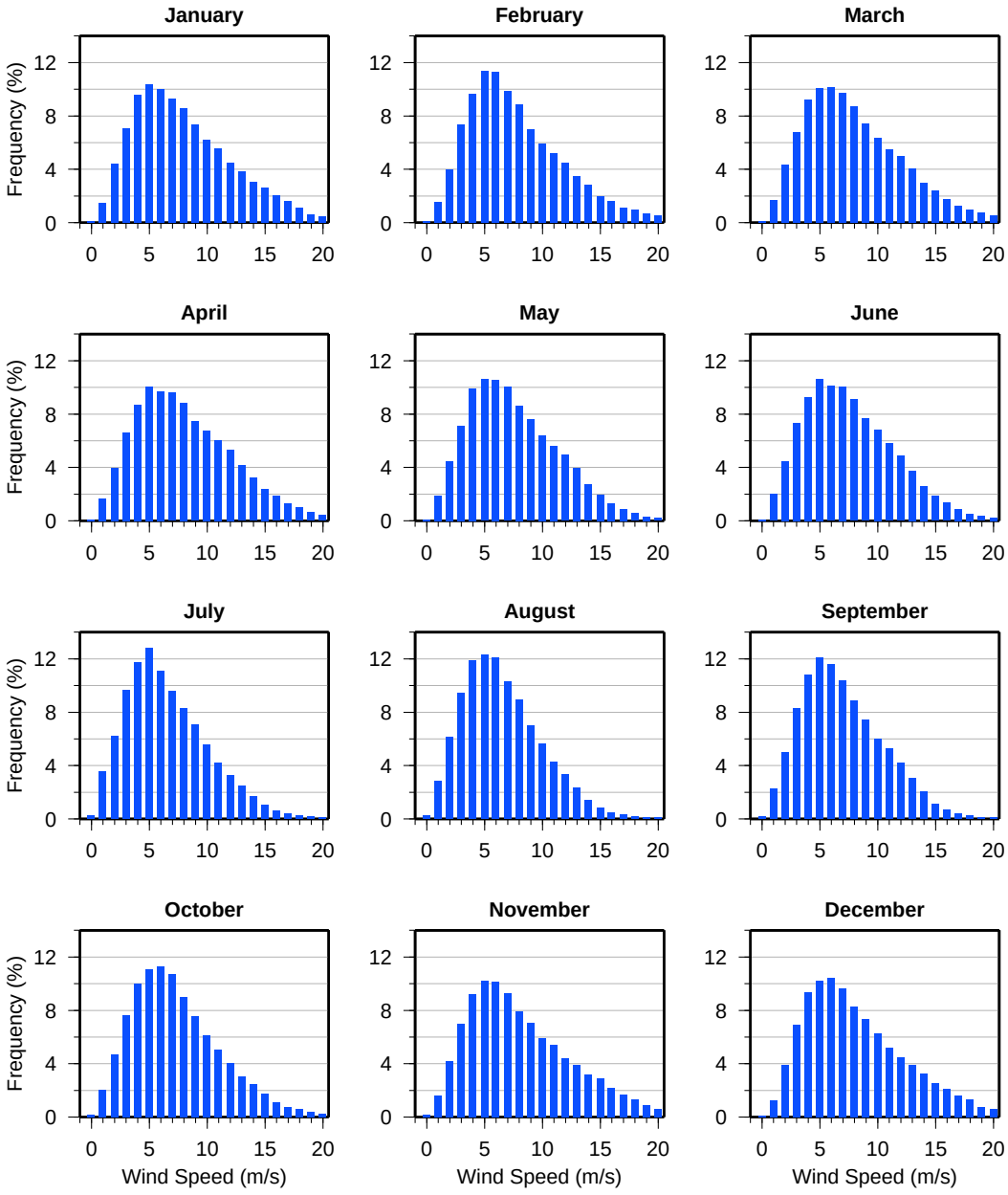

Figure 17: Hourly distribution of simulated project-average wind speed using $1\,m/s$ bins for each calendar month. ($0\,m/s$ bin contains only values ≤ 0.5.)

11.4.4 Wind Direction Distribution

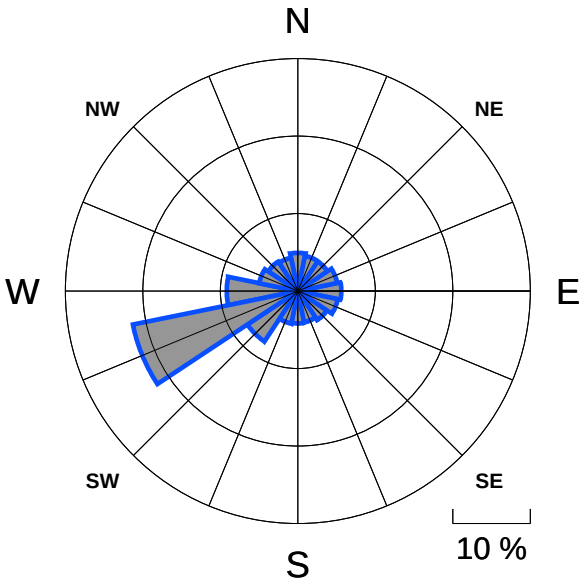

Figure 18: Annual wind rose of the hourly-mean project-average wind direction time series. Directional bins are 22.5° wide, and the radial contour interval is 10%.

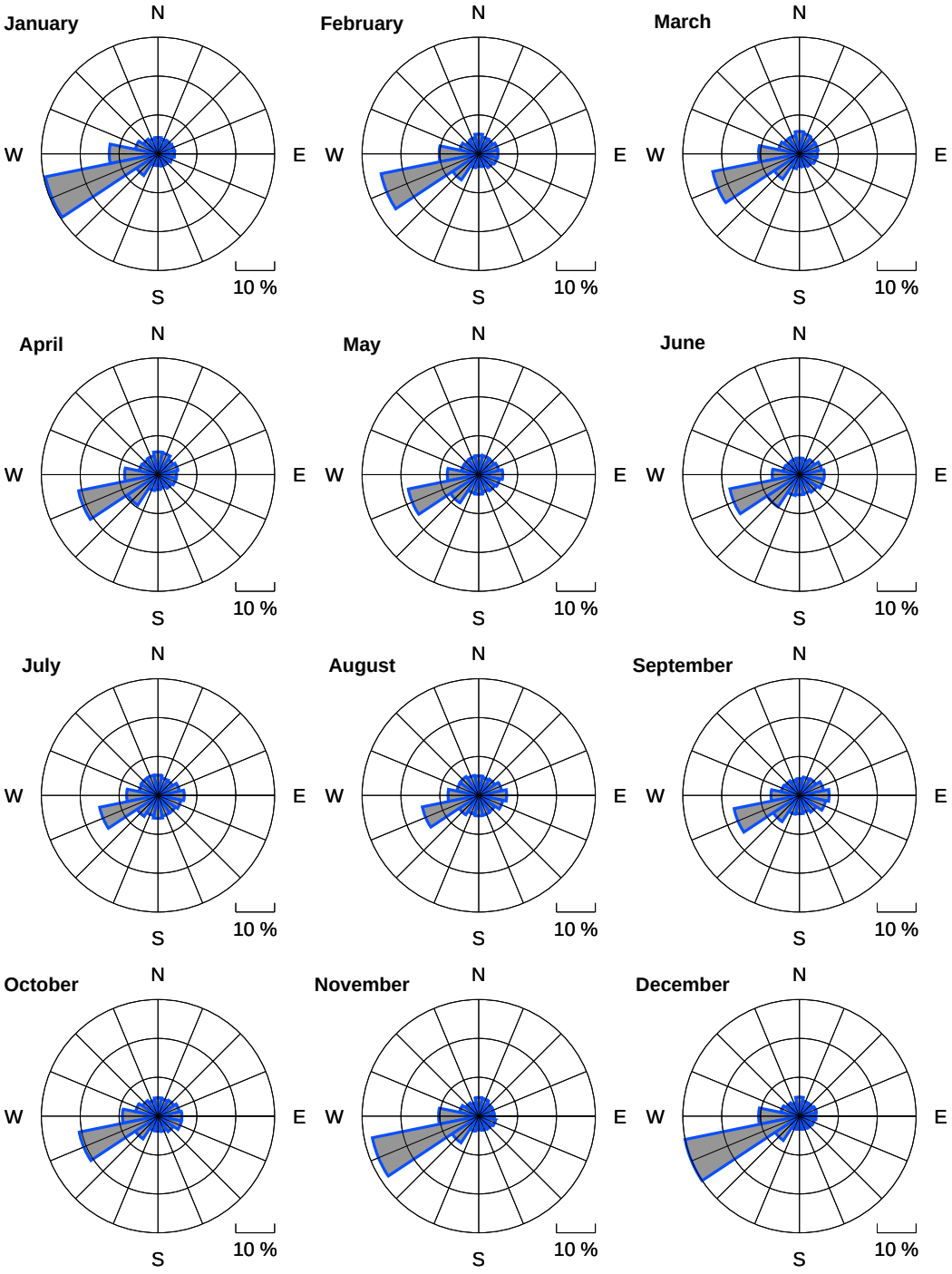

Figure 19: Wind roses of the hourly-mean project-average wind direction time series for each calendar month. Directional bins are 22.5° wide, and the radial contour interval is 10%.

11.4.5 Diurnal Variability of Wind Speed

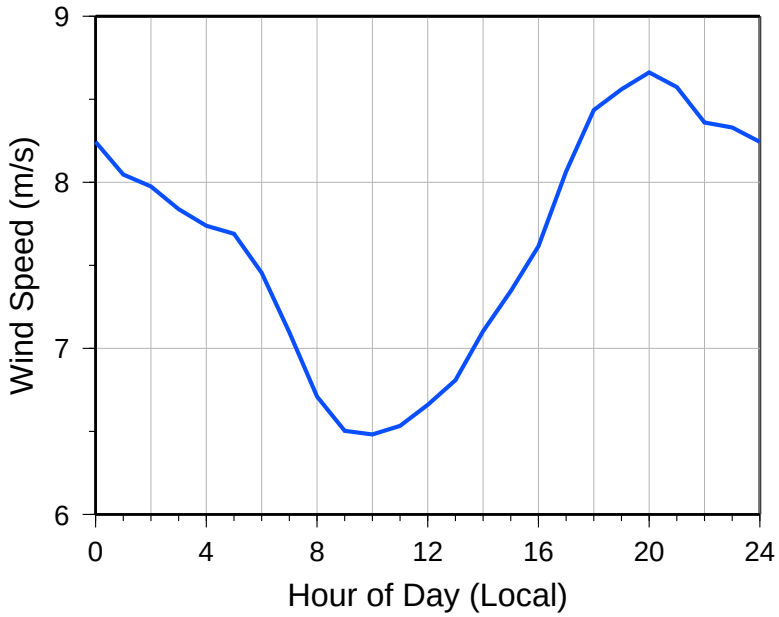

Figure 20: Diurnal cycle of simulated project-average wind speed. The horizontal axis is Mountain Time Zone.

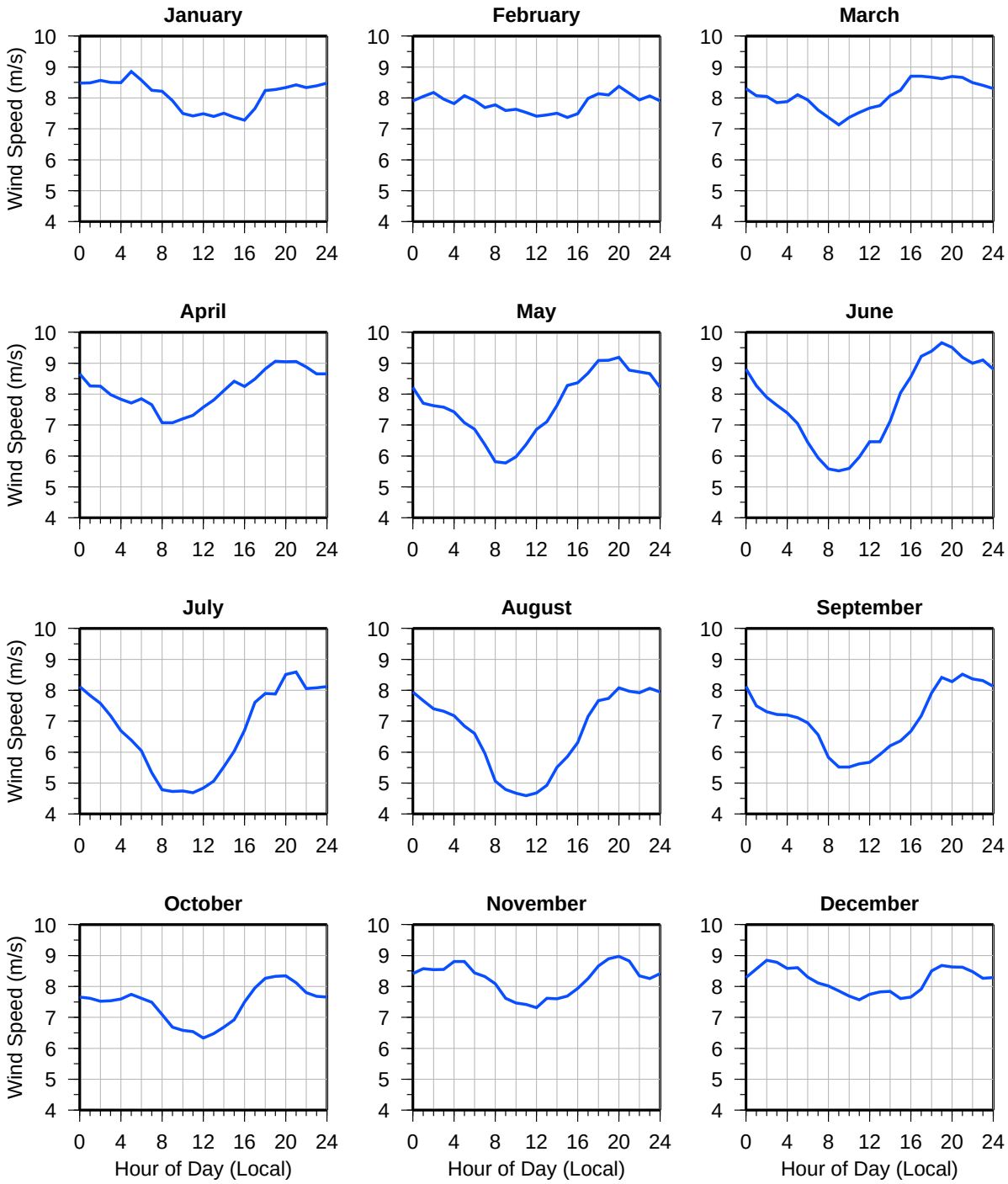

Figure 21: Diurnal cycle of simulated project-average wind speed for each calendar month. The horizontal axis is Mountain Time Zone.

11.4.6 Wind Speed Variability and ENSO

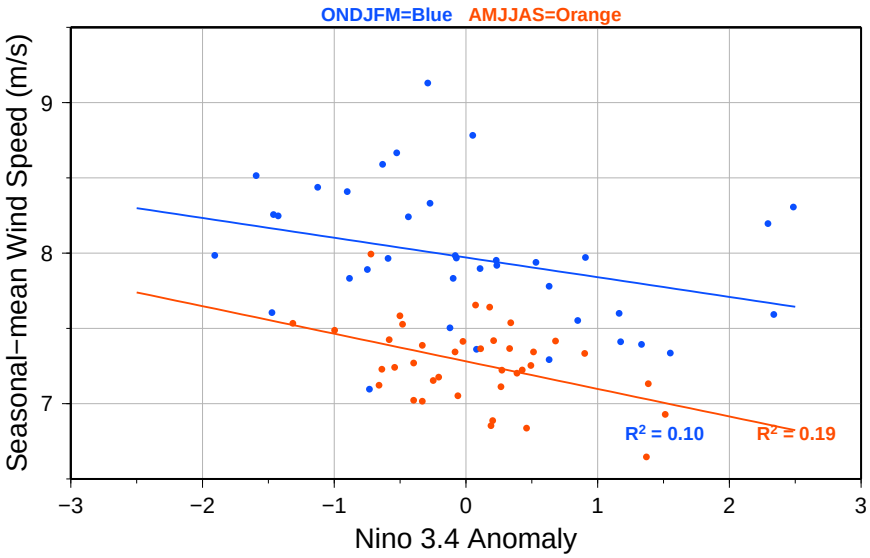

Figure 22: Scatter plot of Niño 3.4 anomalies vs. 6-month seasonal-mean project-average wind speed. Blue dots denote the mean during ONDJFM (October, November, December, January, February, and March); orange dots denote the mean during AMJJAS (April, May, June, July, August and September).

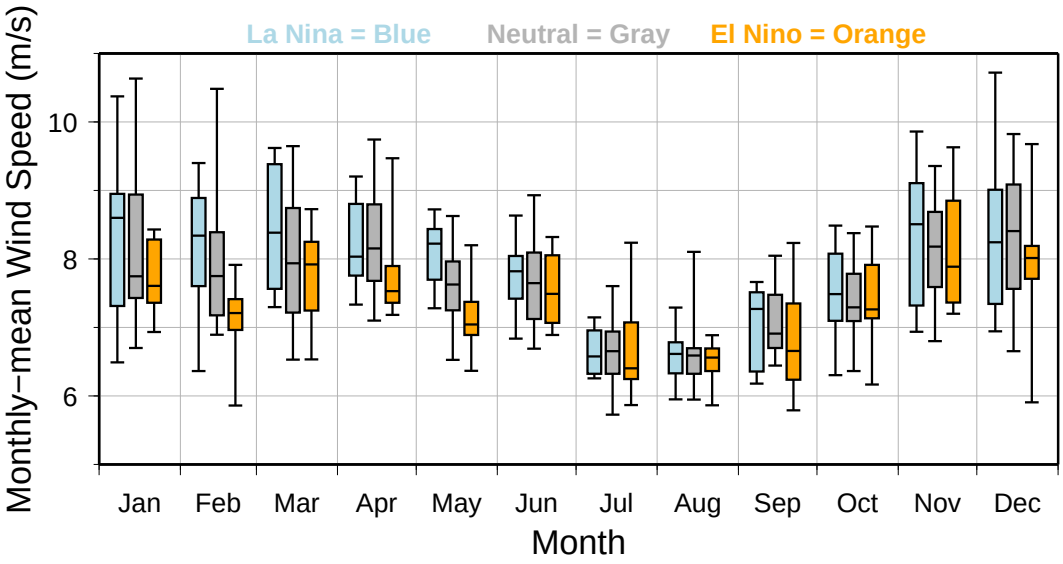

Figure 23: Box-and-whisker plot of monthly-mean project-average wind speed for La Niña (blue), neutral (gray), and El Niño (orange) phases of ENSO. Median wind speed denoted by solid line within the shaded box. Upper and lower boundaries of the shaded box correspond to the 75% and 25% quartiles, while the whiskers denote the maximum and minimum wind speeds.

11.4.7 Tabular Data

Hour of Day (Local)	Jan	Feb	Mar	Apr	May	Jun	Jly	Aug	Sep	Oct	Nov	Dec	Avg
0	8.48	7.90	8.31	8.66	8.21	8.81	8.12	7.94	8.13	7.66	8.41	8.29	8.24
1	8.48	8.05	8.07	8.27	7.70	8.27	7.83	7.67	7.49	7.62	8.58	8.57	8.05
2	8.57	8.17	8.05	8.26	7.62	7.89	7.57	7.40	7.30	7.52	8.54	8.84	7.98
3	8.50	7.96	7.85	7.99	7.58	7.64	7.18	7.32	7.22	7.54	8.55	8.78	7.84
4	8.50	7.82	7.88	7.83	7.43	7.40	6.69	7.18	7.20	7.60	8.81	8.58	7.74
5	8.86	8.07	8.11	7.71	7.08	7.05	6.38	6.85	7.12	7.75	8.80	8.61	7.69
6	8.57	7.92	7.94	7.85	6.86	6.44	6.04	6.61	6.95	7.62	8.44	8.30	7.45
7	8.25	7.69	7.61	7.66	6.36	5.94	5.33	5.95	6.56	7.49	8.32	8.11	7.10
8	8.22	7.78	7.37	7.07	5.81	5.58	4.78	5.06	5.83	7.09	8.09	8.02	6.71
9	7.91	7.60	7.13	7.08	5.77	5.52	4.72	4.79	5.52	6.69	7.62	7.86	6.50
10	7.50	7.63	7.37	7.20	5.97	5.60	4.74	4.67	5.52	6.58	7.47	7.69	6.48
11	7.41	7.53	7.53	7.32	6.37	5.96	4.69	4.59	5.62	6.54	7.42	7.57	6.53
12	7.49	7.41	7.67	7.58	6.86	6.46	4.83	4.68	5.67	6.33	7.31	7.75	6.66
13	7.40	7.45	7.75	7.81	7.10	6.46	5.06	4.93	5.93	6.48	7.61	7.83	6.81
14	7.50	7.51	8.07	8.11	7.64	7.12	5.52	5.51	6.21	6.68	7.60	7.84	7.10
15	7.37	7.37	8.25	8.42	8.28	8.04	6.02	5.85	6.36	6.92	7.69	7.61	7.35
16	7.28	7.49	8.70	8.24	8.36	8.56	6.70	6.30	6.68	7.49	7.93	7.65	7.62
17	7.67	7.96	8.69	8.46	8.68	9.21	7.70	7.16	7.15	7.91	8.27	7.93	8.06
18	8.27	8.11	8.69	8.77	9.07	9.37	7.97	7.66	7.91	8.23	8.68	8.51	8.44
19	8.31	8.08	8.59	9.07	9.05	9.68	7.91	7.73	8.42	8.32	8.90	8.68	8.56
20	8.36	8.38	8.67	9.05	9.12	9.54	8.55	8.09	8.29	8.30	8.99	8.63	8.66
21	8.46	8.14	8.63	9.06	8.74	9.20	8.63	7.95	8.53	8.10	8.80	8.64	8.57
22	8.36	7.92	8.43	8.94	8.66	9.04	8.10	7.90	8.36	7.80	8.33	8.49	8.36
23	8.41	8.04	8.34	8.72	8.62	9.13	8.12	8.02	8.33	7.68	8.24	8.28	8.33
Avg	8.09	7.83	8.07	8.13	7.62	7.66	6.63	6.58	7.01	7.41	8.23	8.21	7.62

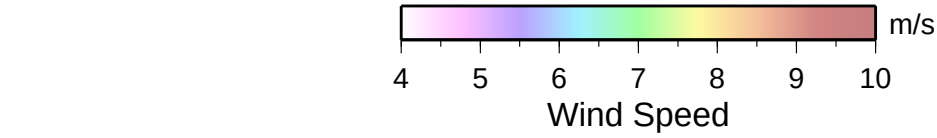

Figure 24: Hourly-mean values of simulated project-average wind speed. Vertical axis is local time.

Year	Jan	Feb	Mar	Apr	May	Jun	Jly	Aug	Sep	Oct	Nov	Dec	Avg
1980	8.43	7.92	9.09	7.31	7.96	8.25	6.78	8.10	7.43	7.09	7.59	7.55	7.79
1981	6.70	7.86	8.24	8.30	8.17	8.09	6.73	6.33	6.70	8.38	8.25	8.81	7.71
1982	10.63	7.64	8.99	8.83	7.06	7.23	7.19	6.36	7.32	7.87	8.45	9.19	8.07
1983	7.50	7.91	8.25	7.90	7.73	7.63	7.60	6.60	7.76	7.39	9.11	7.84	7.76
1984	6.94	8.39	7.68	8.83	7.63	8.04	6.99	6.32	7.36	8.08	9.86	9.11	7.93
1985	6.49	7.46	9.62	7.76	7.28	7.19	6.32	7.11	7.71	7.55	8.16	6.67	7.44
1986	8.45	9.40	7.56	8.84	7.70	7.07	7.51	6.59	8.23	7.17	8.86	5.91	7.75
1987	8.42	7.21	8.05	7.35	7.37	7.00	8.24	6.69	6.13	6.17	7.56	8.01	7.36
1988	8.42	7.23	7.94	7.68	8.72	7.42	6.58	7.29	7.51	6.30	8.90	8.24	7.69
1989	9.11	6.36	8.99	7.33	7.70	6.84	6.80	6.96	7.11	7.25	8.46	6.65	7.47
1990	9.63	8.03	6.97	7.33	8.45	8.66	6.33	6.84	6.57	7.77	8.90	7.56	7.75
1991	6.85	6.98	9.65	7.80	8.65	8.05	6.42	6.18	6.96	7.18	7.71	7.22	7.47
1992	7.36	7.41	7.14	7.18	6.71	6.78	6.65	6.22	7.48	6.91	6.80	9.09	7.14
1993	7.43	7.41	6.53	7.66	6.89	8.32	7.41	6.75	6.50	6.36	8.20	8.47	7.32
1994	7.64	9.05	7.67	8.12	7.25	7.67	6.32	6.43	6.87	7.26	9.63	7.71	7.62
1995	7.69	7.26	8.27	8.09	7.67	7.62	6.60	6.58	6.36	7.55	8.31	7.02	7.42
1996	8.95	7.82	7.36	8.59	7.82	6.69	5.97	6.13	6.91	8.07	7.61	10.72	7.72
1997	8.60	6.89	7.55	7.27	6.37	7.07	7.07	5.86	6.24	8.09	7.21	7.76	7.17
1998	8.28	6.96	7.25	7.40	8.20	8.63	6.26	5.95	7.00	7.49	8.51	7.31	7.44
1999	8.69	9.31	8.18	8.80	8.06	7.80	7.15	6.78	6.33	6.88	7.28	7.95	7.76
2000	7.92	8.31	7.30	7.96	8.44	7.84	6.50	6.53	7.27	7.14	6.94	7.34	7.45
2001	6.99	7.60	6.57	9.12	6.84	7.83	7.13	6.70	6.44	7.95	7.36	8.34	7.40
2002	7.96	7.86	8.32	8.69	7.70	8.01	5.87	6.89	7.35	6.62	7.34	8.19	7.56
2003	6.93	6.83	8.56	9.74	7.49	6.97	6.94	6.59	6.75	7.34	8.82	9.29	7.69
2004	7.86	7.14	7.07	7.60	8.22	7.12	6.02	6.65	7.60	8.47	7.20	8.70	7.47
2005	8.11	7.18	7.97	8.18	7.45	8.21	6.79	6.14	7.74	7.20	9.36	8.60	7.74
2006	10.37	7.36	9.11	9.28	6.53	7.35	5.88	5.95	6.35	7.34	8.07	8.02	7.63
2007	7.58	8.46	7.22	7.62	6.92	7.43	5.81	6.68	7.66	8.08	7.32	9.01	7.47
2008	9.93	8.37	8.38	8.11	8.39	7.35	6.49	6.65	6.63	7.22	7.45	9.62	7.89
2009	8.61	9.26	9.38	8.80	7.14	7.84	6.17	6.75	6.64	7.91	7.36	8.12	7.82
2010	7.31	5.86	7.79	9.47	8.63	8.10	6.96	7.22	7.59	7.53	8.95	8.52	7.84
2011	7.31	8.89	8.34	9.20	8.30	8.51	6.76	6.55	6.18	7.10	9.73	6.94	7.80
2012	8.68	8.57	9.43	7.82	7.92	8.93	6.25	6.63	5.79	7.34	8.69	9.53	7.96
2013	7.54	7.34	7.47	7.10	7.27	7.98	6.34	6.32	8.05	7.78	8.00	8.19	7.45
2014	8.58	8.63	8.81	8.32	7.51	8.61	6.20	6.70	6.88	6.83	9.24	7.11	7.77
2015	6.95	7.08	6.53	8.11	7.03	6.89	6.39	6.49	6.67	7.13	8.85	9.68	7.32
2016	7.61	7.85	8.73	7.36	7.47	6.80	6.94	6.29	7.46	8.49	8.30	9.82	7.76
2017	8.94	10.48	8.74	8.06	7.03	7.35	5.73	6.07	6.88				--
Avg	8.09	7.83	8.07	8.13	7.62	7.66	6.63	6.58	7.01	7.41	8.23	8.21	**7.62**

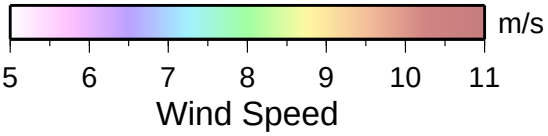

Figure 25: Monthly-mean values of simulated project-average wind speed.

Sector	Mean Speed(m/s)	Weibull Scale(A)	Weibull Shape(k)	Frequency(%)
N	6.74	7.60	1.96	4.92
NNE	5.64	6.36	1.98	4.63
NE	4.99	5.64	1.99	4.60
ENE	4.89	5.52	2.08	5.19
E	5.07	5.73	2.20	5.61
ESE	5.38	6.08	2.26	5.26
SE	5.82	6.57	2.22	4.50
SSE	6.52	7.37	2.06	4.10
S	7.97	8.99	1.99	4.18
SSW	8.08	9.13	2.08	4.28
SW	9.15	10.33	2.34	7.80
WSW	10.92	12.26	2.87	21.73
W	8.18	9.23	2.36	9.17
WNW	6.42	7.25	2.31	5.09
NW	6.73	7.59	2.07	4.58
NNW	6.70	7.57	2.05	4.38
ALL	**7.62**	**8.59**	**1.96**	**100.00**

Table 18: Simulated project-average mean wind speed, Weibull parameters, and frequency. Blank values correspond to times with less than 10 data points.

Wind Speed (m/s)	N	NNE	NE	ENE	E	ESE	SE	SSE	S	SSW	SW	WSW	W	WNW	NW	NNW	All
0 - 0.5	0.01	0.01	0.01	0.02	0.02	0.02	0.01	0.01	0.00	0.00	0.00	0.00	0.00	0.00	0.00	0.00	0.14
0.5 - 1.5	0.13	0.20	0.24	0.26	0.23	0.17	0.13	0.10	0.07	0.06	0.05	0.05	0.06	0.07	0.07	0.09	1.98
1.5 - 2.5	0.30	0.37	0.47	0.53	0.47	0.36	0.29	0.25	0.20	0.19	0.20	0.19	0.20	0.21	0.20	0.23	4.64
2.5 - 3.5	0.46	0.59	0.69	0.78	0.75	0.62	0.46	0.39	0.32	0.30	0.32	0.36	0.38	0.39	0.38	0.39	7.58
3.5 - 4.5	0.58	0.69	0.79	0.91	0.98	0.87	0.62	0.46	0.37	0.35	0.44	0.55	0.64	0.57	0.56	0.53	9.91
4.5 - 5.5	0.61	0.67	0.73	0.87	1.00	0.92	0.71	0.53	0.39	0.42	0.54	0.75	0.86	0.75	0.62	0.57	10.94
5.5 - 6.5	0.52	0.56	0.54	0.68	0.81	0.78	0.65	0.51	0.40	0.42	0.63	1.03	1.08	0.85	0.64	0.55	10.66
6.5 - 7.5	0.51	0.45	0.42	0.45	0.56	0.61	0.57	0.48	0.38	0.37	0.69	1.32	1.14	0.77	0.62	0.51	9.84
7.5 - 8.5	0.47	0.35	0.28	0.29	0.36	0.39	0.41	0.39	0.37	0.36	0.73	1.66	1.10	0.60	0.46	0.41	8.63
8.5 - 9.5	0.38	0.26	0.17	0.17	0.19	0.24	0.26	0.31	0.33	0.33	0.76	2.00	0.95	0.35	0.29	0.32	7.30
9.5 - 10.5	0.28	0.16	0.09	0.10	0.11	0.13	0.15	0.22	0.29	0.30	0.74	2.22	0.73	0.20	0.19	0.23	6.14
10.5 - 11.5	0.20	0.13	0.06	0.05	0.05	0.06	0.08	0.14	0.23	0.27	0.64	2.36	0.55	0.11	0.14	0.16	5.23
11.5 - 12.5	0.13	0.07	0.04	0.03	0.03	0.04	0.06	0.10	0.21	0.23	0.55	2.22	0.40	0.06	0.10	0.11	4.38
12.5 - 13.5	0.09	0.04	0.02	0.02	0.02	0.02	0.03	0.07	0.16	0.20	0.42	1.88	0.29	0.04	0.08	0.08	3.47
13.5 - 14.5	0.07	0.03	0.01	0.01	0.01	0.01	0.02	0.04	0.12	0.15	0.30	1.46	0.22	0.03	0.06	0.05	2.59
14.5 - 15.5	0.05	0.01	0.01	0.01	0.01	0.01	0.01	0.04	0.10	0.12	0.21	1.07	0.17	0.03	0.05	0.04	1.93
15.5 - 16.5	0.04	0.01	0.01	0.00	0.01	0.01	0.01	0.02	0.07	0.08	0.17	0.78	0.11	0.02	0.04	0.03	1.41
16.5 - 17.5	0.03	0.01	0.01	0.00	0.00	0.00	0.00	0.02	0.06	0.05	0.12	0.56	0.09	0.01	0.02	0.02	1.01
17.5 - 18.5	0.02	0.01	0.00	0.00	0.00	0.00	0.01	0.01	0.04	0.03	0.09	0.41	0.07	0.01	0.02	0.02	0.74
18.5 - 19.5	0.01	0.00	0.00	0.00	0.00	0.00	0.00	0.01	0.03	0.02	0.07	0.26	0.05	0.01	0.01	0.01	0.47
19.5 - 20.5	0.01	0.00	0.00	0.00	0.00	0.00	0.00	0.00	0.01	0.01	0.05	0.20	0.03	0.00	0.01	0.00	0.34
20.5 - 21.5	0.01	0.00	0.00	0.00	0.00	0.00	0.00	0.00	0.01	0.00	0.03	0.12	0.02	0.00	0.01	0.00	0.22
21.5 - 22.5	0.01	0.00	0.00	0.00	0.00	0.00	0.00	0.00	0.01	0.01	0.02	0.09	0.01	0.00	0.00	0.00	0.15
22.5 - 23.5	0.00	0.00	0.00	0.00	0.00	0.00	0.00	0.00	0.00	0.00	0.01	0.07	0.01	0.00	0.00	0.00	0.10
23.5 - 24.5	0.00	0.00	0.00	0.00	0.00	0.00	0.00	0.00	0.00	0.00	0.01	0.05	0.01	0.00	0.00	0.00	0.08
$>$ 24.5	0.00	0.00	0.00	0.00	0.00	0.00	0.00	0.00	0.00	0.00	0.02	0.07	0.01	0.00	0.00	0.00	0.11

Table 19: Distribution of simulated project-average wind speed by direction.

11.5 Project-average Long-term Gross Power Capacity Assessment

11.5.1 Monthly-mean Variability of Power Capacity

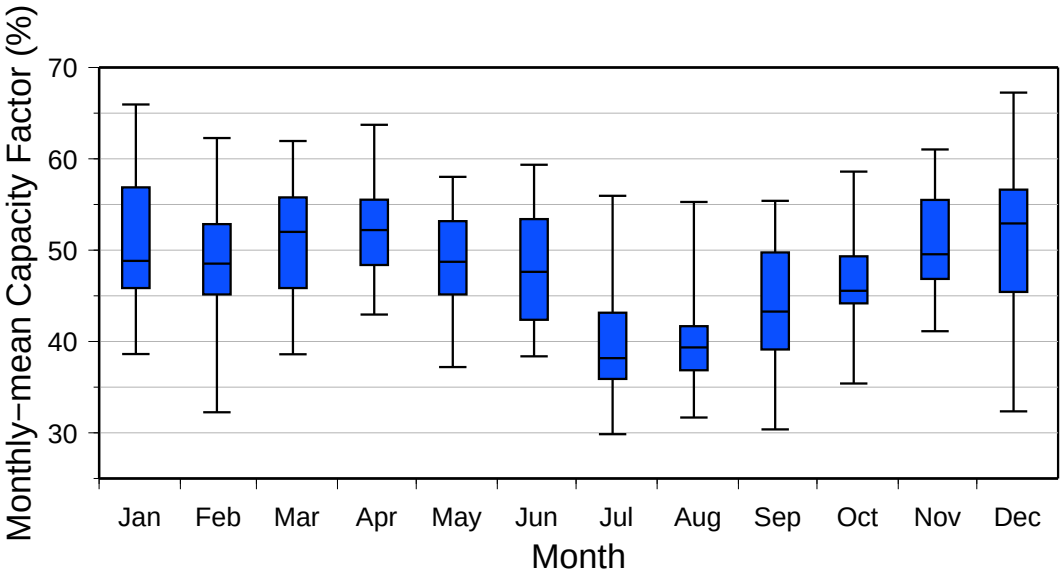

Figure 26: Box-and-whisker plot of monthly-mean project-average gross power capacity. This figure displays the expected variability of monthly-mean project-average gross power capacities. Median power capacity denoted by solid line within the shaded box. Upper and lower boundaries of the shaded box correspond to the 75% and 25% quartiles, while the whiskers denote the maximum and minimum monthly-mean power capacities.

11.5.2 Annual-mean Variability of Power Capacity

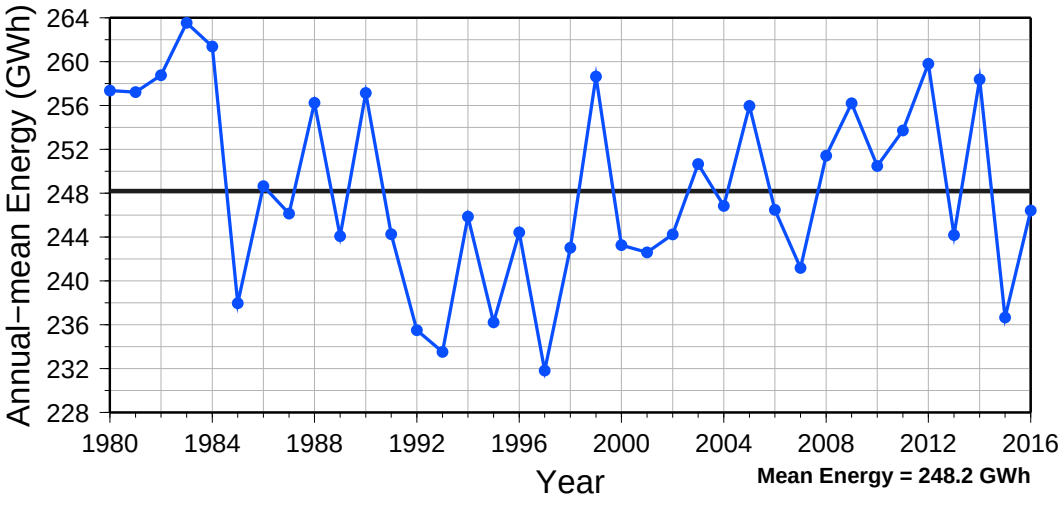

Figure 27: Time series of annual-mean project-average gross energy. Black line denotes the long-term mean.

11.5.3 Power Direction Distribution

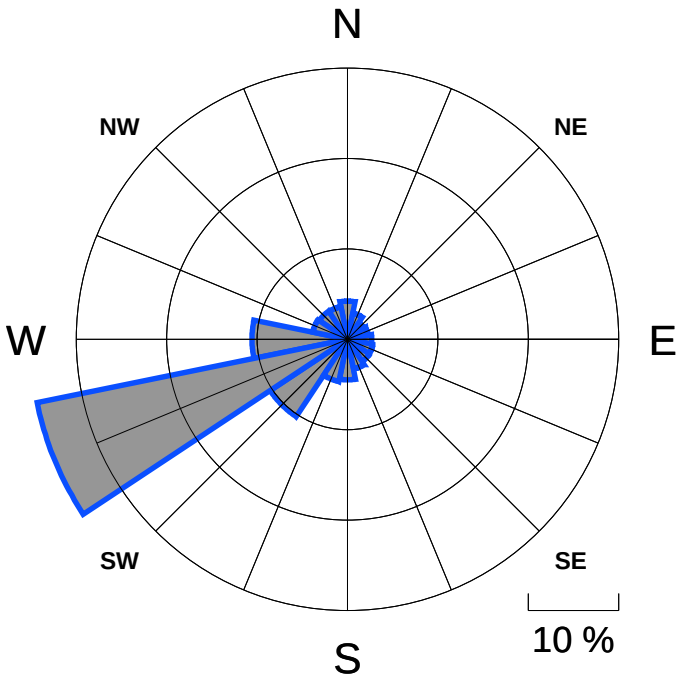

Figure 28: Annual power rose of the hourly-mean project-average gross capacity factor time series. Power rose shows the percent of total power within each sector. Directional bins are 22.5° wide, and the radial contour interval is 10%.

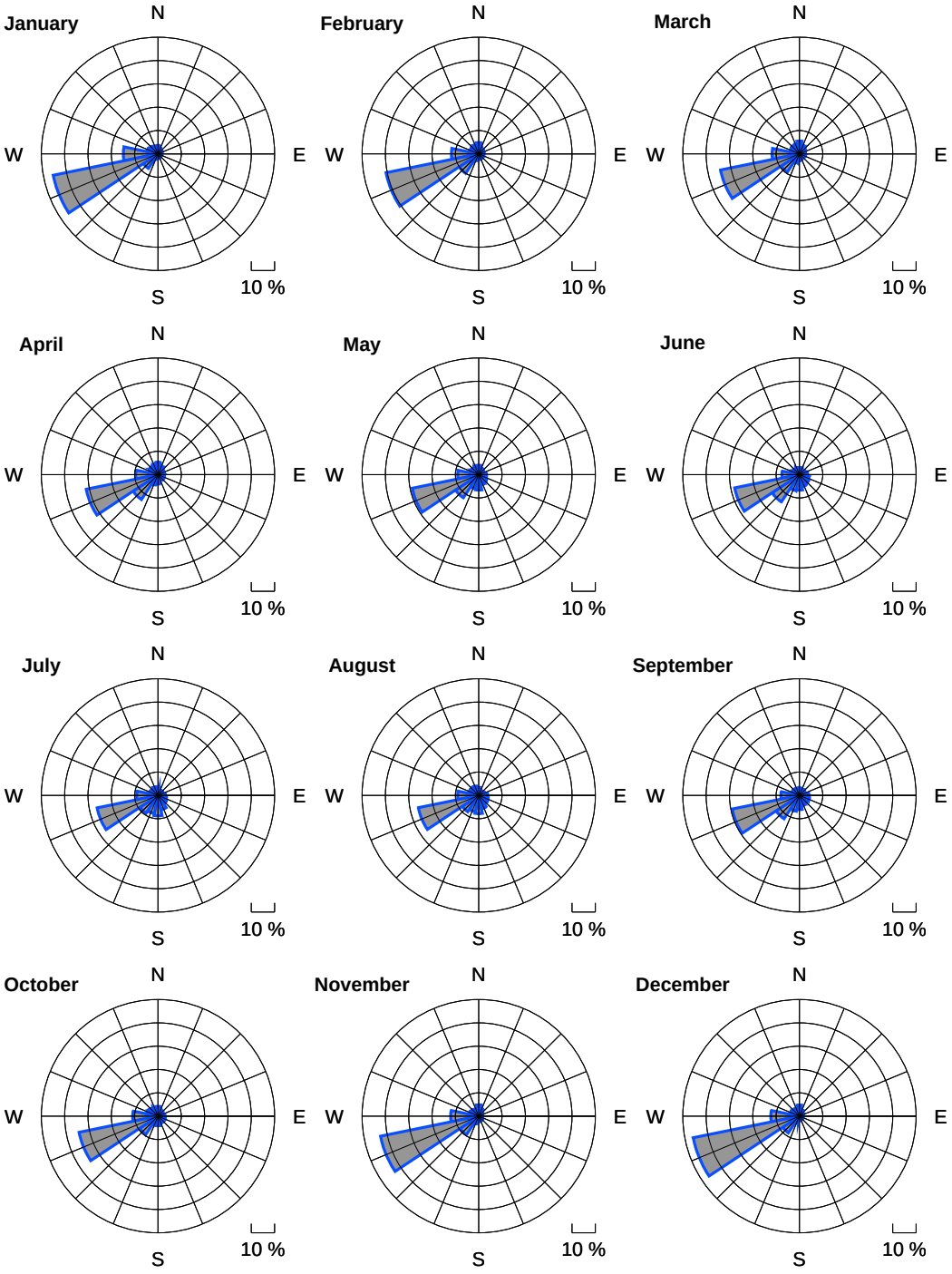

Figure 29: Power roses of the hourly-mean project-average gross capacity factor time series for each calendar month. Directional bins are 22.5° wide, and the radial contour interval is 10%.

11.5.4 Diurnal Variability of Power Capacity

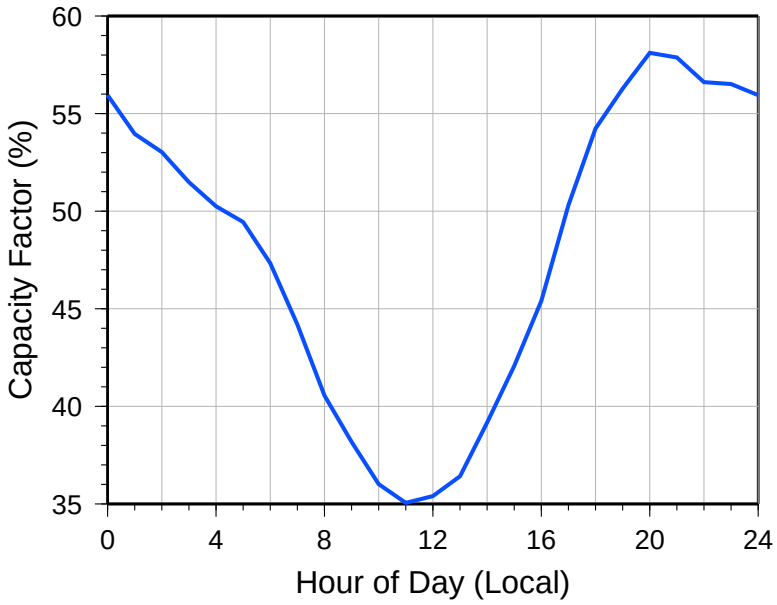

Figure 30: Diurnal cycle of simulated project-average gross power capacity. The horizontal axis is Mountain Time Zone.

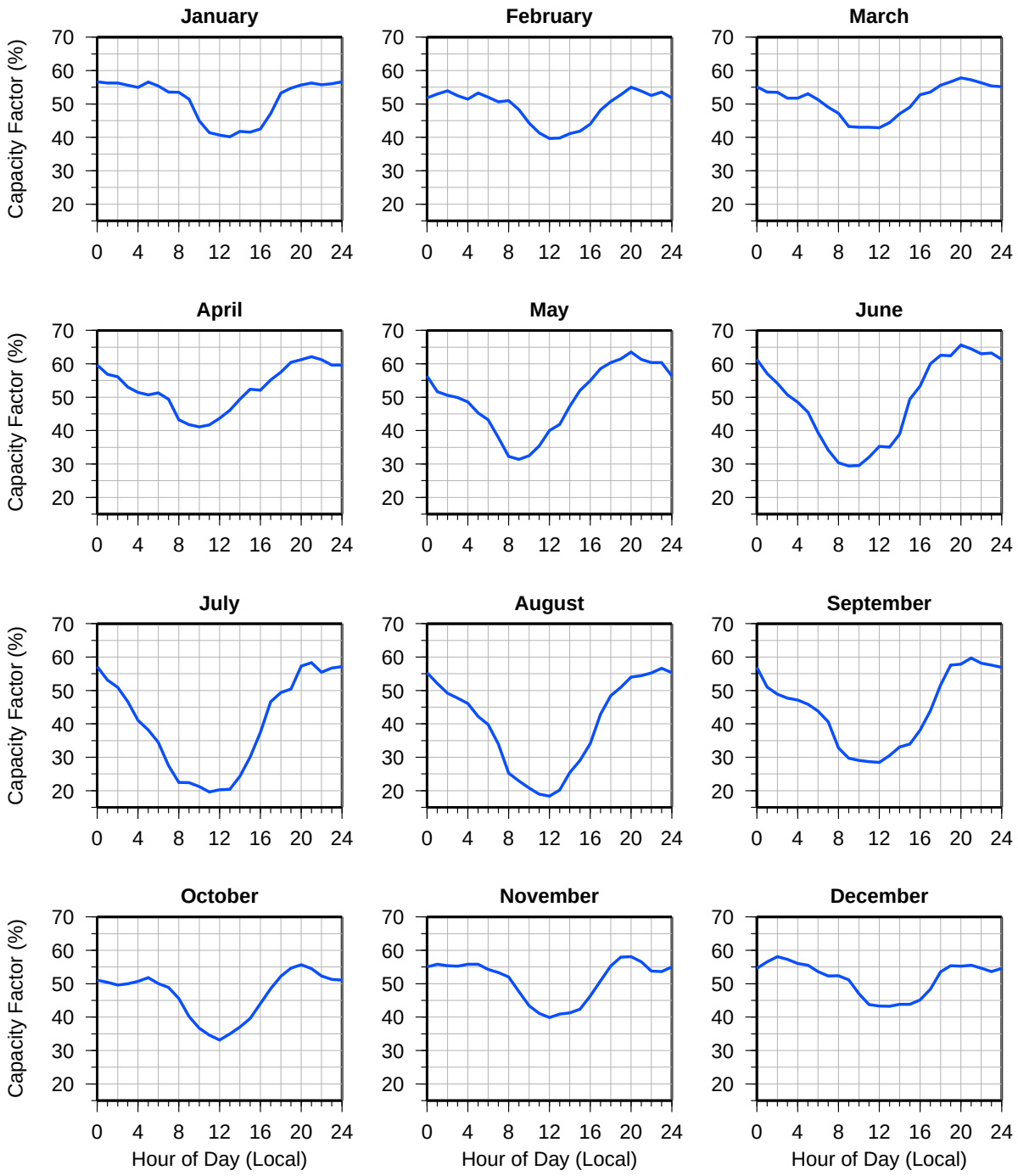

Figure 31: Diurnal cycle of simulated project-average gross power capacity for each calendar month. The horizontal axis is Mountain Time Zone.

11.5.5 Power Capacity Variability and ENSO

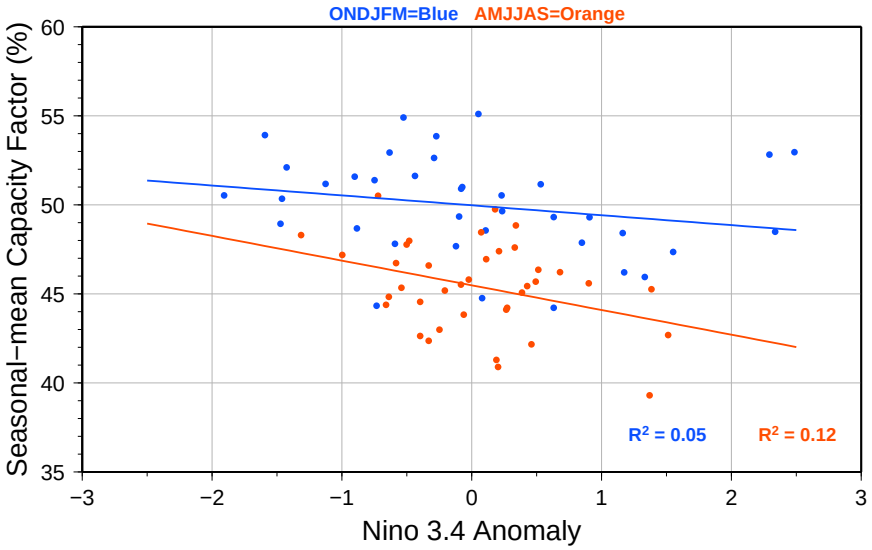

Figure 32: Scatter plot of Niño 3.4 anomalies vs. 6-month seasonal-mean gross power capacity. Blue dots denote the mean during ONDJFM (October, November, December, January, February, and March); orange dots denote the mean during AMJJAS (April, May, June, July, August and September).

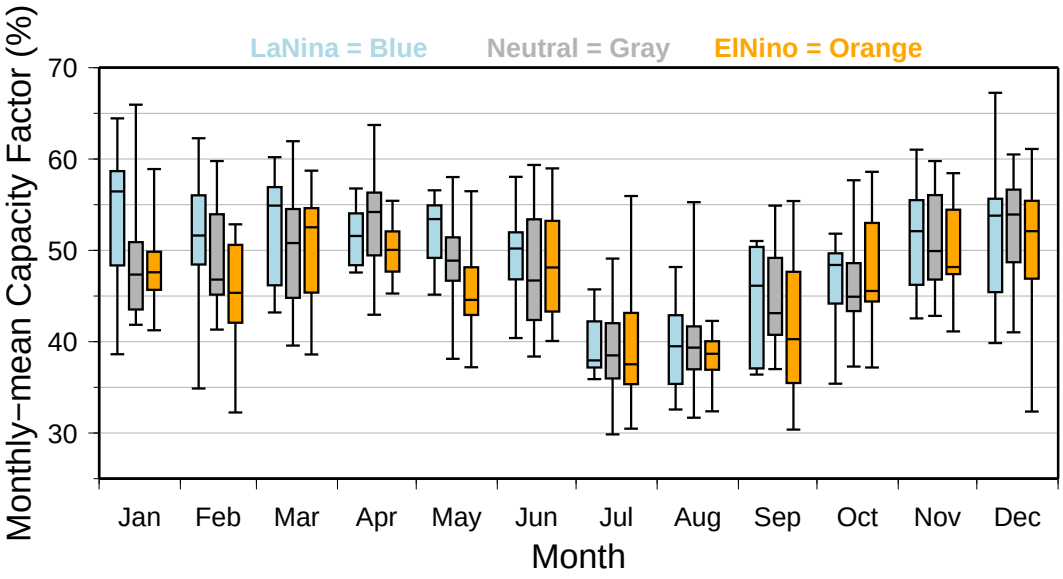

Figure 33: Box-and-whisker plot of monthly-mean project-average gross power capacity for La Niña (blue), neutral (gray), and El Niño (orange) phases of ENSO. Median power capacity denoted by solid line within the shaded box. Upper and lower boundaries of the shaded box correspond to the 75% and 25% quartiles, while the whiskers denote the maximum and minimum power capacities.

11.5.6 Tabular Data

Hour of Day (Local)	Jan	Feb	Mar	Apr	May	Jun	Jly	Aug	Sep	Oct	Nov	Dec	Avg
0	56.6	51.8	55.2	59.7	56.3	61.3	57.1	55.3	57.0	51.1	55.0	54.6	55.9
1	56.3	53.0	53.6	56.9	51.7	57.1	53.1	52.1	51.0	50.4	55.8	56.6	54.0
2	56.3	54.0	53.5	56.1	50.6	54.1	50.9	49.1	48.8	49.6	55.4	58.1	53.0
3	55.6	52.5	51.7	53.1	49.9	50.7	46.7	47.7	47.7	50.0	55.3	57.3	51.5
4	55.0	51.4	51.8	51.4	48.6	48.5	41.0	46.1	47.2	50.7	55.8	56.1	50.3
5	56.6	53.3	53.0	50.7	45.3	45.5	38.2	42.3	45.9	51.8	55.9	55.6	49.4
6	55.4	52.0	51.3	51.3	43.3	39.4	34.5	39.8	43.9	50.1	54.3	53.7	47.3
7	53.6	50.6	49.1	49.4	37.9	34.2	27.5	34.0	40.6	48.9	53.3	52.3	44.2
8	53.5	51.0	47.2	43.2	32.3	30.4	22.5	25.3	32.8	45.6	52.0	52.4	40.6
9	51.4	48.3	43.3	41.8	31.4	29.4	22.4	22.9	29.7	40.2	47.7	51.1	38.2
10	44.9	44.3	43.0	41.1	32.5	29.6	21.2	20.8	29.0	36.7	43.4	47.0	36.0
11	41.4	41.4	43.0	41.7	35.4	32.0	19.6	19.0	28.7	34.6	41.1	43.8	35.1
12	40.7	39.7	42.9	43.7	40.0	35.3	20.2	18.4	28.5	33.2	39.9	43.3	35.4
13	40.2	39.8	44.4	46.1	41.9	35.1	20.4	20.2	30.5	34.9	40.9	43.2	36.4
14	41.8	41.1	47.0	49.4	47.3	39.0	24.3	25.4	33.0	37.0	41.3	43.9	39.2
15	41.6	41.9	49.0	52.4	52.1	49.4	30.0	29.1	33.9	39.6	42.4	43.8	42.1
16	42.5	44.0	52.8	52.1	55.0	53.4	37.5	34.1	38.1	44.1	46.4	45.1	45.4
17	47.0	48.0	53.5	54.7	58.6	60.4	47.0	43.0	43.8	48.1	50.9	48.7	50.3
18	53.5	50.6	55.7	57.1	60.3	62.6	49.8	48.5	51.5	52.0	55.4	53.7	54.2
19	55.0	52.5	56.5	60.6	61.0	62.8	50.8	50.6	57.6	54.5	58.0	55.4	56.3
20	55.7	55.1	57.7	61.3	63.0	65.7	57.6	54.0	58.0	55.4	58.4	55.4	58.1
21	56.4	53.6	57.2	61.9	61.0	64.7	58.7	54.2	59.9	54.2	56.7	55.8	57.9
22	55.8	52.3	56.1	61.5	59.6	63.7	56.0	54.8	58.2	52.2	53.9	54.9	56.6
23	56.3	53.2	55.2	59.9	59.8	63.7	57.0	56.4	57.6	51.4	53.6	53.9	56.5
Avg	51.0	49.0	51.0	52.4	48.9	48.7	39.3	39.3	43.9	46.5	50.9	51.5	47.7

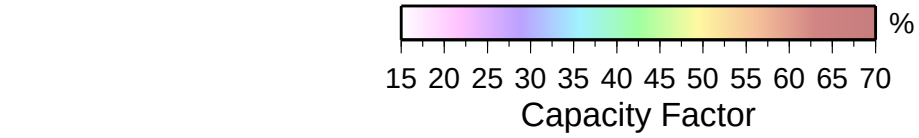

Figure 34: Hourly-mean values of simulated project-average gross capacity factor. Vertical axis is local time.

Year	Jan	Feb	Mar	Apr	May	Jun	Jly	Aug	Sep	Oct	Nov	Dec	Avg
1980	46.8	46.8	62.0	45.3	50.5	59.0	39.9	55.3	48.6	43.4	46.8	48.7	49.4
1981	41.9	51.9	53.4	55.4	53.2	53.4	41.4	35.4	40.8	57.7	52.1	56.6	49.4
1982	62.3	49.3	52.6	54.3	44.4	44.6	45.9	37.3	47.0	53.0	48.3	57.1	49.7
1983	49.8	52.8	55.9	52.1	48.3	51.4	48.8	41.1	51.3	48.5	59.4	48.4	50.6
1984	45.9	56.9	49.1	60.5	48.9	52.0	43.3	36.8	46.5	50.5	55.5	57.4	50.2
1985	38.6	48.1	56.9	48.4	45.1	42.7	37.2	44.8	50.8	44.6	50.6	41.0	45.7
1986	57.1	47.7	45.9	55.8	48.9	42.3	49.1	39.2	55.4	45.4	54.5	32.3	47.8
1987	58.9	45.4	54.1	50.6	48.1	42.3	56.0	40.0	34.6	37.2	48.1	51.5	47.3
1988	56.1	43.0	51.4	50.5	56.6	46.8	37.9	48.2	49.8	35.4	61.0	53.8	49.2
1989	63.0	34.9	55.2	47.6	49.2	40.4	42.0	42.6	44.5	46.8	53.3	41.9	46.9
1990	65.9	46.8	41.3	46.8	57.1	59.4	36.4	42.2	39.8	53.6	58.4	44.8	49.4
1991	43.5	44.9	58.0	51.6	57.9	53.2	37.6	34.4	43.4	45.2	48.0	45.4	46.9
1992	48.9	51.3	45.4	47.7	40.4	38.4	40.5	37.0	49.2	42.2	42.8	59.4	45.2
1993	43.3	41.3	39.6	49.5	42.9	54.7	46.6	41.7	38.7	37.3	49.2	53.5	44.8
1994	49.4	57.3	44.8	55.5	46.7	46.7	36.0	36.9	42.8	44.4	58.5	49.1	47.2
1995	47.5	43.2	53.2	52.0	46.7	45.1	38.4	39.2	36.7	49.7	53.0	39.8	45.4
1996	52.0	51.3	46.2	54.3	51.4	39.4	33.2	33.4	42.5	45.2	47.2	67.3	46.9
1997	56.4	44.2	49.4	44.3	37.2	43.3	43.1	32.4	35.5	48.0	47.4	52.7	44.5
1998	56.9	40.8	45.2	45.3	56.5	58.1	35.9	32.6	43.8	48.4	51.1	45.4	46.7
1999	54.5	62.3	50.9	54.1	54.9	48.4	45.7	42.9	37.1	44.2	46.2	55.6	49.7
2000	48.4	56.0	43.2	52.9	52.0	52.0	37.9	39.4	46.1	46.4	42.5	44.6	46.7
2001	44.3	48.6	39.6	56.3	41.3	50.9	45.5	42.2	37.0	51.8	45.3	56.6	46.6
2002	50.9	50.6	50.8	57.7	48.9	50.3	30.5	42.3	47.7	39.9	41.1	52.9	46.9
2003	42.5	42.1	58.7	63.7	47.2	42.4	40.2	40.1	41.2	45.1	56.0	58.2	48.1
2004	48.0	46.3	44.3	48.1	58.0	41.9	32.1	40.1	50.2	58.6	45.7	55.4	47.4
2005	47.6	45.2	54.5	54.1	48.0	57.1	38.5	34.0	52.7	43.3	59.8	55.6	49.2
2006	64.4	48.4	57.8	61.4	38.1	45.8	31.7	31.7	36.8	47.0	49.1	56.1	47.3
2007	42.8	54.0	47.0	48.8	44.2	42.4	30.0	40.0	50.4	51.8	44.0	61.2	46.3
2008	59.1	52.5	54.9	50.2	54.8	46.7	37.2	39.3	39.1	44.4	46.2	55.0	48.3
2009	57.5	58.3	56.2	61.7	45.3	52.2	34.0	40.1	39.3	53.0	46.9	46.9	49.2
2010	45.7	32.3	51.0	52.3	55.7	55.5	42.2	46.9	50.4	44.5	49.5	50.2	48.1
2011	48.8	55.2	53.9	56.8	56.1	56.9	41.4	39.0	36.4	43.6	54.7	43.0	48.7
2012	56.9	51.2	60.2	49.5	50.9	59.2	35.4	40.0	30.4	46.5	58.2	60.5	49.9
2013	46.7	46.2	47.3	42.9	47.5	51.6	36.8	37.4	54.9	48.6	48.6	54.4	46.9
2014	58.7	57.1	55.8	57.8	50.0	57.3	35.9	41.5	43.1	41.3	56.5	41.8	49.6
2015	41.2	46.0	38.6	55.4	44.7	40.1	37.5	37.2	41.2	45.6	57.3	61.1	45.4
2016	48.6	50.6	54.6	45.5	48.6	39.7	43.4	34.9	51.0	49.3	52.1	49.8	47.3
2017	45.9	59.8	59.0	53.8	43.7	46.0	29.8	33.7	40.8				--
Avg	51.0	49.0	51.0	52.4	48.9	48.7	39.3	39.3	43.9	46.5	50.9	51.5	**47.7**

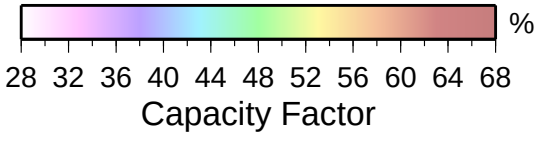

Figure 35: Monthly-mean values of simulated project-average gross capacity factor.

Sector	Mean Capacity Factor(%)	Percent Total Power(%)
N	40.9	4.2
NNE	30.3	2.9
NE	22.9	2.2
ENE	21.5	2.3
E	22.8	2.7
ESE	26.0	2.9
SE	31.1	2.9
SSE	38.8	3.3
S	51.1	4.5
SSW	53.0	4.8
SW	62.7	10.3
WSW	76.9	35.0
W	54.9	10.6
WNW	36.7	3.9
NW	39.0	3.7
NNW	40.2	3.7
ALL	**47.7**	**100.0**

Table 20: Simulated project-average gross mean power capacity factor and percent of total power. Blank values correspond to times with less than 10 data points.

Power Capacity (%)	N	NNE	NE	ENE	E	ESE	SE	SSE	S	SSW	SW	WSW	W	WNW	NW	NNW	All
0 - 5%	1.00	1.30	1.56	1.75	1.65	1.31	0.98	0.82	0.67	0.61	0.69	0.97	0.75	0.74	0.76	0.82	16.35
5% - 15%	0.79	0.91	1.03	1.20	1.33	1.21	0.89	0.66	0.50	0.51	0.65	0.87	0.95	0.84	0.76	0.72	13.84
15% - 25%	0.54	0.57	0.60	0.72	0.84	0.80	0.64	0.49	0.37	0.39	0.56	0.85	0.87	0.72	0.60	0.51	10.08
25% - 35%	0.34	0.35	0.34	0.42	0.50	0.51	0.44	0.33	0.28	0.28	0.45	0.81	0.78	0.59	0.44	0.37	7.25
35% - 45%	0.30	0.27	0.25	0.26	0.34	0.36	0.33	0.29	0.23	0.23	0.41	0.80	0.66	0.46	0.36	0.29	5.84
45% - 55%	0.26	0.20	0.18	0.20	0.23	0.26	0.25	0.22	0.20	0.18	0.38	0.81	0.59	0.35	0.28	0.25	4.83
55% - 65%	0.21	0.16	0.13	0.14	0.17	0.18	0.19	0.18	0.19	0.18	0.36	0.83	0.56	0.32	0.24	0.21	4.24
65% - 75%	0.20	0.15	0.10	0.11	0.14	0.14	0.16	0.17	0.16	0.17	0.38	0.89	0.55	0.28	0.20	0.17	3.99
75% - 85%	0.20	0.13	0.09	0.10	0.11	0.14	0.14	0.18	0.20	0.20	0.44	1.15	0.59	0.24	0.18	0.18	4.27
85% - 95%	0.27	0.17	0.10	0.10	0.11	0.15	0.18	0.23	0.29	0.31	0.74	2.41	0.81	0.21	0.21	0.24	6.52
95% - 100%	0.81	0.42	0.22	0.19	0.19	0.21	0.29	0.52	1.10	1.21	2.74	11.34	2.05	0.34	0.55	0.63	22.79

Table 21: Distribution of simulated project-average gross power capacity by direction.

11.6 Long-term Wind Resource Assessment for Tower M0571 at 80 m

11.6.1 Tabular Data

Sector	Mean Speed(m/s)	Weibull Scale(A)	Weibull Shape(k)	Frequency(%)
N	6.84	7.71	1.91	4.84
NNE	5.69	6.41	1.88	4.57
NE	4.97	5.59	1.86	4.60
ENE	4.96	5.59	1.93	5.05
E	5.14	5.80	2.07	5.66
ESE	5.38	6.08	2.10	5.60
SE	5.82	6.57	2.11	4.86
SSE	6.62	7.47	2.00	4.21
S	7.93	8.94	1.93	4.08
SSW	7.81	8.81	2.07	4.23
SW	9.21	10.40	2.33	9.22
WSW	10.47	11.77	2.73	22.91
W	7.84	8.86	2.21	8.01
WNW	5.92	6.69	2.15	4.01
NW	6.36	7.17	1.93	3.97
NNW	6.67	7.52	1.94	4.17
ALL	**7.52**	**8.48**	**1.93**	**100.00**

Table 22: Simulated mean wind speed, Weibull parameters, and frequency for Tower M0571 at 80 m. Blank values correspond to times with less than 10 data points.

Wind Speed (m/s)	N	NNE	NE	ENE	E	ESE	SE	SSE	S	SSW	SW	WSW	W	WNW	NW	NNW	All
0 - 0.5	0.01	0.03	0.05	0.08	0.09	0.07	0.03	0.01	0.00	0.00	0.00	0.00	0.00	0.00	0.00	0.01	0.40
0.5 - 1.5	0.15	0.22	0.27	0.27	0.24	0.24	0.19	0.10	0.05	0.04	0.04	0.03	0.04	0.05	0.07	0.09	2.08
1.5 - 2.5	0.28	0.39	0.51	0.49	0.43	0.40	0.34	0.29	0.22	0.16	0.14	0.14	0.16	0.17	0.19	0.23	4.54
2.5 - 3.5	0.44	0.57	0.65	0.73	0.71	0.63	0.47	0.39	0.35	0.33	0.33	0.34	0.38	0.38	0.41	0.40	7.52
3.5 - 4.5	0.56	0.66	0.75	0.83	0.94	0.85	0.66	0.48	0.40	0.43	0.50	0.63	0.71	0.64	0.55	0.53	10.12
4.5 - 5.5	0.58	0.63	0.70	0.83	0.96	0.93	0.70	0.51	0.39	0.46	0.71	1.01	1.01	0.76	0.64	0.56	11.37
5.5 - 6.5	0.52	0.53	0.54	0.62	0.81	0.80	0.68	0.50	0.36	0.44	0.82	1.36	1.12	0.75	0.64	0.51	10.99
6.5 - 7.5	0.50	0.44	0.40	0.46	0.58	0.66	0.61	0.46	0.37	0.40	0.92	1.74	1.03	0.51	0.46	0.44	9.98
7.5 - 8.5	0.44	0.34	0.28	0.29	0.37	0.41	0.43	0.42	0.33	0.34	0.94	2.13	0.83	0.28	0.27	0.35	8.48
8.5 - 9.5	0.38	0.26	0.17	0.19	0.22	0.27	0.29	0.32	0.31	0.34	0.96	2.49	0.65	0.16	0.18	0.29	7.47
9.5 - 10.5	0.26	0.16	0.09	0.09	0.12	0.14	0.18	0.21	0.24	0.27	0.82	2.45	0.47	0.08	0.11	0.20	5.89
10.5 - 11.5	0.20	0.13	0.07	0.06	0.07	0.08	0.11	0.17	0.24	0.26	0.73	2.46	0.41	0.07	0.09	0.15	5.32
11.5 - 12.5	0.15	0.08	0.04	0.04	0.03	0.05	0.06	0.11	0.19	0.21	0.59	2.04	0.31	0.04	0.08	0.10	4.11
12.5 - 13.5	0.09	0.05	0.03	0.02	0.02	0.02	0.04	0.07	0.15	0.16	0.43	1.59	0.22	0.02	0.06	0.08	3.05
13.5 - 14.5	0.07	0.03	0.02	0.01	0.02	0.02	0.02	0.05	0.12	0.12	0.33	1.20	0.18	0.02	0.05	0.05	2.30
14.5 - 15.5	0.06	0.02	0.01	0.01	0.01	0.01	0.02	0.03	0.10	0.10	0.24	0.88	0.13	0.02	0.04	0.04	1.70
15.5 - 16.5	0.04	0.02	0.01	0.01	0.01	0.01	0.01	0.03	0.07	0.07	0.18	0.67	0.11	0.01	0.03	0.03	1.32
16.5 - 17.5	0.03	0.01	0.01	0.00	0.00	0.01	0.01	0.02	0.06	0.04	0.15	0.49	0.07	0.01	0.03	0.03	0.97
17.5 - 18.5	0.03	0.01	0.00	0.00	0.00	0.00	0.01	0.02	0.05	0.03	0.11	0.37	0.06	0.01	0.02	0.02	0.75
18.5 - 19.5	0.02	0.00	0.00	0.00	0.00	0.00	0.00	0.01	0.03	0.02	0.08	0.24	0.04	0.01	0.01	0.02	0.49
19.5 - 20.5	0.01	0.00	0.00	0.00	0.00	0.00	0.00	0.01	0.02	0.01	0.06	0.20	0.04	0.01	0.01	0.01	0.39
20.5 - 21.5	0.01	0.00	0.00	0.00	0.00	0.00	0.00	0.00	0.01	0.01	0.05	0.13	0.03	0.00	0.01	0.00	0.25
21.5 - 22.5	0.01	0.00	0.00	0.00	0.00	0.00	0.00	0.00	0.01	0.00	0.03	0.09	0.01	0.00	0.00	0.00	0.17
22.5 - 23.5	0.00	0.00	0.00	0.00	0.00	0.00	0.00	0.00	0.00	0.00	0.02	0.05	0.01	0.00	0.00	0.00	0.10
23.5 - 24.5	0.00	0.00	0.00	0.00	0.00	0.00	0.00	0.00	0.00	0.00	0.02	0.05	0.01	0.00	0.00	0.00	0.09
$>$ 24.5	0.00	0.00	0.00	0.00	0.00	0.00	0.00	0.00	0.00	0.00	0.04	0.11	0.00	0.00	0.00	0.00	0.18

Table 23: Distribution of simulated wind speed by direction for Tower M0571 at $80\,m$.

11.7 Long-term Wind Resource Assessment for Tower M4666 at 80 m

11.7.1 Tabular Data

Sector	Mean Speed(m/s)	Weibull Scale(A)	Weibull Shape(k)	Frequency(%)
N	5.79	6.51	1.78	4.22
NNE	5.73	6.45	1.86	5.20
NE	4.87	5.48	1.86	5.41
ENE	4.70	5.29	1.89	5.96
E	5.04	5.69	2.02	5.91
ESE	5.55	6.27	2.07	5.18
SE	6.00	6.78	2.05	4.54
SSE	6.44	7.26	1.92	3.82
S	7.12	8.00	1.80	3.95
SSW	6.80	7.67	1.95	5.27
SW	7.61	8.59	2.33	11.54
WSW	9.33	10.52	2.44	20.08
W	7.31	8.24	1.91	7.64
WNW	5.12	5.77	1.85	3.87
NW	5.80	6.48	1.64	3.72
NNW	5.71	6.41	1.77	3.71
ALL	**6.76**	**7.62**	**1.85**	**100.00**

Table 24: Simulated mean wind speed, Weibull parameters, and frequency for Tower M4666 at 80 m. Blank values correspond to times with less than 10 data points.

Wind Speed (m/s)	N	NNE	NE	ENE	E	ESE	SE	SSE	S	SSW	SW	WSW	W	WNW	NW	NNW	All
0 - 0.5	0.04	0.05	0.08	0.11	0.09	0.05	0.03	0.02	0.02	0.01	0.01	0.01	0.01	0.01	0.02	0.03	0.60
0.5 - 1.5	0.22	0.29	0.38	0.42	0.33	0.25	0.16	0.14	0.12	0.12	0.12	0.12	0.13	0.15	0.18	0.18	3.34
1.5 - 2.5	0.37	0.43	0.56	0.61	0.48	0.36	0.30	0.26	0.26	0.29	0.33	0.35	0.38	0.36	0.36	0.35	6.04
2.5 - 3.5	0.53	0.60	0.79	0.92	0.77	0.52	0.46	0.39	0.40	0.51	0.68	0.78	0.71	0.64	0.55	0.50	9.77
3.5 - 4.5	0.60	0.71	0.93	1.06	0.99	0.75	0.60	0.48	0.48	0.70	1.12	1.26	1.03	0.81	0.63	0.59	12.72
4.5 - 5.5	0.52	0.66	0.77	0.92	0.94	0.78	0.62	0.46	0.42	0.69	1.37	1.45	0.91	0.61	0.50	0.45	12.06
5.5 - 6.5	0.41	0.55	0.57	0.64	0.78	0.72	0.57	0.40	0.36	0.54	1.23	1.41	0.71	0.38	0.32	0.36	9.94
6.5 - 7.5	0.41	0.56	0.48	0.51	0.63	0.64	0.55	0.40	0.33	0.53	1.25	1.65	0.63	0.29	0.24	0.32	9.43
7.5 - 8.5	0.31	0.42	0.31	0.30	0.37	0.42	0.40	0.33	0.28	0.40	1.13	1.73	0.55	0.18	0.17	0.24	7.54
8.5 - 9.5	0.25	0.31	0.21	0.19	0.22	0.29	0.32	0.27	0.25	0.35	1.10	1.87	0.51	0.14	0.15	0.18	6.60
9.5 - 10.5	0.19	0.20	0.14	0.11	0.13	0.15	0.19	0.20	0.21	0.28	0.92	1.91	0.45	0.10	0.13	0.16	5.46
10.5 - 11.5	0.12	0.15	0.08	0.06	0.06	0.10	0.13	0.15	0.20	0.24	0.78	1.89	0.39	0.06	0.13	0.11	4.65
11.5 - 12.5	0.07	0.10	0.04	0.04	0.04	0.05	0.07	0.11	0.17	0.18	0.53	1.53	0.32	0.04	0.10	0.09	3.48
12.5 - 13.5	0.05	0.05	0.02	0.02	0.02	0.03	0.04	0.06	0.11	0.12	0.31	0.99	0.20	0.02	0.06	0.05	2.14
13.5 - 14.5	0.04	0.04	0.02	0.01	0.02	0.02	0.03	0.05	0.11	0.10	0.23	0.93	0.21	0.02	0.06	0.04	1.92
14.5 - 15.5	0.03	0.03	0.01	0.01	0.01	0.01	0.02	0.04	0.08	0.07	0.16	0.68	0.16	0.02	0.05	0.03	1.42
15.5 - 16.5	0.02	0.02	0.01	0.01	0.01	0.01	0.02	0.02	0.05	0.05	0.10	0.46	0.12	0.01	0.03	0.01	0.94
16.5 - 17.5	0.02	0.01	0.00	0.00	0.01	0.01	0.01	0.02	0.05	0.04	0.07	0.39	0.10	0.01	0.02	0.01	0.76
17.5 - 18.5	0.01	0.01	0.00	0.00	0.00	0.00	0.01	0.01	0.03	0.02	0.04	0.23	0.05	0.01	0.01	0.01	0.45
18.5 - 19.5	0.01	0.00	0.00	0.00	0.00	0.00	0.00	0.01	0.01	0.01	0.02	0.14	0.03	0.00	0.01	0.00	0.25
19.5 - 20.5	0.00	0.00	0.00	0.00	0.00	0.00	0.00	0.01	0.01	0.01	0.02	0.11	0.02	0.00	0.01	0.00	0.20
20.5 - 21.5	0.00	0.00	0.00	0.00	0.00	0.00	0.00	0.00	0.01	0.01	0.01	0.07	0.01	0.00	0.00	0.00	0.13
21.5 - 22.5	0.00	0.00	0.00	0.00	0.00	0.00	0.00	0.00	0.00	0.00	0.01	0.04	0.01	0.00	0.00	0.00	0.07
22.5 - 23.5	0.00	0.00	0.00	0.00	0.00	0.00	0.00	0.00	0.00	0.00	0.00	0.02	0.00	0.00	0.00	0.00	0.03
23.5 - 24.5	0.00	0.00	0.00	0.00	0.00	0.00	0.00	0.00	0.00	0.00	0.00	0.01	0.00	0.00	0.00	0.00	0.02
$>$ 24.5	0.00	0.00	0.00	0.00	0.00	0.00	0.00	0.00	0.00	0.00	0.00	0.02	0.00	0.00	0.00	0.00	0.04

Table 25: Distribution of simulated wind speed by direction for Tower M4666 at $80\,m$.

12 APPENDIX VALIDATION OF MODEL RESULTS

12.1 Validation of Model Results at Tower M0571

This section examines the quality of the NWP simulations used at a single point within the study area. For this section, the observations were taken at Tower M0571 (latitude 37.75192, longitude -104.45762).

The average observed wind speed (for all valid observational times) at $60\,m$ during the 63 months of the period of record (November, 2008 to January, 2014) is $7.52\,m/s$ with an hourly standard deviation of $4.10\,m/s$ at Tower M0571. This compares to a modeled $59.9\,m$ wind speed of $7.45\,m/s$ with a $3.83\,m/s$ standard deviation for these same times.

Based on a comparison of the NWP model output with observations from each of the meteorological towers for which data were provided, Model Output Statistics (MOS) was constructed. MOS uses a multilinear regression model designed to remove the bias and adjust the variance of the raw NWP simulated wind speed and direction. Applying this statistical model to the simulated data at Tower M0571 results in a MOS-corrected mean value of $7.52\,m/s$ and an hourly standard deviation of $4.10\,m/s$.

This section presents a comparison of the simulated winds with the observations at the reference tower (Tower M0571). The focus of the verification is on the model's ability to reproduce the observed variability of the wind resource at daily and monthly time scales, while preserving the distribution of hourly wind speeds and the diurnal characteristics of the wind.

12.1.1 Observational Data

Approximately 63 months of wind speed data at 60 $meters$ and wind direction data at 57 $meters$ (November, 2008 to January, 2014) from a meteorological tower (Tower M0571) at Busch Ranch II were used in this analysis. This tower will be referred to as the reference tower throughout this section. The data at 59.9 m were used to assess the quality of the model simulations at 59.9 m.

It should be noted that meteorological observations provided to Vaisala are not allowed to influence the raw model simulations.

12.1.2 Model Validation Statistics

Table 26 presents some basic statistical measures of the model performance relative to the measured winds at the reference tower during the observational period. Also shown are values (labeled "MOS-corrected") for model data with the statistical model applied. For reference, the correlation of the reference tower data to itself is perfect and hence the explained variance (r^2) value is 1.0.

The observed and modeled winds in this section represent the mean of all times during the month for which a valid wind speed or direction observation was available. Therefore they should not be interpreted as estimates of the true winds at the site, but rather a verification of the model's ability to reproduce the available observations. Any month or hour missing greater than 50% of the available observations is omitted from the following figures, tables, and statistics.

Comparison	Value
Correlation of monthly-mean simulated wind speed to observed	0.96
RMS error of monthly-mean simulated wind speed	0.33 m/s
Correlation of monthly-mean MOS-corrected wind speed to observed	0.98
RMS error of monthly-mean MOS-corrected wind speed	0.25 m/s
Correlation of daily-mean simulated wind speed to observed	0.88
RMS error of daily-mean simulated wind speed	1.39 m/s
Correlation of daily-mean MOS-corrected wind speed to observed	0.90
RMS error of daily-mean MOS-corrected wind speed	1.28 m/s

Table 26: Correlation and root mean square (RMS) error statistics of modeled wind speeds.

12.1.3 Monthly Mean Wind Speed

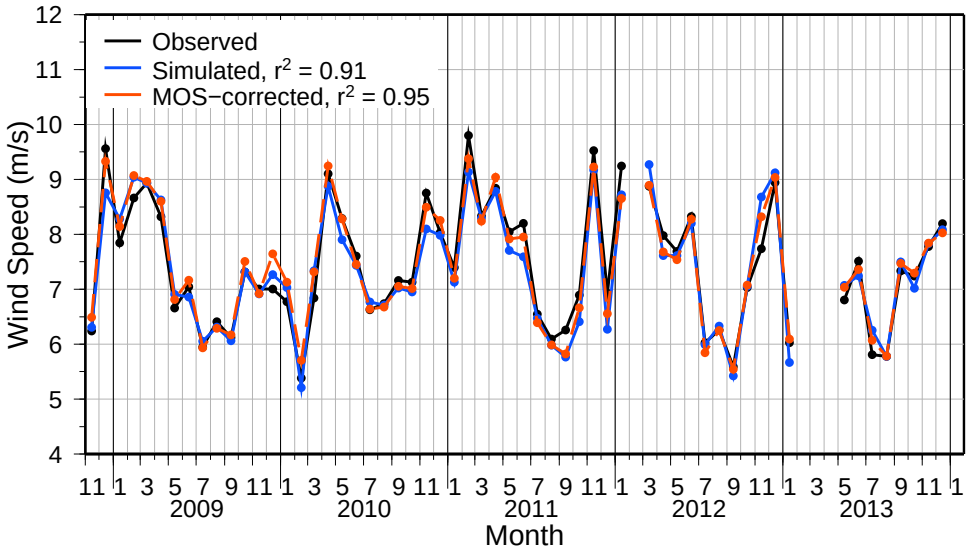

Figure 36: A comparison of the observed, simulated, and MOS-corrected monthly-mean $59.9\,m$ wind speed at Tower M0571. Explained variance(r^2) value of each data source relative to the monthly reference tower wind speeds are shown in the legend. Months missing greater than 50% of the available observations are not plotted. Tabular formatted data are available in Table 27 (p. 73).

12.1.4 Wind Speed Distribution

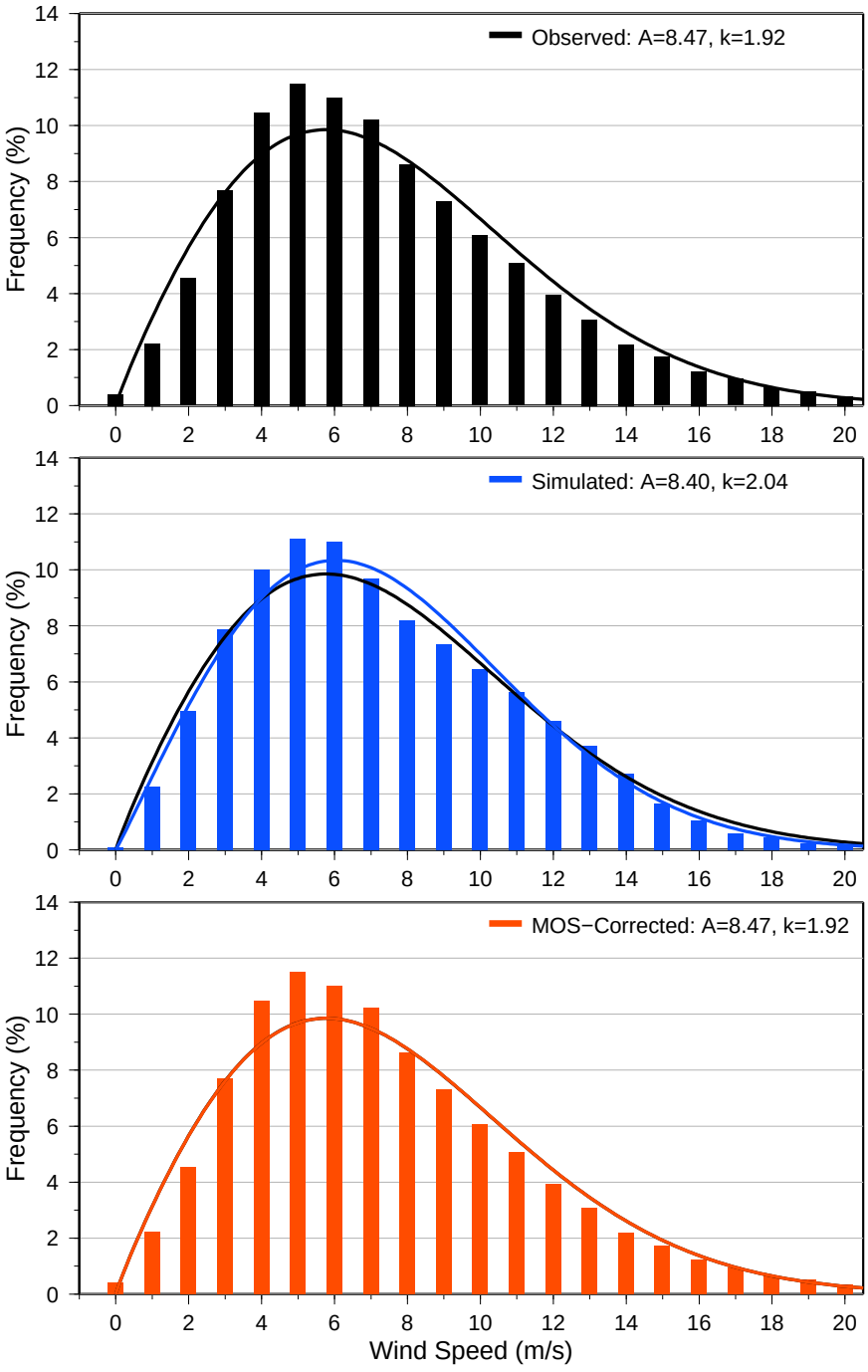

Figure 37: A comparison of the observed, simulated, and MOS-corrected hourly wind speed distributions at $59.9\,m$ at Tower M0571 during the period of record, using $1\,m/s$ bins. ($0\,m/s$ bin contains only values ≤ 0.5) Fitted Weibull distributions are also displayed with the scale(A) and shape(k) parameters listed in the legend. Tabular formatted data are available in Tables 28 and 29 (p. 76 and 77).

12.1.5 Wind Direction Distribution

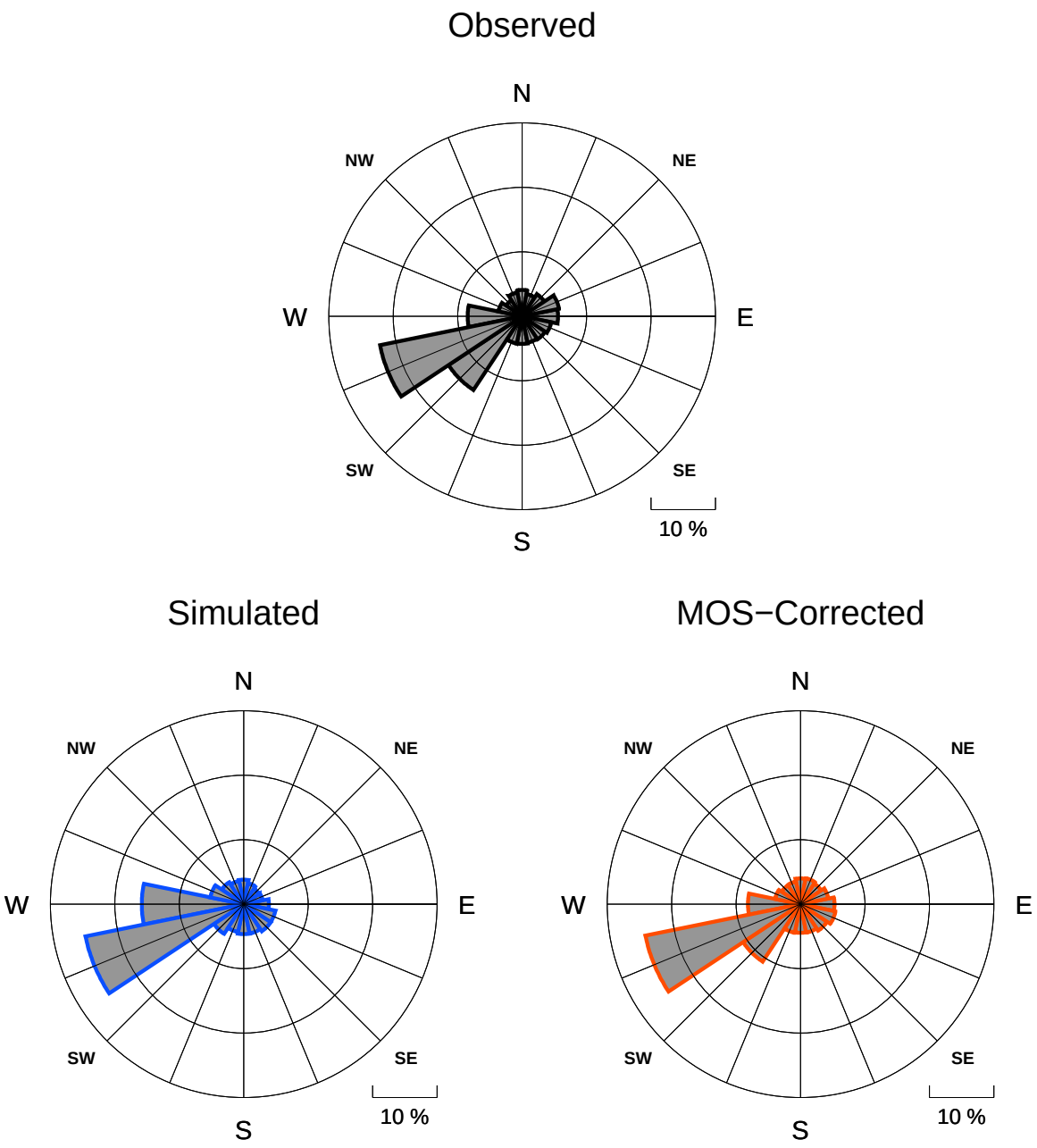

Figure 38: Wind roses at 56.5 m at Tower M0571 for observational data and simulated model data, averaged over the period of record (November, 2008–January, 2014). Directional bins are 22.5° wide, and the radial contour interval is 10%. Tabular formatted data, including mean wind speed values and Weibull parameters for each wind direction sector, are available in Tables 30 and 31 (p. 78).

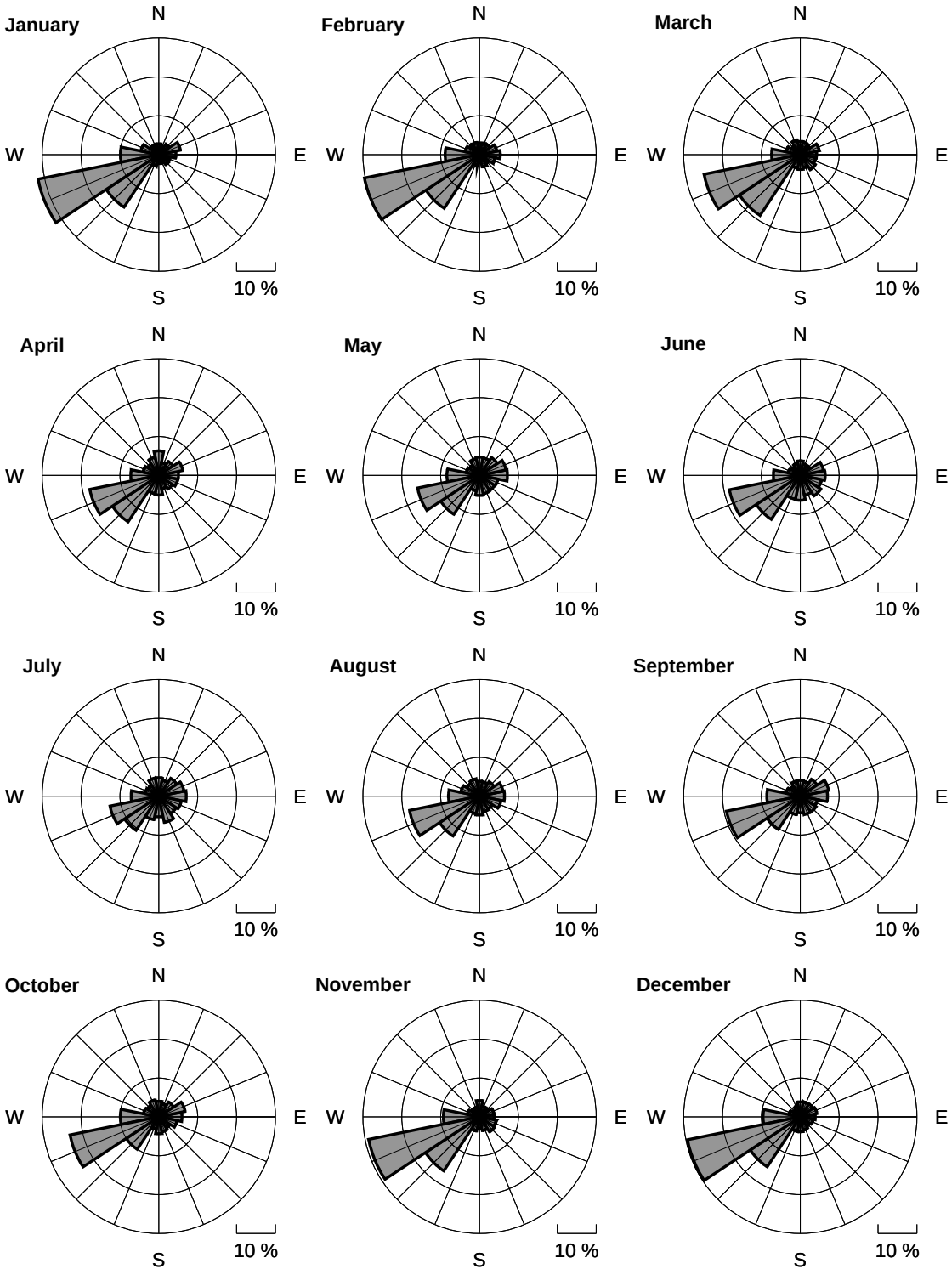

Figure 39: Wind rose of observed wind direction at 56.5 m at Tower M0571 for each calendar month. Directional bins are 22.5° wide, and the radial contour interval is 10%. Months missing greater than 50% of the available observations are not plotted.

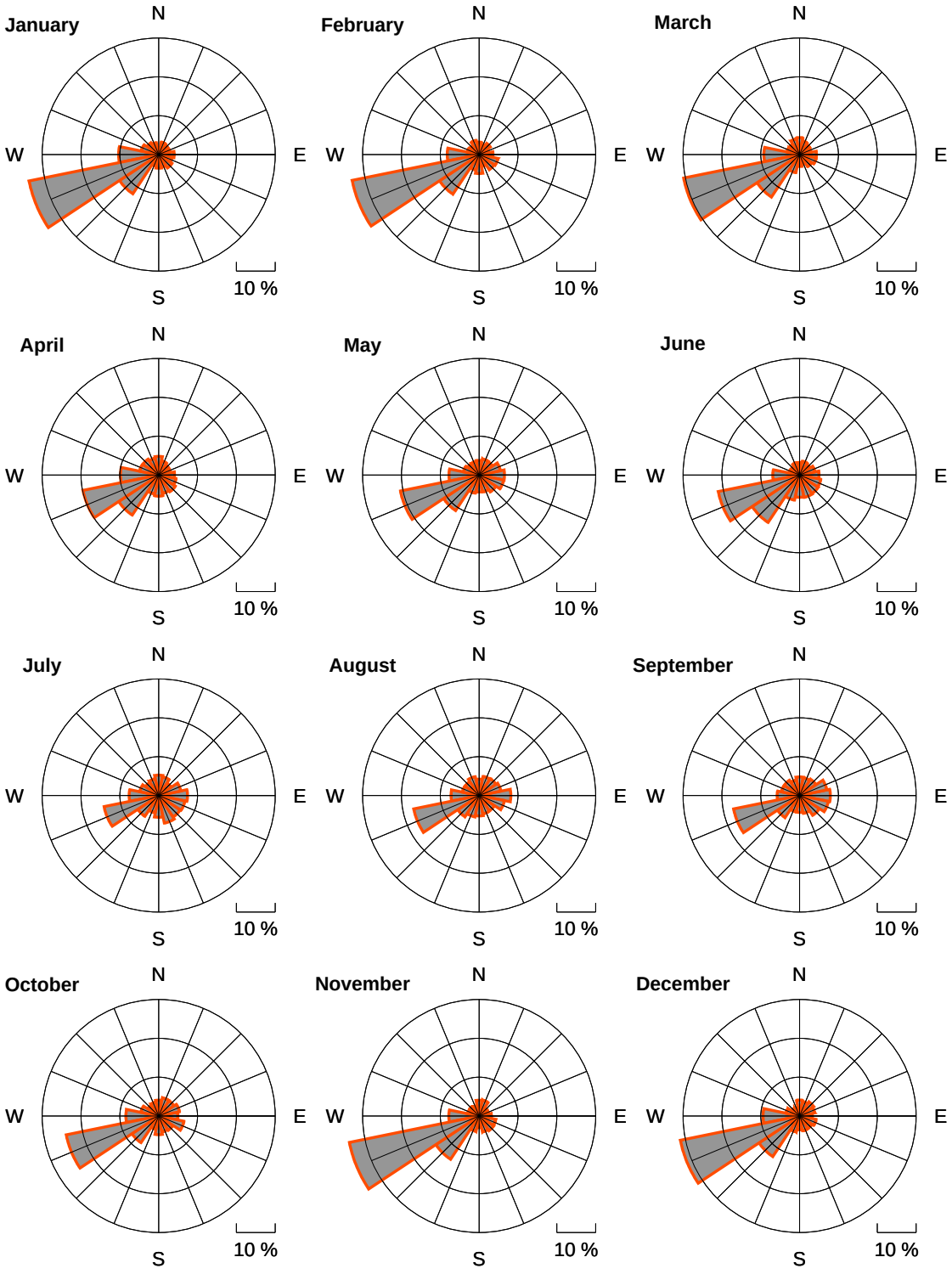

Figure 40: Wind rose of MOS-corrected wind direction at 56.5 m at Tower M0571 for each calendar month. Directional bins are 22.5° wide, and the radial contour interval is 10%. Months missing greater than 50% of the available observations are not plotted.

12.1.6 Diurnal Variability of Wind Speed

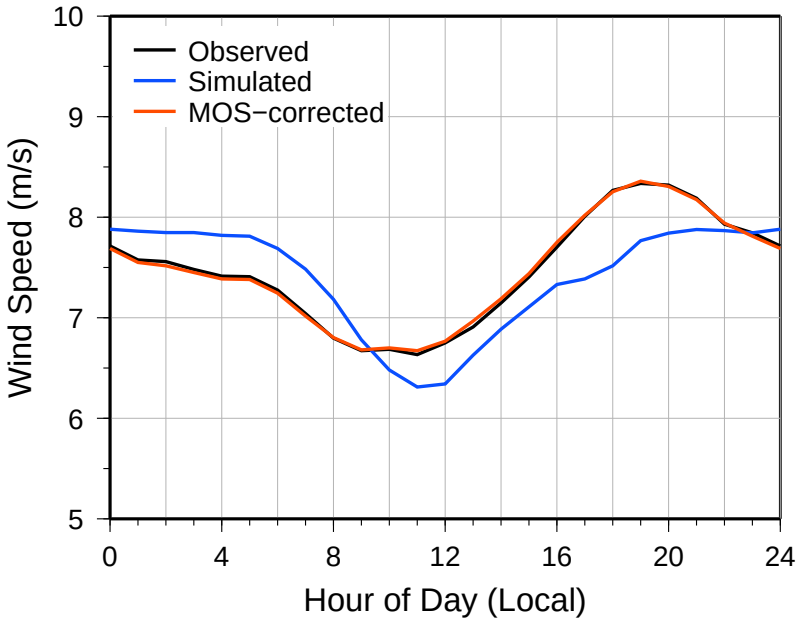

Figure 41: A comparison of the diurnal cycle of observed, simulated, and MOS-corrected 59.9 m wind speed at Tower M0571. Data are averaged over the period of record (November, 2008–January, 2014). Hours missing greater than 15% of the available observations are not plotted. The horizontal axis is Mountain Time Zone. Tabular formatted data are available in Figures 43 and 44 (p. 74 and 75).

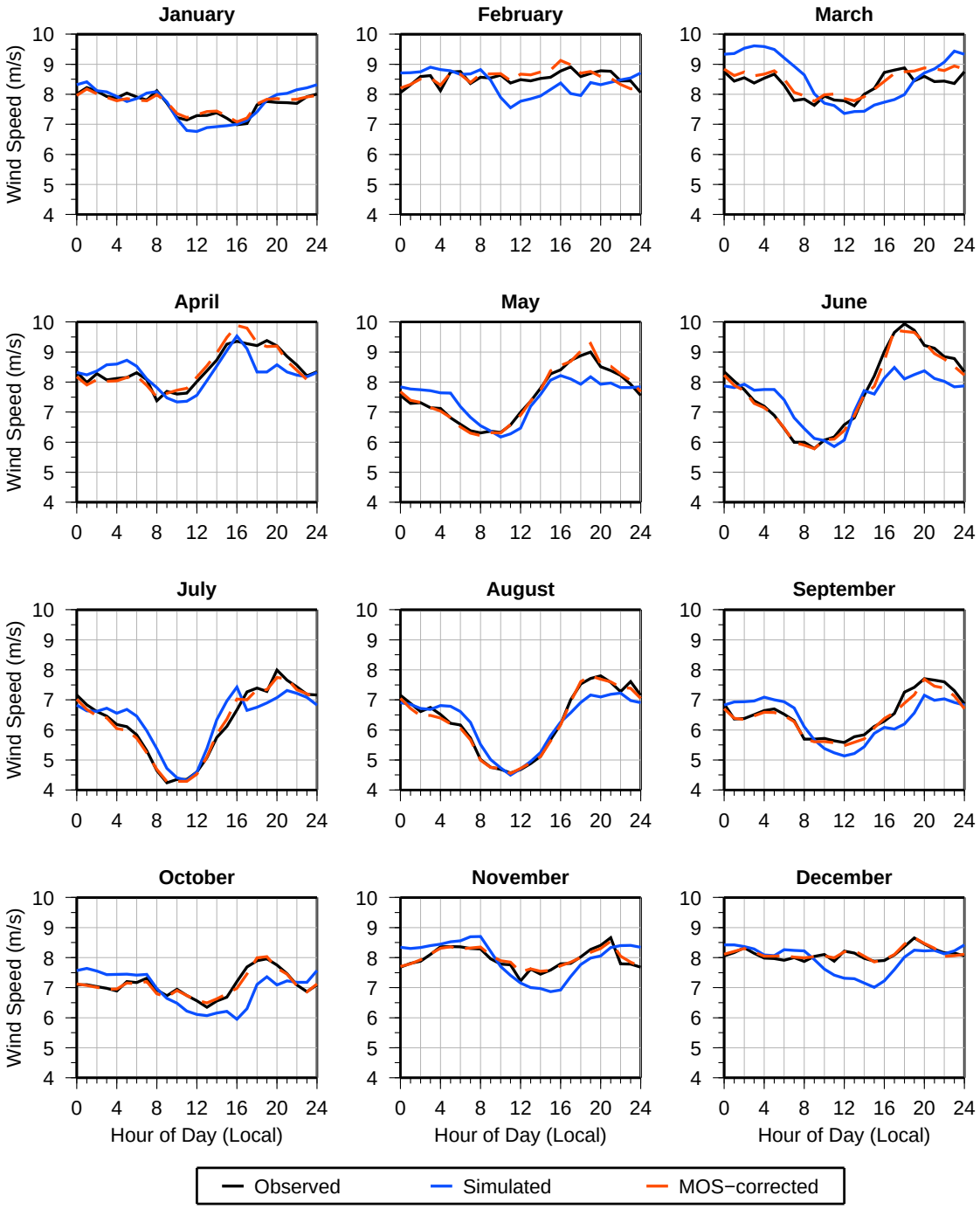

Figure 42: A comparison of the diurnal cycle of observed, simulated, and MOS-corrected $59.9\,m$ wind speed for each calendar month at Tower M0571. Hours missing greater than 50% of the available observations are not plotted. The horizontal axis is Mountain Time Zone. Tabular formatted data available in Figures 43 and 44 (p. 74 and 75).

12.1.7 Tabular Data

Month	Observed	Simulated	Bias	MOS-corrected	Availability(%)
11/2008	6.24	6.31	0.07	6.49	70.7
12/2008	9.56	8.76	-0.80	9.33	96.5
01/2009	7.84	8.28	0.43	8.14	99.6
02/2009	8.66	9.04	0.38	9.07	100.0
03/2009	8.93	8.93	-0.00	8.96	94.0
04/2009	8.32	8.63	0.31	8.60	97.4
05/2009	6.66	6.91	0.25	6.81	100.0
06/2009	7.04	6.86	-0.18	7.17	99.9
07/2009	5.94	6.05	0.11	5.93	99.6
08/2009	6.41	6.31	-0.10	6.29	99.9
09/2009	6.12	6.06	-0.06	6.17	100.0
10/2009	7.31	7.32	0.00	7.51	79.3
11/2009	7.00	6.92	-0.09	6.92	93.5
12/2009	7.01	7.27	0.26	7.64	93.4
01/2010	6.77	7.03	0.26	7.13	94.6
02/2010	5.38	5.21	-0.17	5.71	84.7
03/2010	6.84	7.34	0.50	7.32	83.9
04/2010	9.10	8.88	-0.22	9.24	98.6
05/2010	8.29	7.90	-0.39	8.28	100.0
06/2010	7.61	7.43	-0.17	7.45	99.7
07/2010	6.63	6.77	0.14	6.64	100.0
08/2010	6.74	6.71	-0.03	6.68	99.9
09/2010	7.16	7.02	-0.14	7.05	100.0
10/2010	7.13	6.95	-0.17	7.01	100.0
11/2010	8.75	8.10	-0.66	8.49	98.5
12/2010	8.03	7.98	-0.05	8.25	92.5
01/2011	7.39	7.13	-0.26	7.20	85.8
02/2011	9.80	9.13	-0.66	9.38	81.4
03/2011	8.34	8.29	-0.04	8.24	93.3
04/2011	8.84	8.78	-0.05	9.04	97.6
05/2011	8.04	7.71	-0.34	7.92	99.9
06/2011	8.20	7.59	-0.61	7.95	99.9
07/2011	6.55	6.47	-0.08	6.39	99.7
08/2011	6.09	5.98	-0.11	5.99	100.0
09/2011	6.26	5.76	-0.49	5.82	100.0
10/2011	6.89	6.41	-0.48	6.66	94.4
11/2011	9.53	9.17	-0.35	9.23	97.9
12/2011	6.93	6.27	-0.66	6.56	96.4
01/2012	9.24	8.72	-0.52	8.65	75.8
02/2012	12.48	12.04	-0.45	12.18	36.9
03/2012	8.88	9.27	0.40	8.89	98.9
04/2012	7.98	7.61	-0.36	7.68	97.5
05/2012	7.69	7.61	-0.08	7.54	100.0
06/2012	8.32	8.20	-0.12	8.27	99.6
07/2012	6.03	5.99	-0.04	5.84	99.9
08/2012	6.26	6.33	0.07	6.25	99.9

Table 27: Monthly-mean 59.9 m wind speeds (m/s) at Tower M0571. Time series graph of data is available in Figure 36 (p. 65). (continued on next page)

Month	Observed	Simulated	Bias	MOS-corrected	Availability(%)
09/2012	5.59	5.42	-0.17	5.54	99.9
10/2012	7.03	7.05	0.02	7.08	93.0
11/2012	7.74	8.68	0.94	8.32	97.4
12/2012	8.94	9.12	0.17	9.04	98.5
01/2013	6.03	5.67	-0.36	6.09	53.4
02/2013	–	–	–	–	0.0
03/2013	–	–	–	–	0.0
04/2013	6.55	6.41	-0.14	6.38	28.2
05/2013	6.81	7.07	0.27	7.04	96.5
06/2013	7.51	7.25	-0.27	7.36	99.9
07/2013	5.81	6.25	0.45	6.07	99.9
08/2013	5.78	5.78	0.00	5.78	96.8
09/2013	7.33	7.50	0.16	7.47	100.0
10/2013	7.24	7.02	-0.22	7.29	97.8
11/2013	7.78	7.83	0.05	7.84	86.1
12/2013	8.20	8.08	-0.11	8.03	86.7
01/2014	9.01	9.19	0.18	9.00	45.3
All	**7.52**	**7.45**	**-0.07**	**7.52**	**89.0**

Table 27: Monthly-mean 59.9 m wind speeds (m/s) at Tower M0571. Time series graph of data is available in Figure 36 (p. 65). The average values shown at the bottom of the table, labeled 'All', are computed as the mean of monthly means.

Observed = mean of all available wind speed observations
Simulated = mean of simulated model output for times with observations
Bias = Simulated – Observed
MOS-corrected = mean of MOS-corrected output for times with observations

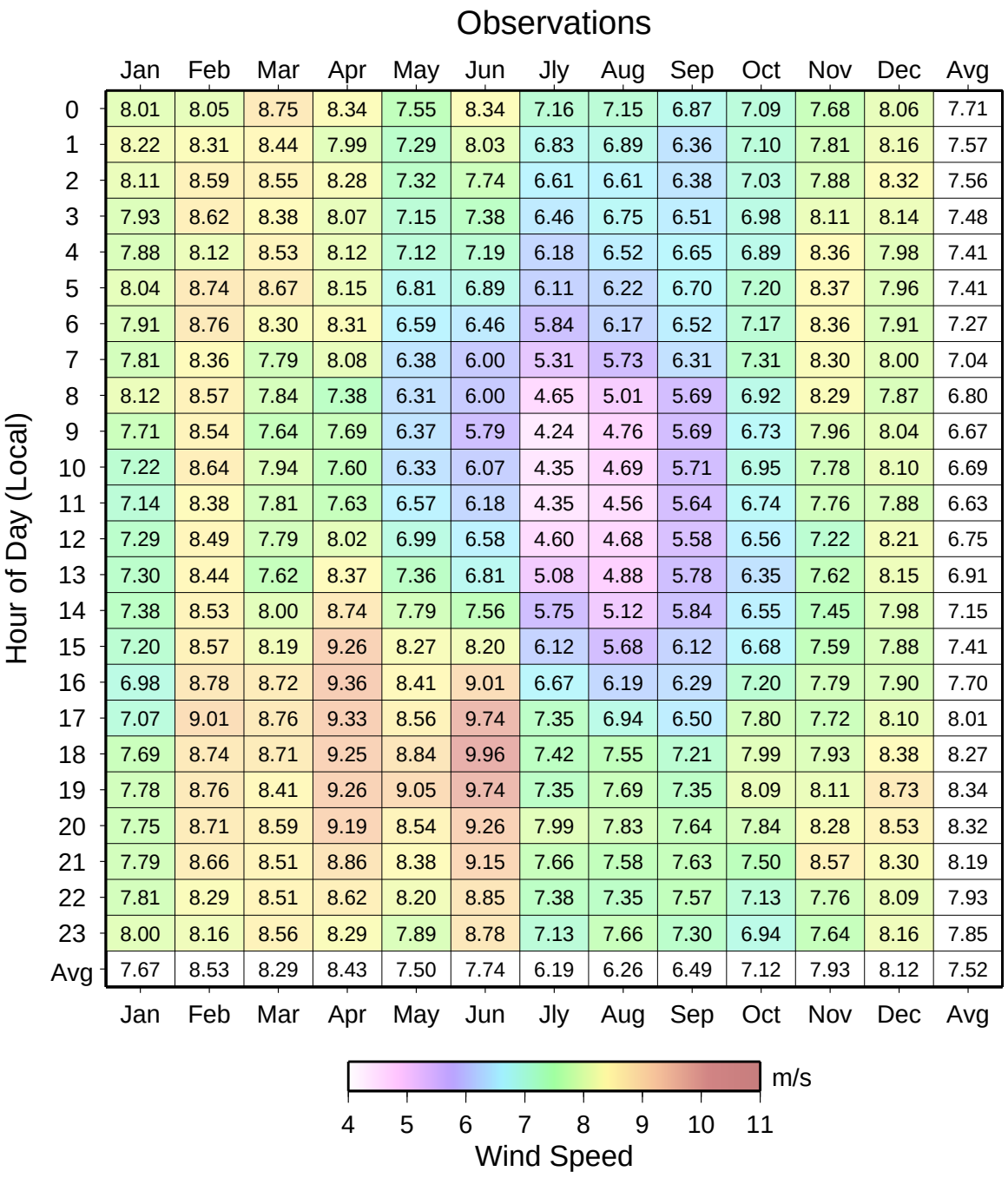

Figure 43: Hourly-mean values of observed $59.9\,m$ wind speed at Tower M0571. Hours missing greater than 50% of the available observations are not plotted. The vertical axis is Mountain Time Zone. Time series graphs of data are available in Figures 41 and 42 (p. 70 and 71).

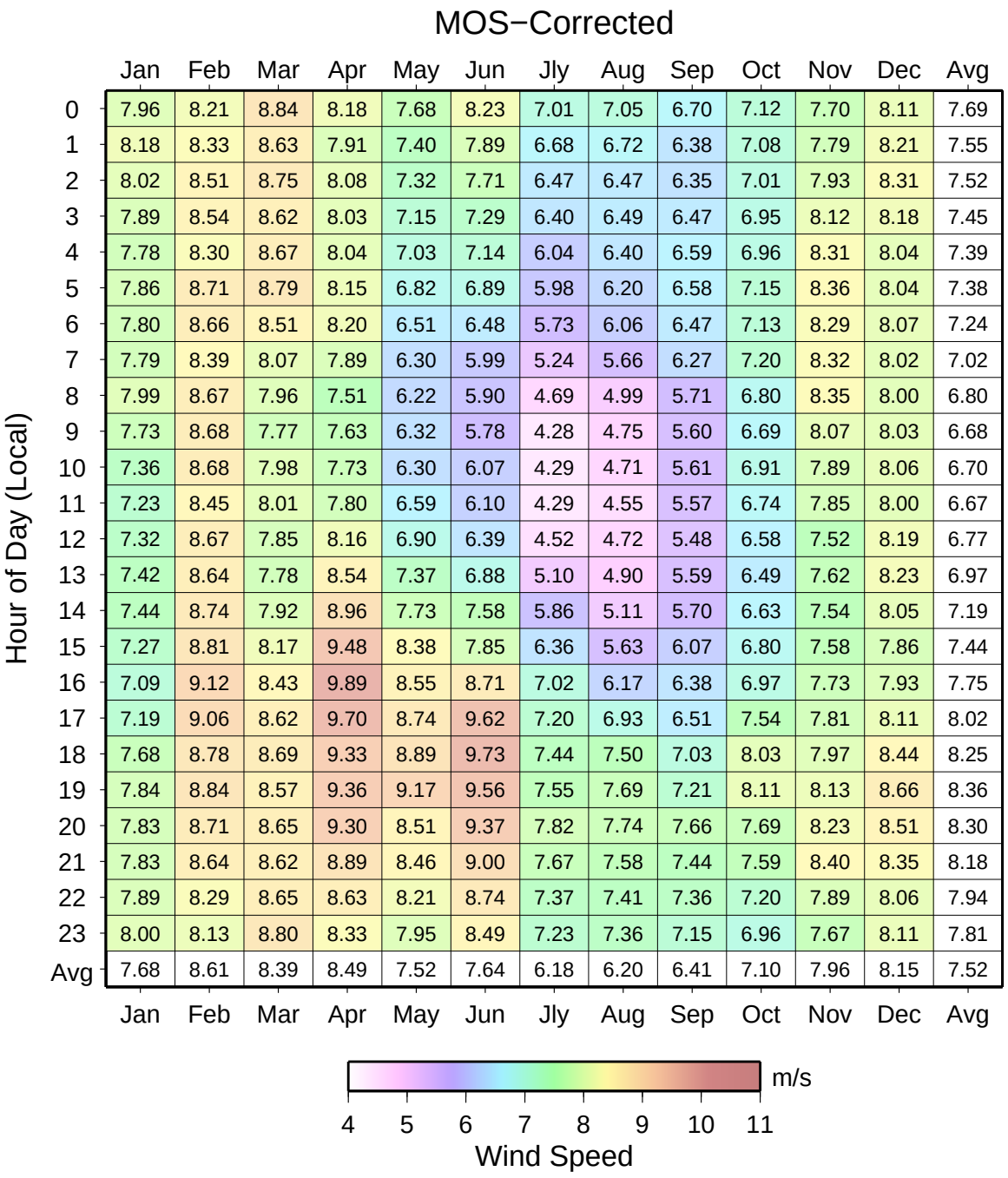

Figure 44: Hourly-mean values of MOS-corrected $59.9\,m$ wind speed at Tower M0571. Hours missing greater than 50% of the available observations are not plotted. The vertical axis is Mountain Time Zone. Time series graphs of data are available in Figures 41 and 42 (p. 70 and 71).

Wind Speed (m/s)	N	NNE	NE	ENE	E	ESE	SE	SSE	S	SSW	SW	WSW	W	WNW	NW	NNW	All
0 - 0.5	0.02	0.01	0.01	0.02	0.03	0.02	0.03	0.03	0.03	0.01	0.03	0.05	0.02	0.01	0.02	0.03	0.40
0.5 - 1.5	0.11	0.12	0.15	0.09	0.12	0.14	0.11	0.18	0.12	0.17	0.17	0.13	0.15	0.15	0.16	0.12	2.21
1.5 - 2.5	0.26	0.24	0.24	0.25	0.27	0.26	0.23	0.25	0.28	0.28	0.35	0.41	0.40	0.30	0.24	0.25	4.51
2.5 - 3.5	0.39	0.40	0.39	0.51	0.59	0.49	0.37	0.37	0.28	0.39	0.58	0.85	0.66	0.55	0.39	0.40	7.63
3.5 - 4.5	0.51	0.50	0.61	0.79	0.69	0.65	0.46	0.46	0.41	0.42	0.78	1.30	1.15	0.67	0.51	0.50	10.41
4.5 - 5.5	0.43	0.48	0.57	0.87	0.85	0.78	0.61	0.45	0.36	0.46	1.03	1.72	1.23	0.69	0.41	0.48	11.43
5.5 - 6.5	0.39	0.38	0.45	0.85	0.89	0.69	0.53	0.45	0.37	0.42	1.22	1.92	1.04	0.52	0.36	0.46	10.94
6.5 - 7.5	0.37	0.36	0.50	0.70	0.75	0.55	0.51	0.41	0.36	0.37	1.37	2.11	0.79	0.32	0.29	0.38	10.16
7.5 - 8.5	0.29	0.29	0.36	0.64	0.59	0.42	0.49	0.39	0.30	0.36	1.22	1.91	0.61	0.18	0.21	0.30	8.56
8.5 - 9.5	0.32	0.22	0.28	0.49	0.33	0.28	0.29	0.36	0.31	0.32	1.12	1.91	0.50	0.11	0.13	0.26	7.26
9.5 - 10.5	0.23	0.14	0.24	0.26	0.25	0.16	0.24	0.29	0.31	0.25	0.97	1.87	0.44	0.09	0.09	0.20	6.04
10.5 - 11.5	0.21	0.11	0.14	0.17	0.12	0.06	0.20	0.19	0.30	0.24	0.93	1.74	0.40	0.06	0.05	0.11	5.04
11.5 - 12.5	0.13	0.08	0.07	0.11	0.05	0.04	0.11	0.10	0.23	0.15	0.77	1.60	0.32	0.03	0.03	0.08	3.92
12.5 - 13.5	0.12	0.06	0.05	0.04	0.03	0.02	0.06	0.09	0.20	0.14	0.61	1.30	0.22	0.01	0.04	0.07	3.05
13.5 - 14.5	0.08	0.04	0.01	0.02	0.00	0.01	0.03	0.07	0.13	0.12	0.52	0.90	0.16	0.01	0.02	0.04	2.16
14.5 - 15.5	0.09	0.02	0.02	0.02	0.00	0.01	0.02	0.03	0.09	0.08	0.47	0.73	0.10	0.01	0.01	0.04	1.73
15.5 - 16.5	0.05	0.02	0.01	0.00	0.00	0.00	0.00	0.01	0.08	0.04	0.31	0.56	0.10	0.01	0.00	0.01	1.22
16.5 - 17.5	0.04	0.01	0.00	0.00	0.00	0.00	0.00	0.02	0.05	0.03	0.30	0.39	0.08	0.01	0.00	0.01	0.95
17.5 - 18.5	0.02	0.00	0.00	0.00	0.00	0.00	0.00	0.00	0.03	0.04	0.23	0.29	0.04	0.00	0.00	0.00	0.64
18.5 - 19.5	0.01	0.00	0.00	0.00	0.00	0.00	0.00	0.00	0.00	0.01	0.18	0.26	0.03	0.00	0.00	0.00	0.51
19.5 - 20.5	0.01	0.00	0.00	0.00	0.00	0.00	0.00	0.00	0.01	0.01	0.13	0.13	0.01	0.00	0.00	0.00	0.33
20.5 - 21.5	0.00	0.00	0.00	0.00	0.00	0.00	0.00	0.00	0.00	0.00	0.10	0.14	0.00	0.00	0.00	0.00	0.26
21.5 - 22.5	0.00	0.00	0.00	0.00	0.00	0.00	0.00	0.00	0.00	0.00	0.09	0.09	0.00	0.00	0.00	0.00	0.19
22.5 - 23.5	0.00	0.00	0.00	0.00	0.00	0.00	0.00	0.00	0.00	0.00	0.07	0.05	0.00	0.00	0.00	0.00	0.13
23.5 - 24.5	0.00	0.00	0.00	0.00	0.00	0.00	0.00	0.00	0.00	0.00	0.07	0.04	0.00	0.00	0.00	0.00	0.11
> 24.5	0.00	0.00	0.00	0.00	0.00	0.00	0.00	0.00	0.00	0.00	0.10	0.10	0.00	0.00	0.00	0.00	0.19

Table 28: Distribution of observed 59.9 *m* wind speed by direction at Tower M0571. Histogram of data is available in Figure 37 (p. 66).

Wind Speed (m/s)	N	NNE	NE	ENE	E	ESE	SE	SSE	S	SSW	SW	WSW	W	WNW	NW	NNW	All
0 - 0.5	0.02	0.03	0.06	0.07	0.09	0.06	0.02	0.01	0.00	0.01	0.00	0.01	0.00	0.00	0.00	0.00	0.40
0.5 - 1.5	0.15	0.25	0.27	0.27	0.26	0.22	0.23	0.12	0.06	0.03	0.03	0.03	0.03	0.05	0.07	0.13	2.21
1.5 - 2.5	0.30	0.40	0.48	0.44	0.40	0.46	0.34	0.31	0.22	0.15	0.13	0.10	0.14	0.17	0.22	0.23	4.52
2.5 - 3.5	0.42	0.52	0.60	0.64	0.71	0.66	0.52	0.42	0.41	0.38	0.36	0.35	0.42	0.44	0.41	0.38	7.65
3.5 - 4.5	0.52	0.65	0.61	0.82	0.88	0.89	0.69	0.43	0.39	0.46	0.58	0.86	0.83	0.67	0.57	0.58	10.41
4.5 - 5.5	0.47	0.59	0.51	0.74	0.83	0.94	0.69	0.52	0.41	0.56	0.79	1.23	1.09	0.94	0.63	0.49	11.42
5.5 - 6.5	0.39	0.41	0.47	0.51	0.68	0.78	0.73	0.54	0.47	0.47	1.00	1.66	1.21	0.72	0.50	0.41	10.94
6.5 - 7.5	0.41	0.38	0.36	0.34	0.57	0.58	0.66	0.49	0.41	0.44	1.28	2.10	1.09	0.39	0.30	0.36	10.16
7.5 - 8.5	0.36	0.26	0.15	0.21	0.39	0.41	0.38	0.47	0.39	0.41	1.18	2.52	0.73	0.23	0.20	0.26	8.56
8.5 - 9.5	0.31	0.18	0.12	0.14	0.18	0.25	0.25	0.30	0.27	0.37	1.05	2.81	0.58	0.12	0.10	0.21	7.25
9.5 - 10.5	0.19	0.11	0.07	0.08	0.12	0.11	0.15	0.27	0.30	0.28	0.99	2.61	0.43	0.08	0.08	0.17	6.04
10.5 - 11.5	0.12	0.10	0.06	0.06	0.06	0.07	0.12	0.19	0.23	0.23	0.75	2.47	0.33	0.05	0.10	0.09	5.04
11.5 - 12.5	0.08	0.09	0.02	0.02	0.03	0.05	0.06	0.15	0.19	0.18	0.58	1.98	0.29	0.03	0.08	0.10	3.91
12.5 - 13.5	0.06	0.05	0.01	0.02	0.01	0.02	0.03	0.09	0.14	0.14	0.46	1.60	0.26	0.03	0.06	0.07	3.05
13.5 - 14.5	0.04	0.02	0.01	0.01	0.01	0.01	0.02	0.03	0.17	0.10	0.31	1.12	0.19	0.04	0.04	0.03	2.16
14.5 - 15.5	0.05	0.01	0.00	0.00	0.00	0.00	0.01	0.05	0.11	0.12	0.26	0.85	0.18	0.02	0.04	0.02	1.72
15.5 - 16.5	0.01	0.02	0.01	0.01	0.01	0.00	0.00	0.03	0.07	0.07	0.22	0.63	0.09	0.01	0.02	0.01	1.22
16.5 - 17.5	0.03	0.00	0.00	0.00	0.01	0.00	0.01	0.02	0.07	0.05	0.16	0.46	0.09	0.00	0.02	0.01	0.95
17.5 - 18.5	0.01	0.00	0.01	0.00	0.00	0.00	0.00	0.03	0.02	0.02	0.12	0.30	0.06	0.01	0.02	0.00	0.64
18.5 - 19.5	0.01	0.00	0.00	0.00	0.01	0.00	0.00	0.00	0.02	0.03	0.12	0.24	0.05	0.01	0.02	0.00	0.51
19.5 - 20.5	0.01	0.00	0.00	0.00	0.00	0.00	0.00	0.00	0.02	0.00	0.08	0.17	0.03	0.00	0.00	0.00	0.33
20.5 - 21.5	0.00	0.00	0.00	0.00	0.00	0.00	0.00	0.00	0.01	0.02	0.07	0.11	0.02	0.00	0.01	0.00	0.26
21.5 - 22.5	0.00	0.00	0.00	0.00	0.00	0.00	0.00	0.00	0.01	0.01	0.04	0.10	0.01	0.00	0.00	0.00	0.19
22.5 - 23.5	0.00	0.00	0.00	0.00	0.00	0.00	0.00	0.00	0.01	0.00	0.05	0.05	0.00	0.00	0.00	0.00	0.13
23.5 - 24.5	0.00	0.00	0.00	0.00	0.00	0.00	0.00	0.00	0.00	0.00	0.03	0.07	0.01	0.00	0.00	0.00	0.11
$>$ 24.5	0.00	0.00	0.00	0.00	0.00	0.00	0.00	0.00	0.02	0.00	0.03	0.13	0.00	0.00	0.00	0.00	0.19

Table 29: Distribution of MOS-corrected $59.9\,m$ wind speed by direction at Tower M0571. All model values are computed only for times with valid observations. Histogram of data is available in Figure 37 (p. 66).

Sector	Mean Speed(m/s)	Weibull Scale(A)	Weibull Shape(k)	Frequency(%)
N	7.02	7.91	1.85	4.09
NNE	6.05	6.82	2.00	3.51
NE	6.03	6.81	2.16	4.12
ENE	6.19	6.98	2.51	5.85
E	5.86	6.61	2.53	5.58
ESE	5.66	6.38	2.37	4.61
SE	6.37	7.19	2.28	4.30
SSE	6.58	7.43	2.02	4.18
S	7.75	8.74	1.93	4.29
SSW	7.10	7.99	1.85	4.31
SW	9.41	10.61	2.03	13.70
WSW	9.40	10.62	2.25	22.52
W	6.95	7.85	1.99	8.45
WNW	5.11	5.77	2.08	3.75
NW	5.35	6.04	1.92	3.00
NNW	6.18	6.97	1.97	3.77
ALL	**7.52**	**8.47**	**1.92**	**100.00**

Table 30: Observed $59.9\,m$ mean wind speed, Weibull parameters, and frequency at Tower M0571. Blank values correspond to times with less than 10 data points. Wind rose of data is available in Figure 38 (p. 67).

Sector	Mean Speed(m/s)	Weibull Scale(A)	Weibull Shape(k)	Frequency(%)
N	6.33	7.12	1.84	3.99
NNE	5.34	6.01	1.83	4.09
NE	4.72	5.31	1.80	3.84
ENE	4.73	5.33	1.91	4.39
E	5.12	5.78	1.98	5.27
ESE	5.24	5.92	2.14	5.53
SE	5.64	6.37	2.10	4.93
SSE	6.72	7.59	1.97	4.50
S	7.95	8.95	1.89	4.44
SSW	7.67	8.66	2.04	4.53
SW	9.20	10.38	2.30	10.68
WSW	10.15	11.42	2.67	24.57
W	7.70	8.70	2.18	8.16
WNW	5.65	6.38	2.22	4.01
NW	6.12	6.89	1.84	3.51
NNW	6.03	6.81	1.99	3.57
ALL	**7.52**	**8.47**	**1.92**	**100.00**

Table 31: MOS-corrected $59.9\,m$ mean wind speed, Weibull parameters, and frequency at Tower M0571. All MOS-corrected model values are computed only for times with valid observations; blank values correspond to times with less than 10 data points. Wind rose of data is available in Figure 38 (p. 67).

12.2 Validation of Model Results at Tower M4666

This section examines the quality of the NWP simulations used at a single point within the study area. For this section, the observations were taken at Tower M4666 (latitude 37.82153, longitude -104.51877).

The average observed wind speed (for all valid observational times) at $59\,m$ during the 13 months of the period of record (April, 2013 to April, 2014) is $6.73\,m/s$ with an hourly standard deviation of $3.72\,m/s$ at Tower M4666. This compares to a modeled $58.5\,m$ wind speed of $6.47\,m/s$ with a $3.58\,m/s$ standard deviation for these same times.

Based on a comparison of the NWP model output with observations from each of the meteorological towers for which data were provided, Model Output Statistics (MOS) was constructed. MOS uses a multilinear regression model designed to remove the bias and adjust the variance of the raw NWP simulated wind speed and direction. Applying this statistical model to the simulated data at Tower M4666 results in a MOS-corrected mean value of $6.73\,m/s$ and an hourly standard deviation of $3.72\,m/s$.

This section presents a comparison of the simulated winds with the observations at the reference tower (Tower M4666). The focus of the verification is on the model's ability to reproduce the observed variability of the wind resource at daily and monthly time scales, while preserving the distribution of hourly wind speeds and the diurnal characteristics of the wind.

12.2.1 Observational Data

Approximately 13 months of wind speed data at 59 *meters* and wind direction data at 57 *meters* (April, 2013 to April, 2014) from a meteorological tower (Tower M4666) at Busch Ranch II were used in this analysis. This tower will be referred to as the reference tower throughout this section. The data at 58.5 m were used to assess the quality of the model simulations at 58.5 m.

It should be noted that meteorological observations provided to Vaisala are not allowed to influence the raw model simulations.

12.2.2 Model Validation Statistics

Table 32 presents some basic statistical measures of the model performance relative to the measured winds at the reference tower during the observational period. Also shown are values (labeled "MOS-corrected") for model data with the statistical model applied. For reference, the correlation of the reference tower data to itself is perfect and hence the explained variance (r^2) value is 1.0.

The observed and modeled winds in this section represent the mean of all times during the month for which a valid wind speed or direction observation was available. Therefore they should not be interpreted as estimates of the true winds at the site, but rather a verification of the model's ability to reproduce the available observations. Any month or hour missing greater than 50% of the available observations is omitted from the following figures, tables, and statistics.

Comparison	Value
Correlation of monthly-mean simulated wind speed to observed	0.83
RMS error of monthly-mean simulated wind speed	0.50 m/s
Correlation of monthly-mean MOS-corrected wind speed to observed	0.99
RMS error of monthly-mean MOS-corrected wind speed	0.11 m/s
Correlation of daily-mean simulated wind speed to observed	0.83
RMS error of daily-mean simulated wind speed	1.43 m/s
Correlation of daily-mean MOS-corrected wind speed to observed	0.86
RMS error of daily-mean MOS-corrected wind speed	1.27 m/s

Table 32: Correlation and root mean square (RMS) error statistics of modeled wind speeds.

12.2.3 Monthly Mean Wind Speed

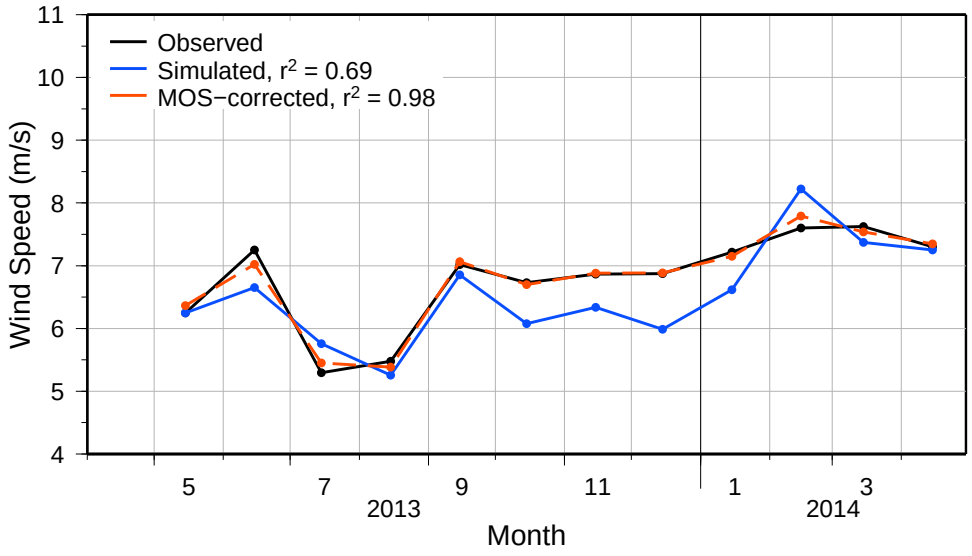

Figure 45: A comparison of the observed, simulated, and MOS-corrected monthly-mean $58.5\,m$ wind speed at Tower M4666. Explained variance(r^2) value of each data source relative to the monthly reference tower wind speeds are shown in the legend. Months missing greater than 50% of the available observations are not plotted. Tabular formatted data are available in Table 33 (p. 88).

12.2.4 Wind Speed Distribution

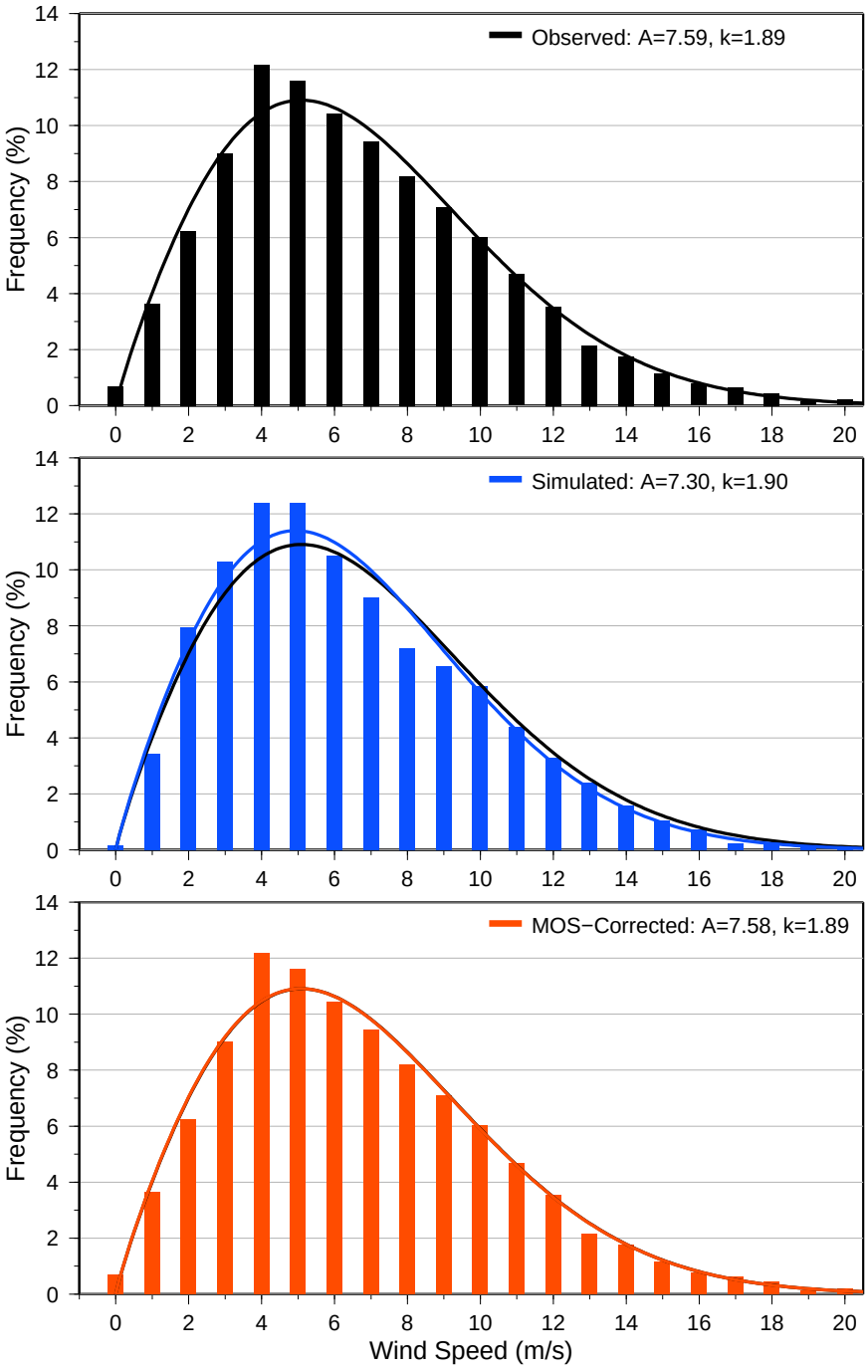

Figure 46: A comparison of the observed, simulated, and MOS-corrected hourly wind speed distributions at $58.5\,m$ at Tower M4666 during the period of record, using $1\,m/s$ bins. ($0\,m/s$ bin contains only values ≤ 0.5) Fitted Weibull distributions are also displayed with the scale(A) and shape(k) parameters listed in the legend. Tabular formatted data are available in Tables 34 and 35 (p. 91 and 92).

12.2.5 Wind Direction Distribution

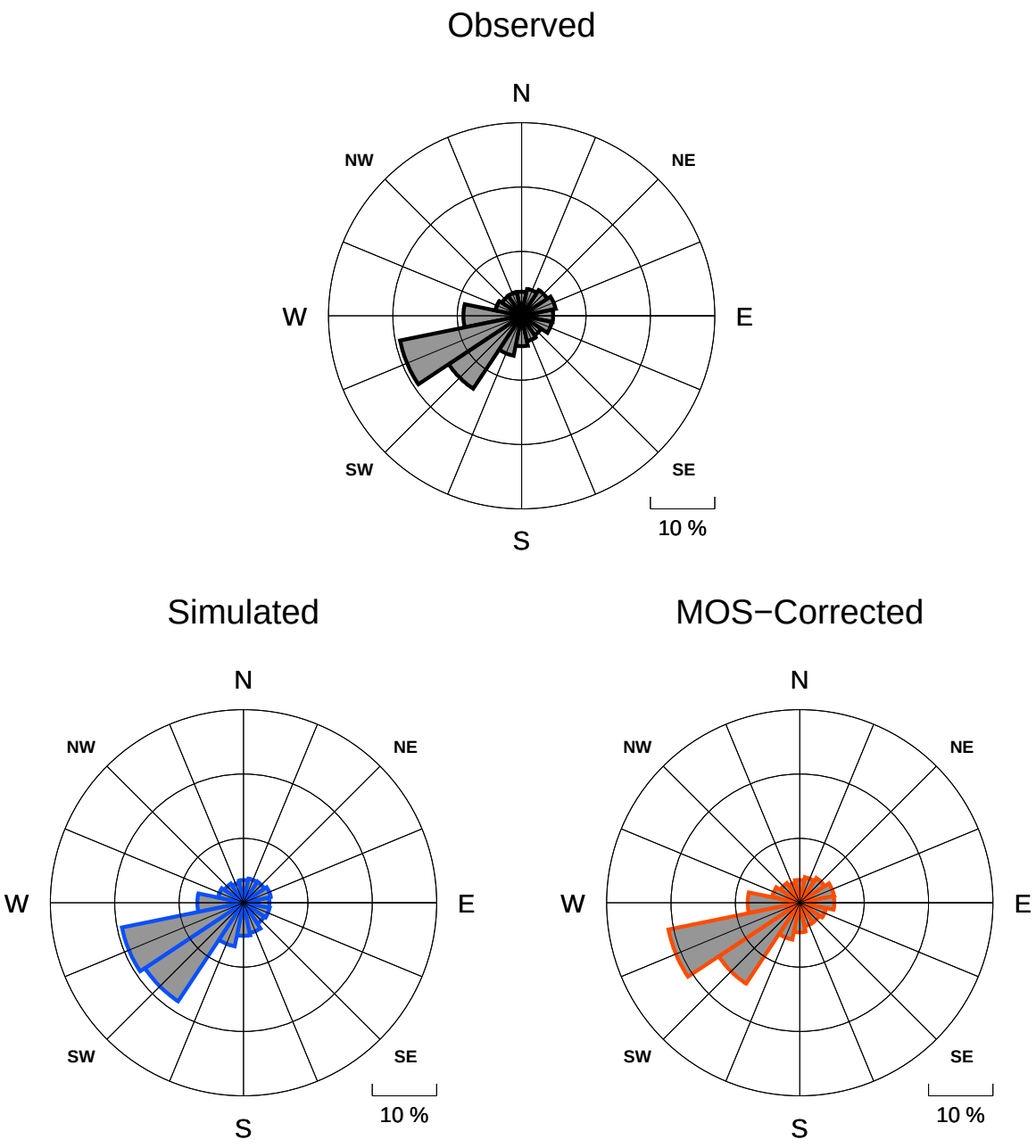

Figure 47: Wind roses at 56.5 m at Tower M4666 for observational data and simulated model data, averaged over the period of record (April, 2013–April, 2014). Directional bins are 22.5° wide, and the radial contour interval is 10%. Tabular formatted data, including mean wind speed values and Weibull parameters for each wind direction sector, are available in Tables 36 and 37 (p. 93).

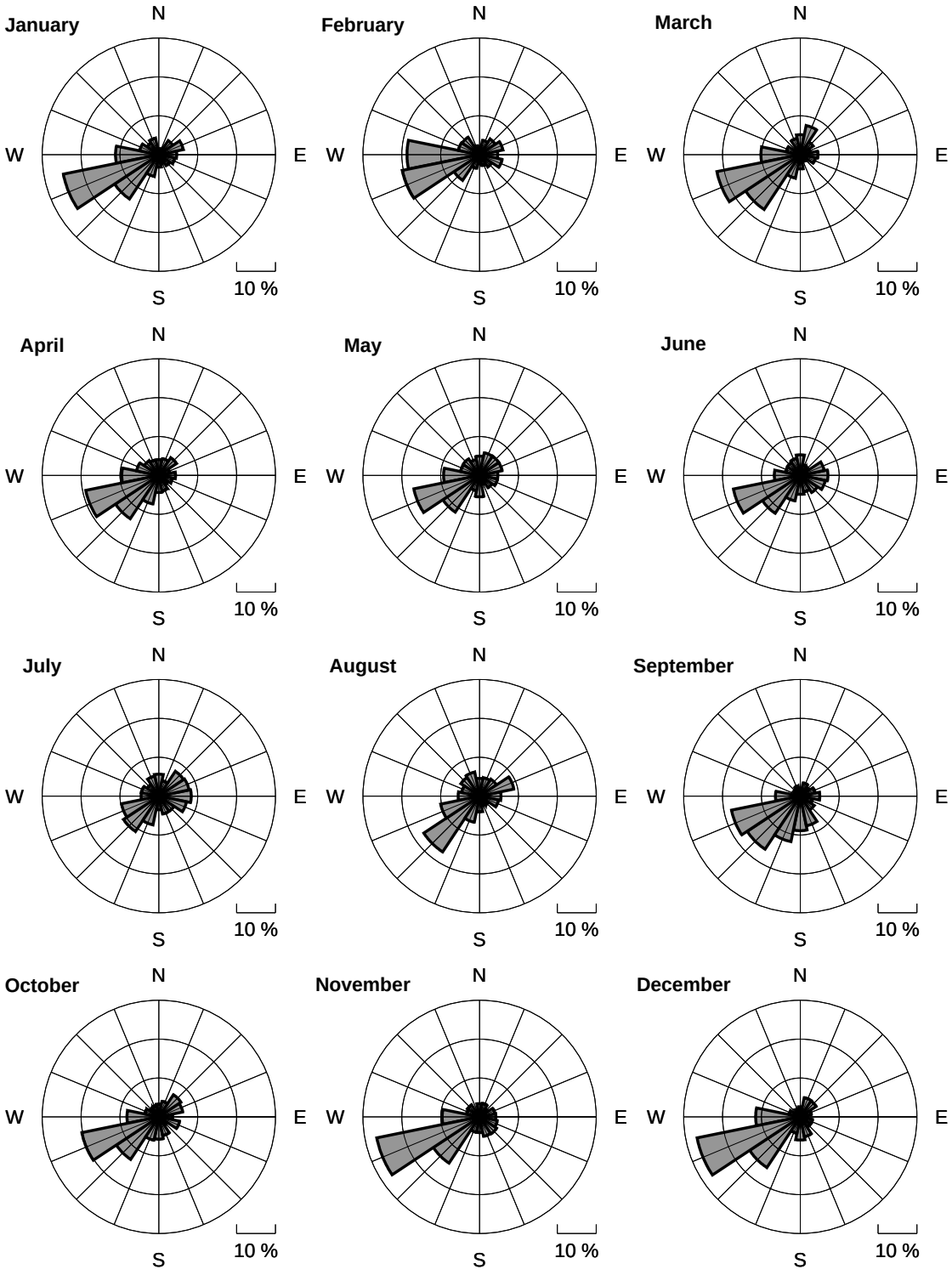

Figure 48: Wind rose of observed wind direction at 56.5 m at Tower M4666 for each calendar month. Directional bins are 22.5° wide, and the radial contour interval is 10%. Months missing greater than 50% of the available observations are not plotted.

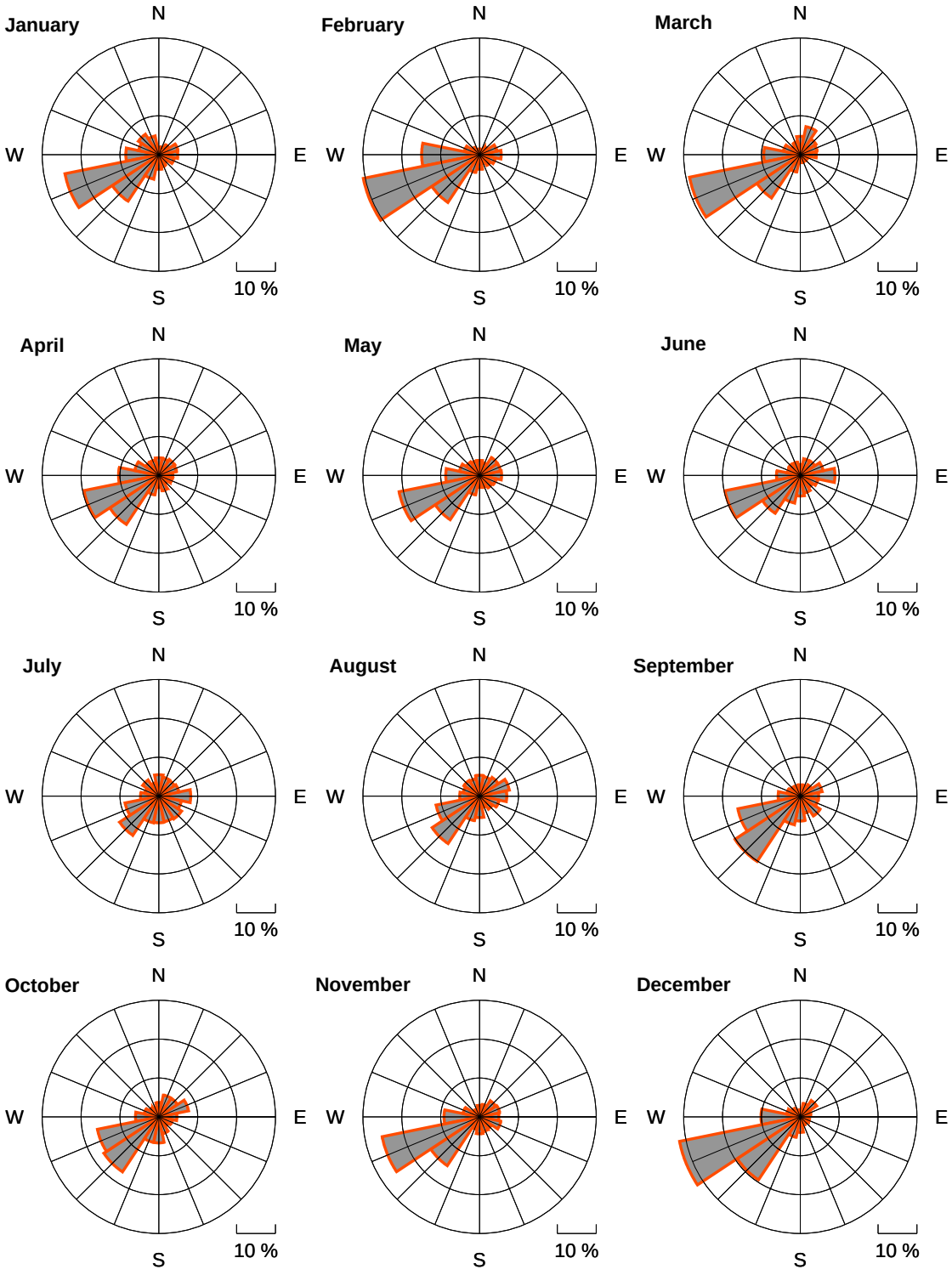

Figure 49: Wind rose of MOS-corrected wind direction at 56.5 m at Tower M4666 for each calendar month. Directional bins are 22.5° wide, and the radial contour interval is 10%. Months missing greater than 50% of the available observations are not plotted.

12.2.6 Diurnal Variability of Wind Speed

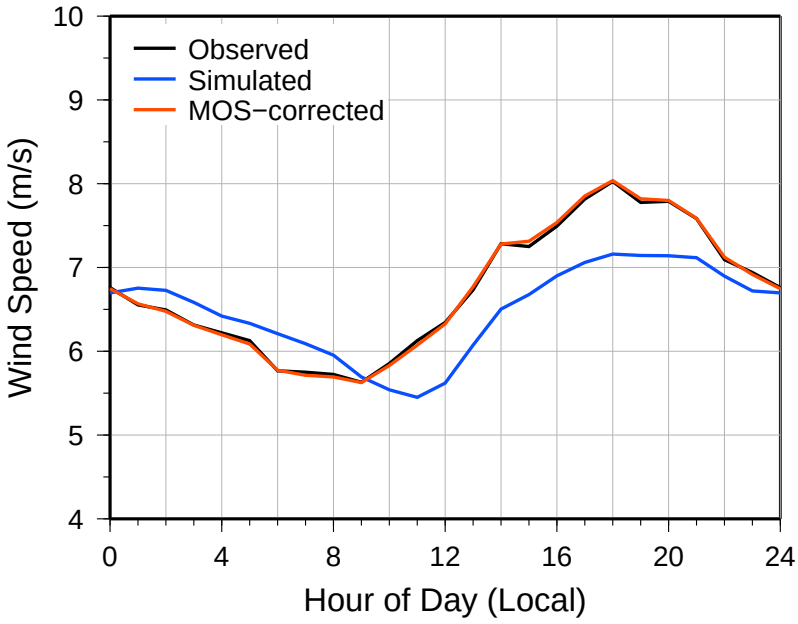

Figure 50: A comparison of the diurnal cycle of observed, simulated, and MOS-corrected 58.5 m wind speed at Tower M4666. Data are averaged over the period of record (April, 2013–April, 2014). Hours missing greater than 15% of the available observations are not plotted. The horizontal axis is Mountain Time Zone. Tabular formatted data are available in Figures 52 and 53 (p. 89 and 90).

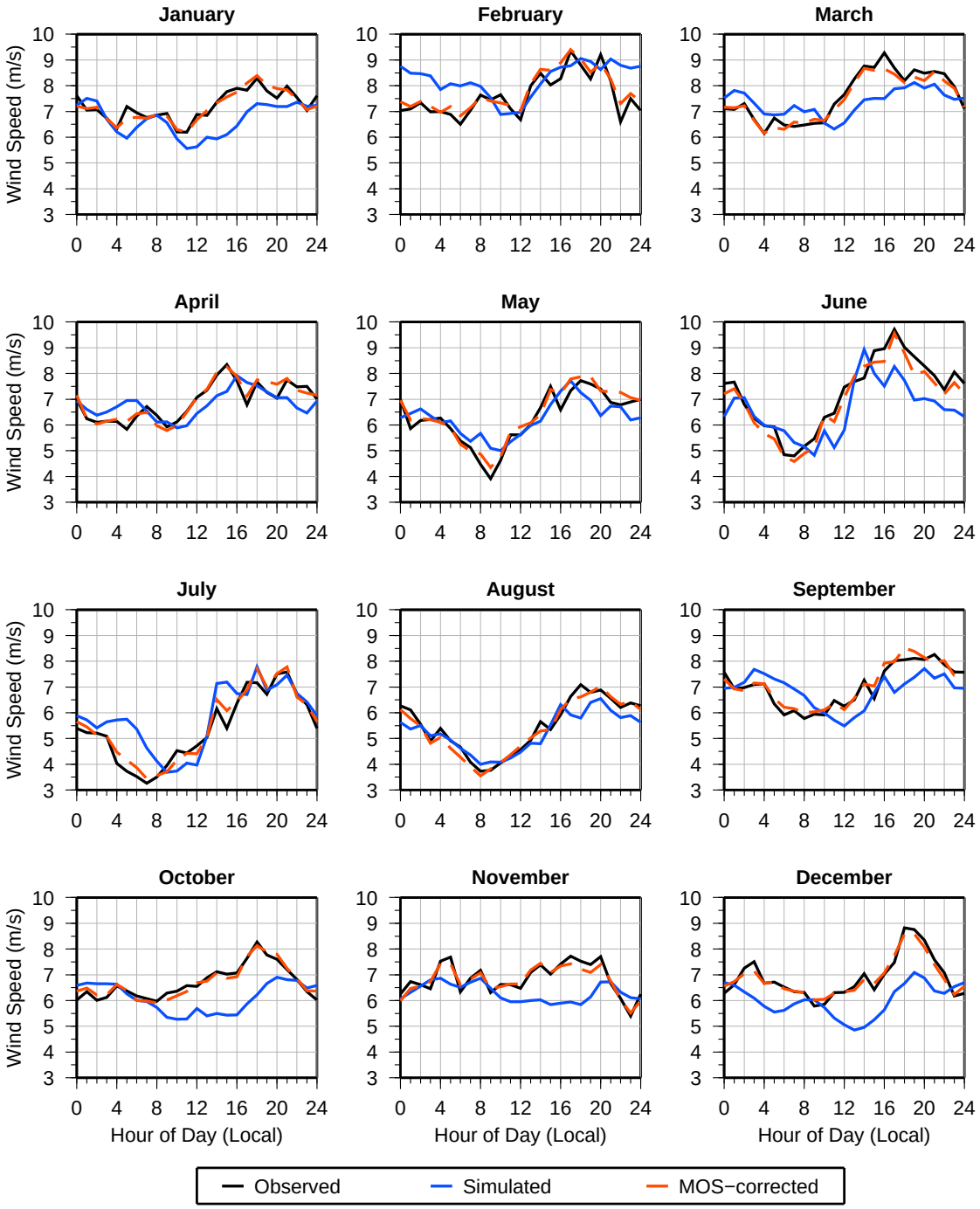

Figure 51: A comparison of the diurnal cycle of observed, simulated, and MOS-corrected $58.5\,m$ wind speed for each calendar month at Tower M4666. Hours missing greater than 50% of the available observations are not plotted. The horizontal axis is Mountain Time Zone. Tabular formatted data available in Figures 52 and 53 (p. 89 and 90).

12.2.7 Tabular Data

Month	Observed	Simulated	Bias	MOS-corrected	Availability(%)
04/2013	5.75	5.41	-0.34	5.67	31.7
05/2013	6.25	6.25	0.00	6.36	97.2
06/2013	7.25	6.65	-0.60	7.02	100.0
07/2013	5.30	5.76	0.46	5.45	99.6
08/2013	5.48	5.26	-0.22	5.38	100.0
09/2013	7.02	6.85	-0.16	7.06	100.0
10/2013	6.73	6.08	-0.65	6.70	98.4
11/2013	6.87	6.34	-0.53	6.88	89.7
12/2013	6.87	5.99	-0.89	6.89	87.8
01/2014	7.21	6.62	-0.60	7.15	96.5
02/2014	7.60	8.22	0.62	7.79	82.9
03/2014	7.62	7.37	-0.25	7.54	91.7
04/2014	7.30	7.25	-0.05	7.35	84.9
All	**6.73**	**6.47**	**-0.26**	**6.73**	**89.2**

Table 33: Monthly-mean $58.5\,m$ wind speeds (m/s) at Tower M4666. Time series graph of data is available in Figure 45 (p. 81). The average values shown at the bottom of the table, labeled 'All', are computed as the mean of monthly means.

Observed = mean of all available wind speed observations
Simulated = mean of simulated model output for times with observations
Bias = Simulated – Observed
MOS-corrected = mean of MOS-corrected output for times with observations

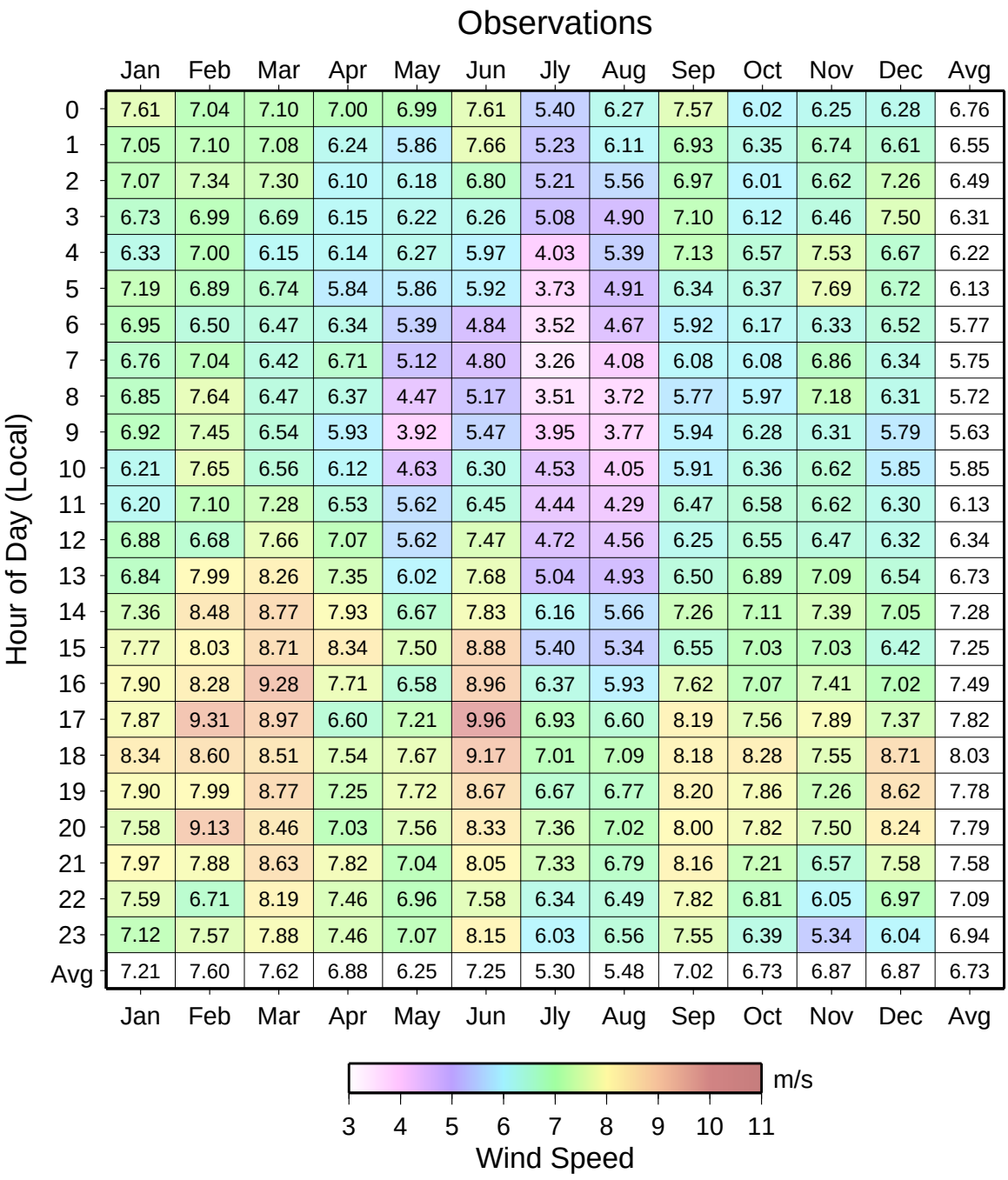

Figure 52: Hourly-mean values of observed $58.5\,m$ wind speed at Tower M4666. Hours missing greater than 50% of the available observations are not plotted. The vertical axis is Mountain Time Zone. Time series graphs of data are available in Figures 50 and 51 (p. 86 and 87).

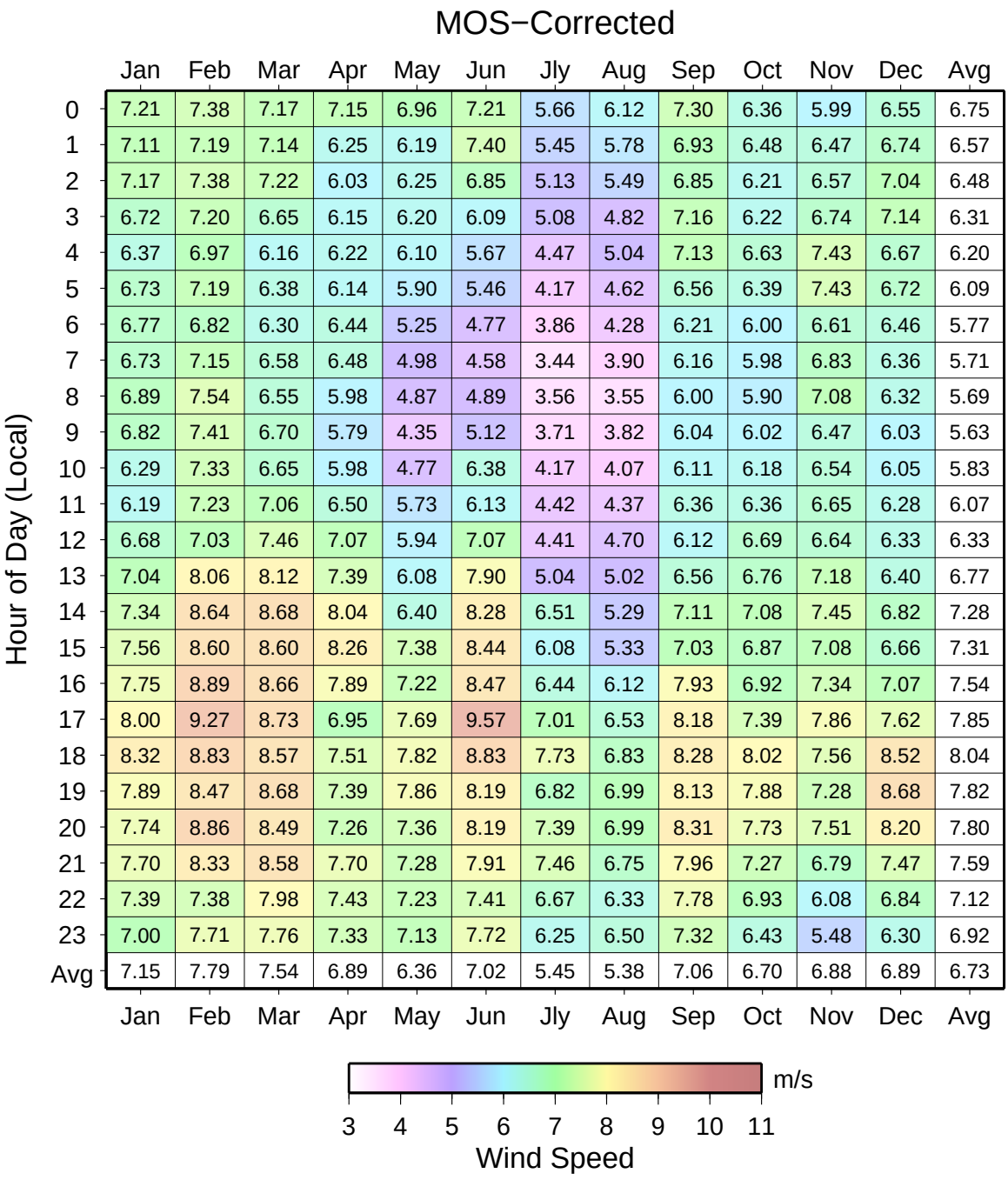

Figure 53: Hourly-mean values of MOS-corrected $58.5\,m$ wind speed at Tower M4666. Hours missing greater than 50% of the available observations are not plotted. The vertical axis is Mountain Time Zone. Time series graphs of data are available in Figures 50 and 51 (p. 86 and 87).

Wind Speed (m/s)	N	NNE	NE	ENE	E	ESE	SE	SSE	S	SSW	SW	WSW	W	WNW	NW	NNW	All
0 - 0.5	0.05	0.02	0.05	0.09	0.00	0.05	0.04	0.06	0.02	0.02	0.01	0.05	0.05	0.05	0.05	0.05	0.65
0.5 - 1.5	0.17	0.19	0.25	0.25	0.17	0.14	0.20	0.19	0.28	0.25	0.26	0.33	0.22	0.32	0.19	0.21	3.61
1.5 - 2.5	0.37	0.32	0.37	0.44	0.33	0.34	0.37	0.32	0.39	0.28	0.54	0.60	0.41	0.45	0.39	0.31	6.22
2.5 - 3.5	0.54	0.42	0.48	0.37	0.40	0.40	0.39	0.34	0.55	0.71	0.92	1.09	0.77	0.60	0.59	0.41	8.99
3.5 - 4.5	0.54	0.68	0.80	1.05	0.61	0.71	0.54	0.48	0.55	0.88	0.96	1.24	1.09	0.77	0.68	0.57	12.17
4.5 - 5.5	0.61	0.64	0.78	0.68	0.80	0.74	0.46	0.59	0.45	0.65	1.70	1.05	0.84	0.65	0.59	0.35	11.59
5.5 - 6.5	0.44	0.52	0.60	0.71	0.83	0.71	0.51	0.41	0.37	0.68	1.57	1.19	0.68	0.40	0.32	0.48	10.42
6.5 - 7.5	0.24	0.32	0.39	0.59	0.65	0.54	0.41	0.40	0.39	0.51	1.72	1.55	0.73	0.27	0.29	0.42	9.43
7.5 - 8.5	0.21	0.24	0.34	0.45	0.41	0.34	0.28	0.31	0.29	0.58	1.91	1.53	0.68	0.18	0.18	0.24	8.18
8.5 - 9.5	0.14	0.27	0.22	0.33	0.26	0.28	0.15	0.32	0.39	0.48	1.36	1.53	0.65	0.15	0.13	0.39	7.07
9.5 - 10.5	0.13	0.17	0.20	0.20	0.19	0.27	0.09	0.26	0.25	0.39	0.90	1.95	0.71	0.11	0.04	0.17	6.01
10.5 - 11.5	0.08	0.12	0.09	0.12	0.12	0.17	0.09	0.12	0.18	0.24	0.55	1.89	0.67	0.08	0.06	0.11	4.68
11.5 - 12.5	0.06	0.13	0.07	0.01	0.11	0.06	0.07	0.11	0.20	0.31	0.32	1.50	0.48	0.04	0.06	0.01	3.53
12.5 - 13.5	0.05	0.07	0.04	0.01	0.02	0.02	0.01	0.01	0.15	0.11	0.20	1.12	0.27	0.04	0.00	0.01	2.14
13.5 - 14.5	0.02	0.04	0.04	0.04	0.00	0.00	0.01	0.04	0.09	0.08	0.27	0.76	0.29	0.04	0.04	0.00	1.75
14.5 - 15.5	0.04	0.01	0.02	0.00	0.00	0.01	0.00	0.04	0.07	0.08	0.13	0.52	0.20	0.02	0.01	0.00	1.16
15.5 - 16.5	0.01	0.02	0.04	0.01	0.00	0.00	0.00	0.02	0.01	0.04	0.08	0.45	0.05	0.00	0.02	0.02	0.78
16.5 - 17.5	0.02	0.07	0.00	0.00	0.00	0.00	0.00	0.00	0.05	0.02	0.06	0.27	0.09	0.00	0.04	0.00	0.63
17.5 - 18.5	0.00	0.00	0.00	0.00	0.00	0.00	0.00	0.00	0.02	0.00	0.06	0.26	0.07	0.00	0.01	0.00	0.42
18.5 - 19.5	0.00	0.01	0.01	0.00	0.00	0.00	0.00	0.00	0.00	0.00	0.01	0.08	0.02	0.00	0.00	0.00	0.14
19.5 - 20.5	0.01	0.00	0.00	0.01	0.00	0.00	0.00	0.00	0.00	0.00	0.04	0.13	0.02	0.00	0.00	0.00	0.21
20.5 - 21.5	0.00	0.00	0.00	0.00	0.00	0.00	0.00	0.00	0.00	0.00	0.01	0.05	0.01	0.00	0.00	0.00	0.07
21.5 - 22.5	0.00	0.00	0.00	0.00	0.00	0.00	0.00	0.00	0.00	0.00	0.00	0.06	0.00	0.00	0.00	0.00	0.06
22.5 - 23.5	0.00	0.00	0.00	0.00	0.00	0.00	0.00	0.00	0.00	0.00	0.00	0.02	0.00	0.00	0.00	0.00	0.02
23.5 - 24.5	0.00	0.00	0.00	0.00	0.00	0.00	0.00	0.00	0.00	0.00	0.01	0.01	0.00	0.00	0.00	0.00	0.02
> 24.5	0.00	0.00	0.00	0.00	0.00	0.00	0.00	0.00	0.00	0.00	0.00	0.01	0.01	0.00	0.00	0.00	0.02

Table 34: Distribution of observed 58.5 m wind speed by direction at Tower M4666. Histogram of data is available in Figure 46 (p. 82).

Wind Speed (m/s)	N	NNE	NE	ENE	E	ESE	SE	SSE	S	SSW	SW	WSW	W	WNW	NW	NNW	All
0 - 0.5	0.06	0.04	0.15	0.06	0.11	0.05	0.01	0.05	0.01	0.00	0.01	0.02	0.02	0.00	0.02	0.06	0.67
0.5 - 1.5	0.29	0.26	0.31	0.52	0.46	0.20	0.09	0.12	0.13	0.12	0.25	0.11	0.13	0.18	0.24	0.22	3.62
1.5 - 2.5	0.34	0.44	0.51	0.76	0.54	0.33	0.31	0.24	0.28	0.29	0.27	0.37	0.39	0.45	0.27	0.44	6.22
2.5 - 3.5	0.46	0.59	0.76	0.72	0.61	0.33	0.26	0.31	0.44	0.55	0.52	0.85	0.80	0.71	0.58	0.48	8.97
3.5 - 4.5	0.65	0.68	0.83	0.96	0.78	0.74	0.47	0.35	0.53	0.61	1.17	1.33	1.11	0.79	0.70	0.46	12.17
4.5 - 5.5	0.48	0.41	0.53	0.77	0.91	0.67	0.54	0.45	0.52	0.93	1.55	1.56	0.99	0.57	0.33	0.38	11.59
5.5 - 6.5	0.33	0.33	0.42	0.55	0.73	0.63	0.54	0.54	0.37	0.55	2.01	1.83	0.51	0.48	0.34	0.25	10.42
6.5 - 7.5	0.32	0.38	0.24	0.48	0.45	0.53	0.40	0.47	0.41	0.68	1.95	1.81	0.65	0.27	0.20	0.18	9.42
7.5 - 8.5	0.22	0.26	0.32	0.17	0.35	0.29	0.40	0.34	0.38	0.59	1.84	2.03	0.47	0.28	0.04	0.19	8.18
8.5 - 9.5	0.14	0.14	0.17	0.14	0.19	0.18	0.28	0.20	0.33	0.46	1.69	2.12	0.57	0.21	0.14	0.11	7.07
9.5 - 10.5	0.06	0.13	0.15	0.08	0.05	0.07	0.15	0.13	0.28	0.29	1.46	2.14	0.61	0.15	0.18	0.06	6.01
10.5 - 11.5	0.02	0.09	0.08	0.05	0.06	0.05	0.06	0.13	0.25	0.20	1.04	2.02	0.37	0.12	0.06	0.09	4.68
11.5 - 12.5	0.06	0.06	0.09	0.06	0.05	0.01	0.04	0.12	0.20	0.20	0.58	1.35	0.40	0.01	0.18	0.13	3.53
12.5 - 13.5	0.04	0.05	0.01	0.06	0.02	0.05	0.04	0.11	0.17	0.09	0.27	0.91	0.19	0.02	0.08	0.04	2.14
13.5 - 14.5	0.01	0.06	0.02	0.02	0.04	0.01	0.01	0.07	0.09	0.09	0.15	0.70	0.26	0.05	0.12	0.04	1.75
14.5 - 15.5	0.01	0.01	0.01	0.00	0.00	0.00	0.00	0.02	0.05	0.05	0.15	0.58	0.20	0.04	0.02	0.01	1.16
15.5 - 16.5	0.01	0.02	0.00	0.01	0.01	0.00	0.01	0.00	0.02	0.02	0.06	0.35	0.15	0.01	0.08	0.00	0.78
16.5 - 17.5	0.00	0.04	0.01	0.00	0.00	0.00	0.00	0.01	0.00	0.01	0.07	0.33	0.13	0.00	0.01	0.01	0.63
17.5 - 18.5	0.02	0.04	0.01	0.01	0.00	0.00	0.00	0.00	0.02	0.00	0.02	0.21	0.07	0.00	0.01	0.00	0.42
18.5 - 19.5	0.00	0.00	0.00	0.01	0.00	0.00	0.01	0.00	0.01	0.01	0.00	0.05	0.04	0.00	0.01	0.00	0.14
19.5 - 20.5	0.00	0.00	0.00	0.00	0.00	0.00	0.00	0.02	0.02	0.01	0.00	0.13	0.01	0.00	0.01	0.00	0.21
20.5 - 21.5	0.00	0.00	0.00	0.00	0.00	0.00	0.01	0.00	0.04	0.00	0.00	0.02	0.00	0.00	0.00	0.00	0.07
21.5 - 22.5	0.00	0.00	0.00	0.00	0.00	0.00	0.00	0.00	0.01	0.00	0.01	0.01	0.01	0.00	0.00	0.01	0.06
22.5 - 23.5	0.00	0.00	0.00	0.00	0.00	0.00	0.00	0.01	0.01	0.00	0.00	0.00	0.00	0.00	0.00	0.00	0.02
23.5 - 24.5	0.00	0.00	0.00	0.00	0.00	0.01	0.00	0.00	0.00	0.01	0.00	0.00	0.00	0.00	0.00	0.00	0.02
$>$ 24.5	0.00	0.00	0.00	0.00	0.00	0.00	0.00	0.01	0.01	0.00	0.00	0.00	0.00	0.00	0.00	0.00	0.02

Table 35: Distribution of MOS-corrected $58.5\,m$ wind speed by direction at Tower M4666. All model values are computed only for times with valid observations. Histogram of data is available in Figure 46 (p. 82).

Sector	Mean Speed(m/s)	Weibull Scale(A)	Weibull Shape(k)	Frequency(%)
N	5.46	6.13	1.78	3.73
NNE	6.00	6.75	1.81	4.26
NE	5.57	6.28	1.93	4.79
ENE	5.47	6.18	2.05	5.36
E	5.77	6.51	2.42	4.90
ESE	5.75	6.49	2.28	4.79
SE	5.31	5.99	2.04	3.64
SSE	6.00	6.76	1.92	4.01
S	6.49	7.29	1.73	4.72
SSW	6.57	7.41	2.02	6.32
SW	7.17	8.09	2.29	13.60
WSW	9.05	10.22	2.24	19.24
W	7.58	8.55	1.95	9.04
WNW	4.85	5.45	1.79	4.16
NW	5.05	5.67	1.73	3.68
NNW	5.58	6.30	2.03	3.75
ALL	**6.73**	**7.59**	**1.89**	**100.00**

Table 36: Observed $58.5\,m$ mean wind speed, Weibull parameters, and frequency at Tower M4666. Blank values correspond to times with less than 10 data points. Wind rose of data is available in Figure 47 (p. 83).

Sector	Mean Speed(m/s)	Weibull Scale(A)	Weibull Shape(k)	Frequency(%)
N	4.96	5.56	1.70	3.54
NNE	5.44	6.08	1.64	4.03
NE	4.85	5.43	1.68	4.63
ENE	4.61	5.17	1.72	5.43
E	4.82	5.42	1.87	5.36
ESE	5.29	5.97	2.05	4.16
SE	5.97	6.74	2.16	3.65
SSE	6.58	7.41	1.88	3.71
S	7.20	8.10	1.82	4.59
SSW	6.64	7.50	2.12	5.81
SW	7.58	8.53	2.70	15.07
WSW	8.88	10.01	2.52	20.82
W	7.47	8.42	1.89	8.09
WNW	5.27	5.94	1.91	4.34
NW	5.99	6.67	1.57	3.62
NNW	5.14	5.72	1.55	3.15
ALL	**6.73**	**7.58**	**1.89**	**100.00**

Table 37: MOS-corrected $58.5\,m$ mean wind speed, Weibull parameters, and frequency at Tower M4666. All MOS-corrected model values are computed only for times with valid observations; blank values correspond to times with less than 10 data points. Wind rose of data is available in Figure 47 (p. 83).

REFERENCES

[1] O. Arino, P. Bicheron, F. Achard, J. Latham, R. Witt, and J. Weber, "Globcover: The Most Detailed Portrait of Earth," *ESA Bulletin*, vol. 136, 2008.

[2] A. J. et al., "Hole-filled seamless SRTM data V4." International Centre for Tropical Agriculture (CIAT), available from http://srtm.csi.cgiar.org, 2008.

[3] M. Liu and M. Yocke, "Siting of Wind Turbine Generators in Complex Terrain," *Journal of Energy*, vol. 4, pp. 10–16, 1980.

[4] D. P. Dee, S. M. Uppala, A. J. Simmons, P. Berrisford, P. Poli, S. Kobayashi, U. Andrae, M. A. Balmaseda, G. Balsamo, P. Bauer, P. Bechtold, A. C. M. Beljaars, L. van de Berg, J. Bidlot, N. Bormann, C. Delsol, R. Dragani, M. Fuentes, A. J. Geer, L. Haimberger, S. B. Healy, H. Hersbach, E. V. Hlm, L. Isaksen, P. Kllberg, M. Khler, M. Matricardi, A. P. McNally, B. M. Monge-Sanz, J.-J. Morcrette, B.-K. Park, C. Peubey, P. de Rosnay, C. Tavolato, J.-N. Thpaut, and F. Vitart, "The ERA-Interim Reanalysis: Configuration and Performance of the Data Assimilation System," *Quart. J. Roy. Meteor. Soc.*, vol. 137, pp. 553–597, 2011.

[5] E. Kalnay, M. Kanamitsu, R. Kistler, W. Collins, D. Deaven, L. Gandin, M. Iredell, S. Saha, G. White, J. Woollen, Y. Zhu, M. Chelliah, W. Ebisuzaki, W.Higgins, J. Janowiak, K. C. Mo, C. Ropelewski, J. Wang, A. Leetmaa, R. Reynolds, R. Jenne, and D. Joseph, "The NCEP/NCAR 40-year Reanalysis Project," *Bull. Amer. Meteor. Soc.*, vol. 77, pp. 437–470, 1996.

[6] R. D. Koster, M. G. Bosilovich, S. Akella, C. Lawrence, R. Cullather, C. Draper, R. Gelaro, R. Kovach, Q. Liu, A. Molod, *et al.*, "Technical Report Series on Global Modeling and Data Assimilation," *MERRA-2 Initial Evaluation of the Climate*, vol. 43, 2015.

[7] G. Larsen, J. Hjstrup, and H. A. Madsen, "Wind Fields in Wakes," in *Proceedings EWEC 1996*, (Göteborg, Sweden), pp. 764–768, 1996.

[8] T. Sorensen, P. Nielsen, and M. L. Thgersen, "Recalibrating Wind Turbine Wake Model Parameters - Validating the Wake Model Performance for Large Offshore Wind Farms," in *Proceedings EWEC 2006*, (Athens, Greece), 2006.

[9] "Obstruction Evaluation / Airport Airspace Analysis." https://oeaaa.faa.gov/oeaaa/external/gisTools/gisAction.jsp, 2017.